SCHOOL OF
CIVIL ENGINEERING

INDIANA
DEPARTMENT OF TRANSPORTATION

JOINT HIGHWAY RESEARCH PROJECT

FHWA/IN/JHRP-94/3
Final Report

ASPHALT MIX DESIGN AND PERFORMANCE

Shakor R.B. Badaruddin
Thomas D. White

PURDUE UNIVERSITY

JOINT HIGHWAY RESEARCH PROJECT

FHWA/IN/JHRP-94/3
Final Report

ASPHALT MIX DESIGN AND PERFORMANCE

Shakor R.B. Badaruddin
Thomas D. White

Final Report

ASPHALT MIX DESIGN AND PERFORMANCE

Shakor Ramat Bin Badaruddin, P.E.
Materials and Research Engineer

Thomas D. White
Professor of Civil Engineering
Purdue University

Joint Highway Research Project

Project No: C-36-55I
File No: 2-12-9

Conducted in cooperation with the

Indiana Department of Transportation

and

Federal Highway Administration

The contents of this report reflect the views of the authors who are responsible for the facts and the accuracy of the data presented herein. The contents do not necessarily reflect the official views of policies of the Federal Highway Administration and the Indiana Department of Transportation. This report does not constitute a standard, specification or regulation.

Purdue University
West Lafayette, IN 47907
May 10, 1994

Revised January 11, 1995

TECHNICAL REPORT STANDARD TITLE PAGE

1. Report No.	2. Government Accession No.	3. Recipient's Catalog No.
FHWA/IN/JHRP-94/3		

4. Title and Subtitle	5. Report Date
Asphalt Mix Design and Performance	May 9, 1994
	6. Performing Organization Code
7. Author(s) Shakor Badaruddin and Thomas White	8. Performing Organization Report No. JHRP-94/3
9. Performing Organization Name and Address Joint Highway Research Project Civil Engineering Building Purdue University West Lafayette, IN 47907	10. Work Unit No. 11. Contract or Grant No. Indiana-HPR-2013
12. Sponsoring Agency Name and Address Indiana Department of Transportation State Office Building 100 North Senate Avenue Indianapolis, IN 46204	13. Type of Report and Period Covered Final Report 14. Sponsoring Agency Code

15. Supplementary Notes

Prepared in cooperation with the U.S. Department of Transportation, Federal Highway Administration

16. Abstract

Premature flexible pavement distress became a major concern in Indiana. As a result, a study was conducted investigating the major underlying factors.

Pavement sections were investigated based on a factorial study with four factors comprised of climate, truck traffic, pavement base type, and wheel path. The distresses evaluated were rutting, thermal cracking and stripping. All were evaluated agaist control sections with zero distress. The pavement condition of each section was determined. Laboratory tests of field samples included physical properties, dynamic creep and recompaction.

Results of the study indicate that the Asphalt Institute mix design criteria identify an asphalt content that is too high. Inplace densities were found to be inadequate and a recommendation was made to use higher field compactive effort. The USAE Gyratory Testing Machine (GTM) was used in laboratory studies to recompact bulk samples of mixtures. Good agreement was shown between GTM and in situ bulk density and air voids. Tests confirm that the in situ asphalt content was too high. Gap graded gradations were found to be prone to rutting. Benefit is shown in using dynamic modulus to evaluate mixtures. A statistical analysis method, discriminant analysis, was used to accurately predict mixture field performance using laboratory data.

17. Key Words	18. Distribution Statement
Rutting, Thermal Cracking, Stripping, Dynamic Creep, Discriminant Analysis, Recompaction Analysis	No restrictions. This document is available to the public through the National Technical Information Service, Springfield, Virginia 22161

19. Security Classif. (of this report)	20. Security Classif. (of this page)	21. No. of Pages	22. Price
Unclassified	Unclassified		

Form DOT F 1700.7 (8-69)

IMPLEMENTATION REPORT

Instances of early distress of asphalt pavement surfaces in the State of Indiana in the last several years have created concern. Among the critical distresses included in this study are rutting, thermal cracking, and fatigue cracking. Rutting has occurred on newly laid pavements as well as those several years old. Among the reasons suggested for the early distresses are increase in truck traffic and truck tire pressure. Questions were directed at the adequacy of the mix design method used by INDOT to sustain the increase in truck tire pressure.

Thermal cracking allows for entry of moisture into the pavement structure that leads to other types of distresses. Stripping or loss of asphalt from the aggregate in a bituminous concrete matrix has been observed to cause premature failure both in high as well as low volume roads. Stripping is a complex phenomenon caused by a combination of internal and external effects acting to dislodge the asphalt film coating the aggregate. The internal effect is the type of asphalt and aggregate which might not be compatible; the external effect is moisture, traffic and their combination.

To achieve improved performance of asphalt concrete pavements, it is necessary to understand the mechanisms that influence this performance. This includes asphalt mixture specification, mix design, construction and also a measure of the qualitative performance. Performance can be judged by the frequency and severity of the various distresses and failures that occur on the pavement.

Mix design procedures currently in use were developed based on wheel loads and tire pressure magnitudes that have been vastly surpassed in recent years due to enhancements in tire technology and truck size. The increase in tire pressure has also been accompanied by a significant increase in truck traffic volume.

Research has been conducted that included a study of distress and materials from in service pavements as well as laboratory prepared asphalt mixtures. Detailed surveys were made of the in service pavements and samples in the wheel path and between the wheel paths were obtained. The effects of various compaction efforts were studied in conducting mix designs. Laboratory tests of field samples included physical properties, dynamic creep, recompaction and silicious sand content.

As a result of this study a number of recommendations are made that could improve asphalt mix designs, construction and performance.

1. An analysis was made of the physical properties of in service pavement samples from in the wheel path and between the wheel path, samples compacted in the laboratory to evaluate mix design criteria, and recompacted samples of materials from the in service pavements. This analysis indicated that the mix design criteria recommended by the Asphalt Institute results in an asphalt content that is too high. The manual Marshall and gyratory compaction efforts are recommended. A mix

design criteria based on an air void content of 5 to 6 percent will result in a reasonable optimum asphalt content.

2. Comparison of bulk densities produced during mix design and those from recompacting material from in service pavements indicates that the constructed density is 6 to 8 pcf lower than that achieved with laboratory compaction. As a result, it is recommended that INDOT require densities 4 to 5 pcf higher.
3. Mixtures from badly rutted pavement sections with high truck traffic tended to be gap graded. Also, in many cases these gradations were out of the specification limits at the coarser end. Quality control for jobs included in this study was not adequate to control the mixture gradations. INDOT should implement quality control processes to minimize deviations from the specified gradation.
4. A gyratory compactive effort of one degree angle of gyration, 120 psi pressure and 60 revolutions at a temperature of 250°F produces a mean bulk density and air voids that compares with those of in service pavements. Recompaction of material from in service pavements using this compaction effort can provide significant information on potential mixture performance.
5. Dynamic testing of field cores produced bituminous concrete modulus values comparable to theoretical dynamic modulus values. Thus, considering the inherent variabilities present in bituminous concrete and given

the uncertain nature of asphalts, the theoretical dynamic modulus of bituminous concrete was shown to be a useful substitute in indicating and predicting mixture behavior. The theoretical dynamic modulus is much easier to obtain and can be used as a check when testing bituminous concrete in the laboratory.

6. The dynamic modulus values for bituminous concrete cores from pavement sections with thermal cracking were consistently high at all test temperatures and loading frequencies. Moduli for rutted pavements were low. As a result, dynamic modulus can be used to identify asphalt mixtures that would be unstable or be prone to thermal cracking.

7. A criterion for identifying mixtures with distress potential using discriminant analysis has been developed. This criterion identifies mixtures that will perform well or rut, thermally crack or strip. Mix designs produced in the laboratory can be evaluated using this criterion prior to use in the field.

It is recognized that INDOT has adopted mix design criteria that is similar to the criteria recommended in this report. Also, quality control procedures now being used should help minimize the variations in gradations and achieve higher and more uniform densities. The tests and analyses utilized in this current study will be helpful in evaluating the benefit of such changes.

TABLE OF CONTENTS

Page

LIST OF TABLES

LIST OF FIGURES

Figure Page

CHAPTER 1. INTRODUCTION

1.1 Background

For satisfactory performance asphalt mixtures need to be well designed, specified and constructed. However, the variability in performance of existing pavements indicate that current mixture and structural design procedures may be inadequate (Roque and Ruth, 1987). In order to improve the end product, that is, the performance of asphalt concrete pavements, it is necessary to understand the mechanisms that influence this performance. This includes asphalt mixture specification, mix design, construction and also a measure of the qualitative performance. Performance can be judged by the frequency and severity of the various distresses and failures that occur on the pavement. It is reflected by the maintenance requirements and cost of repair.

Pavement distress is is a result of gradual deterioration that may take place throughout the pavement life. Some important distress types that are occurring on Indiana highways are rutting, cracking, stripping and raveling which are occurring in new as well as old pavements. The most critical distress currently affecting flexible pavements is rutting which is known to occur even on newly constructed highways (Hughes and Maupin, 1987). Early, excessive rutting is dangerous and results in shortened pavement service life. Pavement distress is an acceptable phenomenon only if it occurs gradually over the entire design life of the pavement.

Mix design procedures currently in use were developed based on wheel loads and tire pressure magnitudes that have been vastly surpassed in recent years due to enhancements in tire technology and truck size. Average truck tire pressures today range between 80 - 120 psi (Hudson and Seeds, 1988) whereas they were well below that during the evolution of mix design methods. The increase in tire pressure has also been accompanied by a significant increase in truck traffic volume. Thus, in addition to evaluating the appropriate mix design processes and its effect on pavement performance, there is a need to identify critical areas of mix design specification and construction control to reduce the distresses occurring on Indiana highways.

1.2 Problem Statement

Recent instances of early distress of asphalt pavement surfaces in the State of Indiana have created concern. Among the critical distresses included in this study are rutting, thermal cracking, and fatigue cracking. Rutting has occurred on newly constructed pavements as well as those several years old. Among the reasons suggested for the early distresses are increase in truck traffic and truck tire pressure. Questions were directed at the adequacy of the mix design method used by INDOT to sustain the increase in truck tire pressure.

Thermal cracking allows for entry of moisture into the pavement structure that leads to other types of distresses. Stripping or loss of asphalt from the aggregate in a bituminous concrete matrix has been observed to cause premature failure in both low and high volume roads.

Stripping is a complex phenomenon caused by a combination of internal and external effects acting to dislodge the asphalt film coating the aggregate. The internal effects are the type of asphalt and aggregate; the external effects are moisture, traffic and their combination. This complexity precludes researchers from conducting accurate tests in the laboratory to predict which mixtures are prone to strip. Available test methods are only partially successful in achieving that goal. In this study samples from distressed pavements will be evaluated in relation to desirable mix design and material properties. The effect of climatic variations, level of truck traffic and type of base beneath the flexible pavement are factors that are included in the study.

1.3 Objective of Study

The objective of this study is to quantitatively analyze cores from distressed pavements. The following tests and evaluations are planned on field and laboratory specimens:

i) Density and subsequently voids.

ii) Dynamic creep tests.

iii) Asphalt content and aggregate gradation.

iv) Physical tests on the recovered asphalt to characterize its in service properties.

v) Sand analysis.

vi) Laboratory compaction studies.

vii) Analysis for criteria to identify bituminous mixtures that are prone to be distressed based on laboratory material properties.

1.4 Organization of Study

Results of this study are presented in the following nine chapters. Chapter 2 presents the results of a literature review of work in the area of asphalt mix design, pavement performance and characterization of bituminous pavements through various test methods. A discussion is also provided of pertinent research on dynamic creep. In Chapter 3, results are presented of the effect on asphalt mix design using different laboratory compaction techniques. Chapter 4 describes the design of experiment methodology used in the study. Chapter 5 explains field data collection and techniques employed in distress measurement. Chapter 6 describes tests of cores. Dynamic creep testing is covered in Chapter 7. Chapter 8 covers the analysis of the results and application of discriminant analysis to identify and group pavements with distinct distresses. Chapter 9 contains the analysis for recompaction of field cores using the gyratory testing machine. The summary and conclusions of the study are included in Chapter 10, followed by recommendations for further research.

1.5 Implementation

Implementation of the results and recommendations in this study is expected to assist INDOT in alleviating distress in asphalt pavements in Indiana. The results could be used to identify distress prone mixtures in the laboratory before they are laid in the field. It would be a step towards reducing the amount and severity of distresses and result in longer asphalt pavement service life. The end result would be a savings in tax dollars.

CHAPTER 2. LITERATURE REVIEW

2.1 Introduction

Significant research has been and is still being conducted on asphalt mix design and evaluation. The reason for this continuing research is that adjustments are required to accommodate the changing parameters that affect asphalt pavement performance, e.g., new loading conditions, new construction materials, and analytical methods. Therefore, asphalt mix design has to be an adaptable process to meet renewed challenges facing the paving industry. However, in a number of cases pavements constructed with asphalt mixtures designed with current mix design procedures have exhibited deficiencies.

2.2 Review of Mix Design Methods And Philosophies

Various studies have been conducted to investigate causes and remedies to distresses like early rutting, cracking and stripping all of which lead to reduced pavement service life. The recent Asphalt Aggregate Materials and Mixture Study (AAMAS) focused on laboratory evaluation of asphaltic concrete mixtures for such distress in developing an improved mix design procedure (Von Quintas et al., 1991). A flow chart of the AAMAS process is shown in Figure 2.1. The ultimate goal was to optimize the structural and mixture design processes to result in a satisfactory pavement design at the least cost.

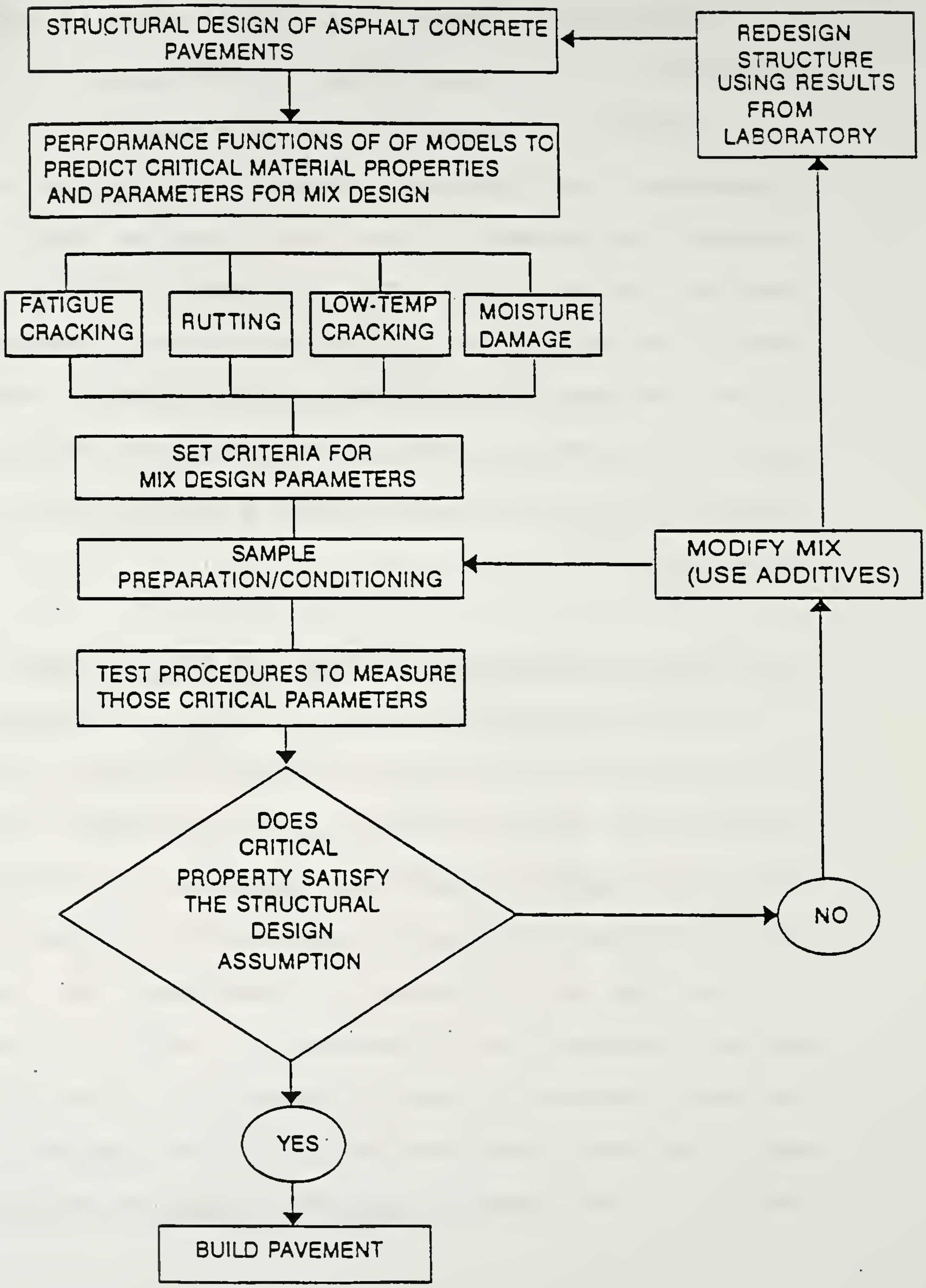

Figure 2.1 Conceptual Flow Chart Illustrating the Different Steps in AAMAS. (Von Quintas, 1991)

The Strategic Highway Research Program (SHRP, 1986) was a two level study where the first level was to incorporate findings from studies like AAMAS in developing a performance based mix design specification for a wide variety of factors such as environment, construction variability and loading conditions (Moulthrop and Cominsky, 1991). The second level was to emphasize evaluation and validation of these mixtures to provide a direct link between the measured fundamental engineering properties in the laboratory to those measured in the field through short and long term observation and testing. Such results would be achieved using conventional test equipment as well as accelerated test facilities. The SHRP Long Term Pavement Performance (LTPP) studies would create a much needed data base consisting of field performance and material properties that would serve as a reference in optimizing the design process.

2.2.1 The Marshall Method

The Marshall Mix Design method is the most commonly used mix design method in the United States although criteria and practice vary in the selection of the optimum asphalt content (Kandhal and Koehler, 1985). The popularity of the Marshall method stems form its simplicity and portability. Even though it is an empirical method, in the absence of other effective methods, the Marshall method serves as an effective guide in setting initial plant mix parameters and monitoring mix production uniformity (White, 1985).

Sources of variation in the mixture plant production process has been shown to outweigh the inherent empricity of mix design methods. Root, 1989 pointed out that many recent pavement failures are not caused by poor mix design methods but rather due to poor specification control during production and construction. Sources of variation include variable stockpile gradations and filler amounts. He also pointed out that lack of quality control frequently produced field mixtures with an optimum asphalt content differing by as much as 0.5 percent from the optimum design value. This aspect of production control is prompting State Highway agencies to implement Quality Assurance Programs [Badaruddin and McDaniel, 1992].

2.2.2 The Hveem Method

The Hveem method of mix design is also a widely used mix design method. Its basic philosophy has been summarized by Vallerga and Lovering (1985) as having the following elements:

i) Asphalt content is estimated based on the aggregate surface area and requires sufficient asphalt cement to provide an optimum coating for the aggregates while also accounting for absorption.

ii) The asphalt content should be such that the compacted aggregate-asphalt matrix is stable, durable and resistant to stripping. Excessive asphalt is indicated by a flushed appearance of compacted cores.

The Hveem method takes into account both frictional and cohesive resistance to deformation of a paving mixture

(Jimenez, 1986).

2.2.3 Other Mix Design Methods

A comprehensive Asphalt Mixture Design System was developed by Monismith et al., 1985 as shown in Figure 2.2. It is essentially an integrated mix design procedure which comprises a series of sub systems which must be executed in a step-wise manner in order to obtain the desired mix design.

Mahboub and Little (1990) introduced a mix design procedure based on mixture stiffness and fatigue characteristics. Subsequently, the mixture is evaluated for rutting and thermal cracking potential using fundamental material properties. The goal was to develop a performance based design procedure.

Yandell and Smith (1985) presented a design method to obtain maximum performance life of bituminous pavements. They illustrated that if the pavement is designed to consist of a stiff, non-plastic surface layer over increasingly soft elasto-plastic layers, then maximum resistance to rutting and cracking could be achieved. In this concept the stiffness of each layer is a function of the asphalt grade with the hardest asphalt in the surface mix and the softest in the base layer.

2.2.4 Indiana D.O.T. Mix Design Method

Indiana uses the Marshall Mix Design method procedures described in MS-2 (1979) of the Asphalt Institute. However, a different criteria is used to select optimum asphalt content. Optimum asphalt content is selected at a given

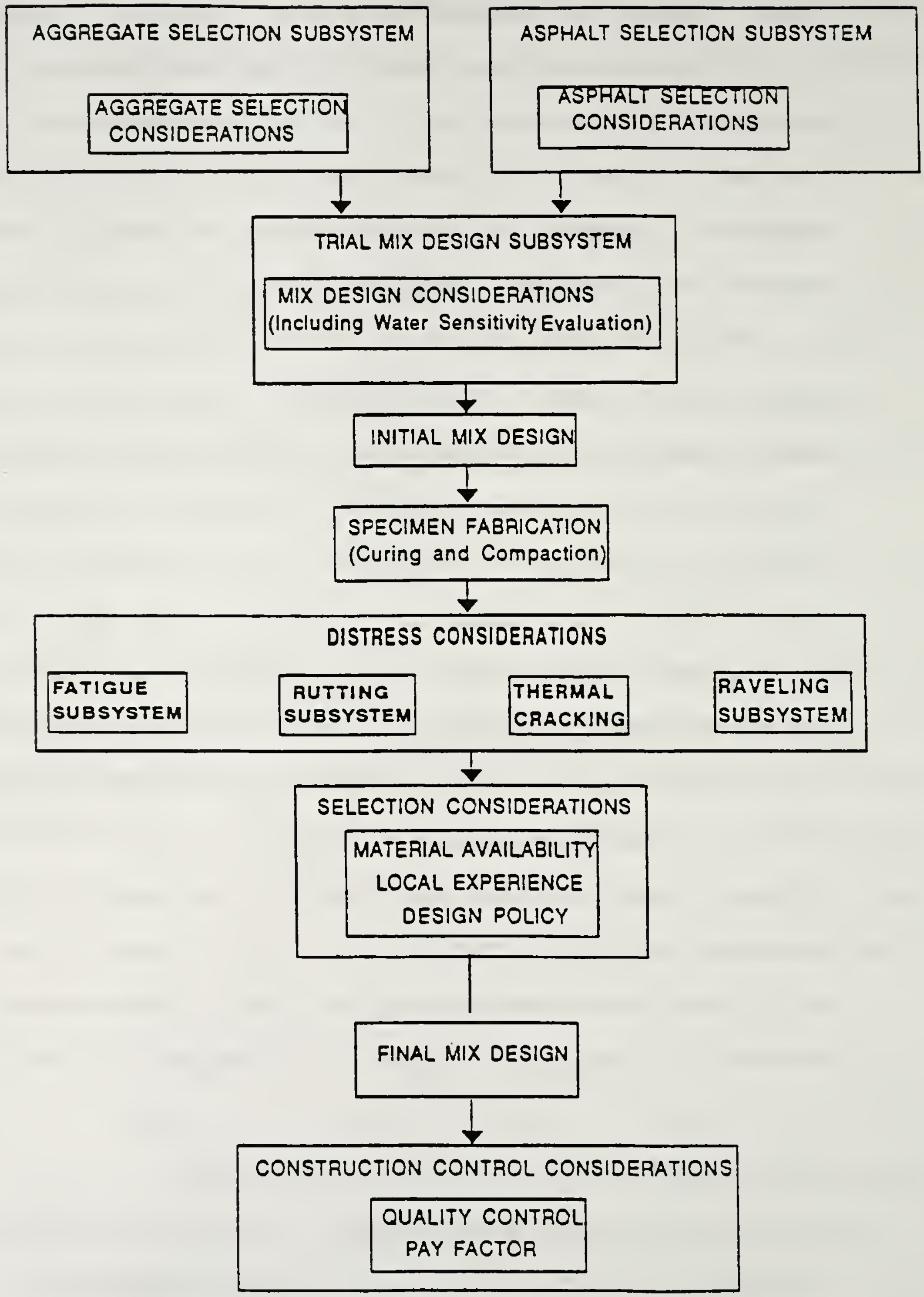

Figure 2.2. A Comprehensive Design System For Asphalt Concrete With or Without Modified Asphalt (Monismith et al., 1985)

percent air voids based on the type of mixture. Subsequently, the stability at optimum asphalt content is checked to insure that the stability is above a minimum. Also, the voids in the mineral aggregate is required to be above a minimum value. The manual Marshall or a calibrated automatic hammer is specified for compaction. AASHTO T209 and T245 are used to specify process control of mixture production (Indiana Specifications, 1988).

2.2.5 Review of Mix Design in Relation to Pavement Performance

The principal aim of mix design is to achieve good performing and long lasting pavements. In fact, mix design has been identified as being one of the two most important factors governing the performance of asphalt pavements (Hughes, 1989). The other factor is compaction. Goetz, 1985 stated that a mix design should fulfill two basic requirements; it must result in adequate void content and the design asphalt content should be sufficient to coat all the aggregates with an optimum film thickness. The simple static creep test was recommended by Shell and others (Shell Pavement Design Manual, 1978, and Van de Loo, 1978) as a means to detect tender mixes that are not detected by tests used for the Marshall and Hveem methods (Brown et al., 1991).

Individual elements that constitute the mix design process; material properties, handling techniques, mixture temperature, compaction and testing have been scrutinized. Material characterization represents a major proportion of the effort of SHRP, 1986. Santucci, 1985 charted the critical factors that affect pavement performance which shows that mix design and materials are among the key elements affecting performance.

2.2.6 Mix Design and Pavement Design

Asphalt mix design and pavement thickness design are inextricably related. Structural properties of the mixture have a direct bearing on pavement performance. However, there seems to be no direct link between the two at the mix design stage. When the asphalt mixture is designed it is done with an 'experienced' hope that it will perform as intended. In pavement design, thickness is selected with a number of parameters which are estimated. The thickness design process hardly uses the mixture properties measured in the laboratory. The exception is the use of static and dynamic creep test in the Shell Pavement Design method (Van de Loo, 1978).

An effort to integrate the two design processes was made by Mahboub and Little, 1990. They showed that hot mix asphalt (HMA) could be designed using fundamental material properties rather than test properties. In their study, distress predictions are carried out on a selected design thickness using nomographs. The AAMAS (Von Quintas et al., 1991) and SHRP, 1986 studies should be able to provide the framework for further integrated design procedures based on the performance based specifications that will be developed.

2.2.7 Quality Assurance in Mix Design

White, 1985 and Root, 1989 pointed out that poor control in any step of the mixture production could lead to field mixtures that are different from that designed. This problem has been acknowledged by INDOT which implemented a Quality Assurance program in 1986 (Walker, 1989). Subsequent evaluation of the results of this implementation indicates a positive improvement in the quality of pavement construction (Badaruddin, 1993). Quality Assurance programs are implemented with the philosophy of transferring responsibility for producing a quality product to the contractor under a penalty and reward system (Dukatz and Marek, 1986). It is in the contractors interest to produce or acquire quality mixtures as specified and construct the pavement to required density in order to be paid in full. A point deduct system is used to quantify deficient materials or work. In this case, the contractor does not get full payment. When the degree of deficiency is too great the contractor may be given an option of leaving the material in place with no payment or removing it and replacing it with acceptable material. Advantages and disadvantages of quality assurance programs are discussed by Dukatz and Marek, 1986.

2.3 Review of Asphalt Pavement Performance

Asphalt pavement performance has been categorized as being structural or functional (Yoder and Witczak, 1975). In this work, reference will be made mainly to functional pavement performance which relates to the condition of the pavement and its riding surface.

2.3.1 Major Distresses in Flexible Pavements

The major distresses that are of concern in flexible pavements (Von Quintas et al., 1991, Scherocman and Wood, 1989, and Sousa et. al., 1991) are:

i) Rutting

ii) Fatigue Cracking

iii) Thermal Cracking

iv) Stripping

Other modes of distress in flexible pavements generally stem from these distresses or are not severe enough to affect the pavements functionally.

2.3.1.1 Rutting

Factors either individually or in combination that can be related to asphalt rutting or permanent deformation are:

i) asphalt content

ii) asphalt grade

iii) aggregate gradation

iv) aggregate type

v) percent crushed aggregate

vi) percent natural sand

vii) density

Analysis of asphalt rutting is compounded if more than one type of distress is present. By far, rutting attracts the greatest attention and concern due to the hazardous situations it leads to if left unmaintained. A discussion of rutting models is given in section 2.5.3.

2.3.1.2 Fatigue Cracking and Fatigue Life

Pavement fatigue is a function of load magnitude and repetitions. Fatigue results in cracking and subsequently structural failure of the pavement. Bonnaure et. al., 1980 used a fatigue model that utilized varying asphalt stiffnesses in the different layers in pavement to predict fatigue life of bituminous mixtures.

2.3.1.3 Thermal Cracking

Thermal or low temperature cracking is the result of increased brittleness of the bituminous matrix at low temperatures. This phenomenon is strongly related to the binder characteristics. Performance of a pavement is more predictable when less temperature susceptible binders are used. McLeod has shown (McLeod, 1976) that the use of Penetration Viscosity Number or PVN could identify such binders. His method identifies the characteristics of the original asphalt because the PVN remains constant irrespective of age of the recovered asphalt. This was verified in another study (Kandhal and Koehler, 1985). The PVN is given by:

$$PVN = (-1.5)(L-X)/(L-M)$$

where:

$$L = 4.258 - 0.79674\{\log Pen@77^{\circ}\ F\}$$

$$M = 3.46829 - 0.61094\{\log Pen@77^{\circ}\ F\}$$

$$X = \log\{Kin.Visc.@\ 275^{\circ}\ F\}$$

Pfeiffer and van Doormal, 1936 used the Penetration Index (PI) to evaluate asphalt temperature susceptibility. Asphalts with lower PI values indicate higher temperature susceptibilities. The Penetration Index is given by :

$$PI = (20 - 500A)/(1 + 50A)$$

Where:

$$A = \{(\log Pen@T1 - \log Pen@T2)\}/\{T1-T2\}$$

$$T1 = 77^{\circ} F$$

$$T2 = \text{Another test temperature (in } ^{\circ}F)$$

Mcleod, 1989, however, showed that the original Pfeiffer and Doormaals' method was applicable only to wax free asphalt and that a revised Penetration Index relationship by Heukelom, 1973 over corrected for wax content.

Thermal cracking in climatic regions with cold winters and hot summers complicates the process of asphalt mix design. As the range of temperature difference widens, the choices of asphalt that can perform satisfactorily diminishes. Modified asphalt and additives have been shown (Lundy et al., 1987) to extend the performance regime of asphalt, but high costs and absence of long term data has largely precluded their extensive use. This is another area of study in SHRP, 1986.

2.3.1.4 Stripping

Stripping in bituminous mixtures is defined in ES-10 (Asphalt Institute, 1981) as "the breaking of the adhesive bond between the aggregate surface and the asphalt cement". However, stripping also occurs as the result of emulsification of the asphalt under conditions of high moisture, hot temperatures and moving, heavy wheel loads. Laboratory methods to predict stripping prone mixtures are discussed by Taylor and Khosla, 1974.

However, the lack of correlation between laboratory predictions of moisture damage to field performance prompted a two phase NCHRP study to establish the link. In Phase I of the study (Lottman, 1978), a laboratory procedure was developed to predict levels of moisture damage similar to that which occurred in the field. In Phase II (Lottmann, 1982), the predictive capability of the test method was assessed and found to be acceptable. The findings in Phase I and II of this study were integrated into a computer program called ACOMODAS C and is considered to be an adequate method for relating laboratory tests to field performance (Terrel and Schute, 1989). Brown and Cross, 1989 indicated that mixtures with Gyratory Shear Index (GSI) values less than unity were prone to strip in the field. This factor could be included in analyzing mix designs in the laboratory for identifying mixtures that may strip.

Stripping mechanisms and pertinent factors that affect the phenomenon of stripping; including material characteristics, anti-strip additives and loading; are discussed in the FHWA State-of-the-Art report (Stuart, 1990).

2.3.2 Influence of Heavy Vehicles on Pavement Performance

Contact pressures at the truck tire and pavement interface have been shown in several studies to be nonuniformly distributed (Huhtala et al., 1989, and Sebaaly and Tabatabee, 1989). The maximum contact pressure due to the reduced contact area can reach as high as 1.75 times the inflation pressure (Huhtala et al., 1989). These high contact pressures are most detrimental to thin pavement sections. Thicker sections with improved load bearing criteria has been recommended by NAPA (Acott, 1986) to sustain the increased loads and contact pressures.

The immediate effect of heavier vehicles on inadequately designed pavements is permanent deformation extending into the subgrade. For well designed and constructed pavements, the effect is a shortening of the fatigue life. Heavier vehicles which are becoming more popular (Sullivan, 1988) account for a greater number of ESAL's in proportion to their number thus contributing to the accumulation of load repetitions. These heavier axles result in an increase in tensile strain at the bottom of the pavement thus causing fatigue of the pavement (Sebaaly and Tabatabee, 1989).

2.3.3 Influence of Climate on Pavement Performance

Asphalt concrete is affected by temperature and by freeze thaw cycles. The changes in the seasons also greatly affect the subgrade support (Bibbens et. al., 1984). Yoder and Colluci-Rios, 1980 established two climatic zones for the State of Indiana. These zones can be used to investigate the effect of climate on asphalt mixtures. Effective evaluation of climate involves comparison of pavement performance and the material characteristics in the different zones.

2.4 Review of Static and Dynamic Creep Characteristics of Asphaltic Mixtures

2.4.1 Rheology of Asphaltic Concrete

Asphaltic concrete is a viscoelastic material consisting of a matrix of packed aggregates bound together by asphalt. Perl et al., 1984 showed that under load the pavement layer undergoes four distinct types of strains; elastic, plastic, viscoelastic and visco-plastic as shown in Figure 4. Each type of strain was shown to be a function of certain factors implicit in the material matrix. They also found that if the applied stress was less than 0.4mPa then the asphaltic concrete deformations were linear and the non-elastic components were insignificant.

Asphalt cement rheology affects mixture durability and resistance to rutting. Roque et al., 1985 showed asphaltic concrete rheology to be a suitable indicator for thermal cracking. However, rheology is complex and results from testing cannot always be extrapolated for general conditions. This effect is confounded by the extreme sensitivity of strain measurements which tends to lead to inaccurate results. Other factors that affect the test results are differences in equipment, operator skills, sample preparation and test method. The magnitude of the strain measurements becomes skewed or amplified by any of these factors.

2.4.2 Static Creep Testing

The static creep test was applied to estimate asphalt mixture rutting potential. Van de Loo, 1978 showed that mix design and pavement design were inextricably linked. Creep and laboratory wheel rutting tests by Bolk, 1981 were shown to correlate well for a small range of static creep stiffness. However, in general, he found that laboratory predictions of rutting underestimated field measured rutting by as much as a factor of two. Van de Loo, 1978 recommended the use of correction factors for the "dynamic effect" in the prediction equations. The most popular static creep test is the unconfined type due to its simplicity. However, the static, confined creep test would simulate field confinement and should provide better indication of pavement performance in the field. The static creep test at best is able to sort between suitable and unsuitable mixes during the mix design stage and be indicative of stable mixtures for field use.

2.4.3 Dynamic Creep Testing

The dynamic creep test has been suggested as the better method to predict field performance than the static creep test. Various researchers have shown repeated load testing gives better predictions of rutting potential of bituminous concrete (Claessen et al., 1977, Van de Loo, 1978, and Valkering et al., 1990). The methods described in the literature to predict mixture rutting potential are analytical in nature and can be divided into two procedural groups; the layer-strain and the visco-elastic procedures (Sousa et al. 1991).

The layer-strain method uses elastic analysis which can either be linear or non-linear. The general linear procedure for this method was proposed by Barksdale, 1972 and Romain, 1972. Brown and Bell, 1977 introduced the use of a non-linear elastic theory. The Shell Pavement Design method makes use of this procedure with the concept of correction factors for various type of pavements. However, Mahboub and Little, 1990 suggested that these correction factors magnify the rutting predictions by 30 to 100 percent when they should be reducing it because dynamic loading causes less deformation than static loading.

The visco-elastic method considers the rheological properties of the mixture in conjunction with moving load. Mechanical models consisting of elements of Maxwell and/or Kelvin are used to represent a loaded system. This method can also incorporate non-linear visco-elasticity as shown by Elliot and Moavenzadeh, 1971. This visco-elastic procedure is applied in VESYS (Kenis, 1977). Because of poor correlation between predicted and measured observations, this procedure is no longer being used.

A list of models for predicting rutting has been summarized by Sousa et al., 1991. In general the layer-strain procedure is more popular than the visco-elastic due to its simplicity. A three dimensional, dynamic finite element method (3D-DFEM) that uses the visco-elastic method is described by Zaghloul and White, 1993. The 3D-DFEM accurately maps distress and deformation in various pavement layers (1993).

CHAPTER 3. LABORATORY EVALUATION OF DIFFERENT COMPACTION TECHNIQUES TO PRODUCE BITUMINOUS MIXTURE DESIGNS

3.1 Introduction

As stated in Chapter 2, the performance of asphalt concrete pavements is affected by two major factors (Hughes, 1989); a properly designed mix and compaction. Correct treatment of these two factors together would be effective in mitigating many pavement distresses. And in general, lead to improved pavement quality and longer service life.

There remains the question "why do not more pavements embody the two salient factors mentioned above"? There are two principal reasons. Firstly, there is the problem of achieving the desired quality of construction even when mixtures are properly designed. Secondly, the mix design process is a function of various factors including material type and compaction technique. For a given mix design method, different laboratory compactors have been shown to produce different results (Fehsenfeld and Kriech, 1991, and Consuegra et al., 1989). The first factor has been addressed through implementation of contractor quality control procedures. One goal of this current study is to clarify questions on mix design.

As part of the current study, five types of laboratory compactors were used in producing mix design specimens. Based on the test results, the compactors are ranked and recommendations made on their use for mix design. Results from this study will be compared to mixture characteristics of recompacted field cores in Chapter 9.

3.2 Laboratory Mix Design Concept and Application

The goal of a laboratory mix design is to determine the proportions of a bituminous mixture that will produce a pavement that is stable, durable and flexible. When the mixture is placed and compacted it should be resistant to major distresses like rutting, thermal cracking and stripping.

Thus the mix design, in concept, is a selection process to identify the optimum asphalt content for a given choice of aggregate type and gradation. In this study, use was made of the Marshall Mix Design Criteria (MS-2 Asphalt Institute, 1979).

Although properly designed and compacted mixtures do produce high quality pavements, laboratory test results, to date, have not proven to be indicators of good field performance. In short, cores made in the laboratory do not possess the same engineering properties as those from the in-situ pavement.

One major discrepancy between laboratory and field compaction is the manner in which the compaction energy is imparted to the mix. (In the laboratory, compaction is imparted to a confined sample by impact, gyratory or kneading type compactors.) Field compaction, on the other hand, is effected by the kneading action of rollers with limited mixture confinement. A rolling process simulating the field conditions would be of benefit.

3.3 Description of Study

A study was undertaken to evaluate and compare five laboratory compaction techniques. The compaction techniques were manual Marshall, mechanical Marshall, slanted foot rotating base (SFRB) Marshall, California kneading compactor and gyratory testing machine. Cores produced from the different compaction methods were tested according to the Marshall design methods for asphalt concrete (MS-2 Asphalt Institute, 1979). The test results were evaluated and ranked for acceptability and versatility.

The main variable in this study was the compaction method. Care was taken to maintain control over all other variables including material type, gradation, and compaction temperature.

3.3.1 Materials

Four inch diameter specimens were made using crushed limestone and dolomite obtained from stockpiles at an asphalt plant in Lafayette, Indiana. The aggregate, originating from a quarry in Monon Indiana, had a gradation meeting No. 9 Binder specification limits (Indiana Specification, 1988). The asphalt cement was an AC-20 (ASTM D-3381) obtained from a tank at the same asphalt plant. The AC-20 specifications and aggregate gradation are shown in Appendix A.

Individual 1400 gram aggregate batches were prepared for sample fabrication. The asphalt was heated in containers that held sufficient asphalt to make 4 cores.

3.4 Laboratory Compaction Techniques

In each of the five compaction techniques the mixing and compaction temperatures were the same. This was considered necessary for making a meaningful comparison. The blended aggregates were heated to a temperature of between 320-340 degrees Farenheight and held for over an hour to ensure dry conditions. The aggregates were then mixed with asphalt at 300 degrees Farenheit. Each specimen was made from an individual batch of aggregates that was hand mixed before compaction at 275 ± 5 degrees Farenheight. Mixing was continued long enough to ensure uniform coating and until the compaction temperature was attained. The entire mixture was then placed into a mold for compaction.

After compaction, the samples in the mold were allowed to cool in air or under a table fan. Three samples at the same asphalt content were made at five asphalt contents for each compaction method. The description of each compaction technique is given below.

3.4.1 Manual Marshall

The manual Marshall compactor specified in ASTM D-1559-82 was used to apply 75 blows to each face of the specimen. After cooling, the specimen was removed from the mold and its height and weights in air and water determined and recorded. The cores were then set aside for testing.

3.4.2 Mechanical Marshall

This technique is similar to the manual Marshall except that the 75 compaction blows are delivered mechanically at a rate of about 55 times a minute.

3.4.3 Slanted Foot Rotating Base (SFRB)

This compactor has two additional features to the above two methods which are:

a. The sample and mold assembly rotates at a speed of about 20 revolutions per minute while the hammer blows are delivered mechanically at about 58 times a minute, and

b. The base plate has a one degree bevel which imparts some kneading action.

The SFRB compactor was also used to apply 75 blows to each face of the specimen.

3.4.4 California Kneading Compactor

With exception of the foot, the compaction techniques utilized with the California kneading compactor follows the procedure described in ASTM D-1561-81. Samples were compacted on one face with 150 tamping repetitions at 500 psi. The compaction was delivered by a special foot with a one degree bevel which imparts additional kneading during compaction when compared to the standard flat foot. This method requires different molds than those of the Marshall compactors and had to be cooled longer.

3.4.5 Gyratory Testing Machine (GTM)

The GTM used is described in ASTM D-3387-83. Samples were subjected to 30 and 60 revolutions of the GTM set at 120 pounds per square inch (psi) with one degree angle of gyration. In this study the GTM was used only as a compactor although it should be noted that the GTM is capable of measuring other mixture characteristics. Physical properties and Marshall stability and flow were determined on the compacted samples.

3.5 Testing

The compacted cores were analyzed in accordance with the Asphalt Institute Marshall Mix Design Method (MS-2 Asphalt Institute). The tests conducted were as follows:

a. Bulk Specific Gravity (SSD) - ASTM D-2726-83.

b. Marshall Stability and Flow - ASTM D-1559-82.

c. Theoretical (Rice) Maximum Specific Gravity - ASTM D-2041-78.

d. Percent Air Voids - ASTM D-3203-83.

The test results are summarized in Table 3.1. Each result represents the average of test values from three samples.

3.6 Analyses of Results

The results in Table 3.1 are plotted in Figures 3.1 to 3.25. A summary of the asphalt contents used in selecting the optimum asphalt content is given in Table 3.2. The test properties at the selected optimum asphalt content for each compaction method is summarized in Table 3.3. As expected,

Table 3.1. Summary of Test Results

COMPACTION METHOD	COMPACTIVE EFFORT	PERCENT ASPHALT CONTENT	BULK SPECIFIC GRAVITY	MAX. SPECIFIC GRAVITY	PERCENT AIR VOIDS	MARSH. STABILITY LBS.	FLOW (0.01")	PERCENT VMA
MANUAL MARSHALL	75 BLOWS	4.0	2.437	2.5962	6.1	2199	9	14.0
	75 BLOWS	4.5	2.4367	2.5752	5.4	2315	11	13.8
	75 BLOWS	5.0	2.4523	2.5546	4.0	2290	12	13.5
	75 BLOWS	5.5	2.4901	2.5343	1.7	2081	14	12.3
	75 BLOWS	6.0	2.4917	2.5143	0.9	1745	17	12.4
	75 BLOWS	6.5	2.4791	2.4946	0.6	1773	23	13.1
MECHANICAL MARSHALL	75 BLOWS	4.0	2.4078	2.5868	6.9	2419	9	15.5
	75 BLOWS	4.5	2.4477	2.5661	4.6	2512	11	14.6
	75 BLOWS	5.0	2.5034	2.5456	1.7	2503	12	13.1
	75 BLOWS	5.5	2.5116	2.5255	0.6	2293	13	13.2
	75 BLOWS	6.0	2.5	2.5057	0.2	1733	19	14.1
	75 BLOWS	6.5	2.4761	2.4862	0.4	1832	23	15.4
SLANTED FOOT ROTATING BASE	75 BLOWS	4.0	2.4628	2.5935	5.0	2373	13	13.2
	75 BLOWS	4.5	2.4808	2.5726	3.6	2621	15	13.2
	75 BLOWS	5.0	2.5368	2.5521	0.6	2843	17	11.3
	75 BLOWS	5.5	2.5241	2.5318	0.3	2848	16	11.7
	75 BLOWS	6.0	2.5118	2.5151	0.1	2186	20	12.2
	75 BLOWS	6.5	2.482	2.4822	0.0	1975	23	13.2
CALIFORNIA KNEADING COMPACTOR [one face only]	150 REPS.	4.0	2.4348	2.5632	5.0	1918	9	14.6
	150 REPS.	4.5	2.4574	2.5431	3.4	2043	11	14.2
	150 REPS.	5.0	2.4799	2.5233	1.7	2052	12	12.8
	150 REPS.	5.5	2.4906	2.5038	0.5	2221	13	14.0
	150 REPS.	6.0	2.4962	2.4998	0.1	2124	14	14.8
	150 REPS.	6.5	2.4884	2.4899	0.1	2161	16	16.0
GYRATORY TESTING MACHINE	60 REV.	4.0	2.4582	2.5798	5	1995	11	14.7
	60 REV.	4.5	2.4989	2.5736	3.0	2325	13	13.7
	60 REV.	5.0	2.5411	2.5556	2.4	2113	14	12.7
	60 REV.	5.5	2.5096	2.5353	0.9	2162	15	14.3
	60 REV.	6.0	2.4962	2.5153	1.0	1747	16	15.1
	60 REV.	6.5	2.4669	2.4915	1.0	1654	17	16.6

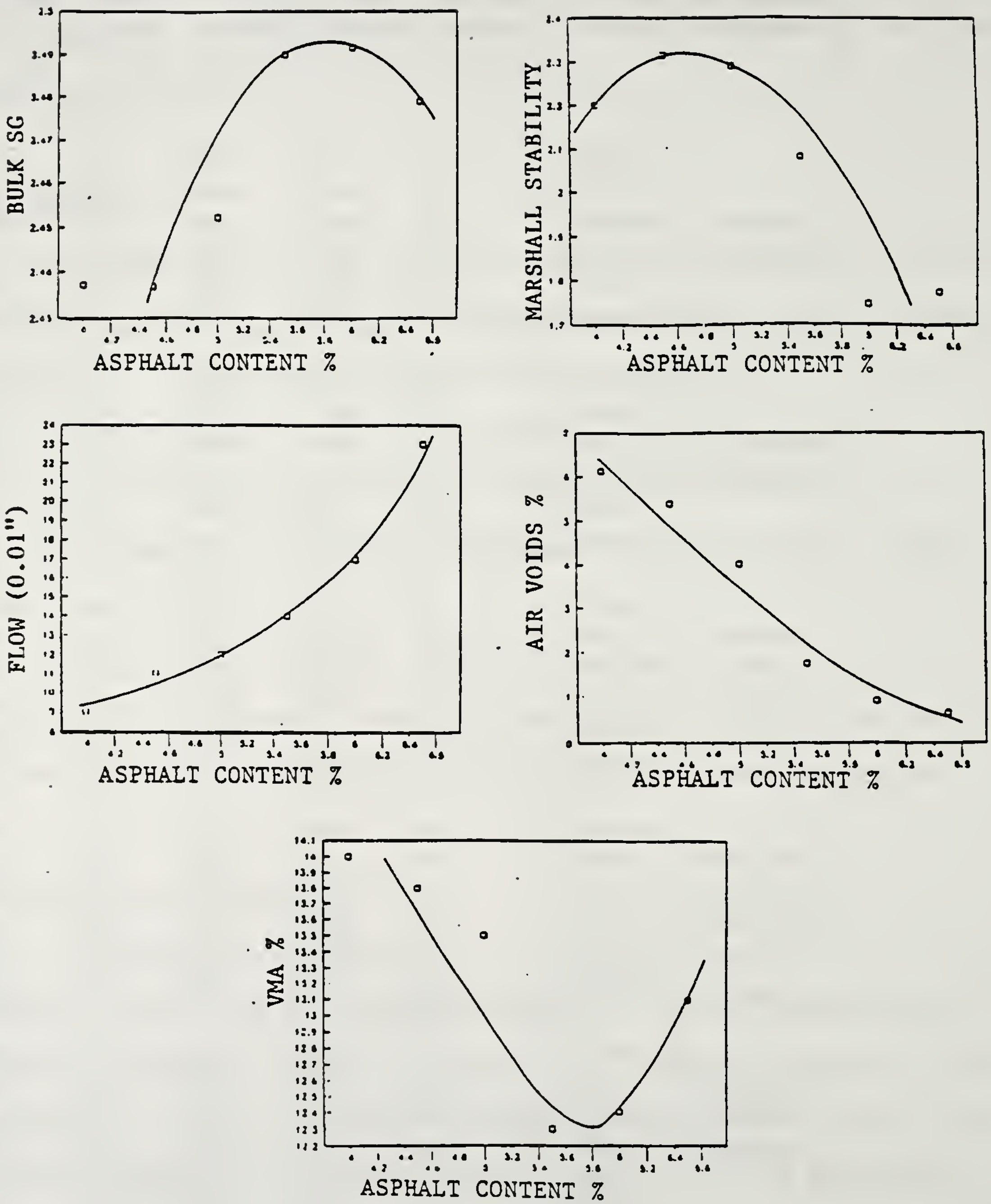

Figure 3.1. Mix Design Using Manual Marshall Compactor

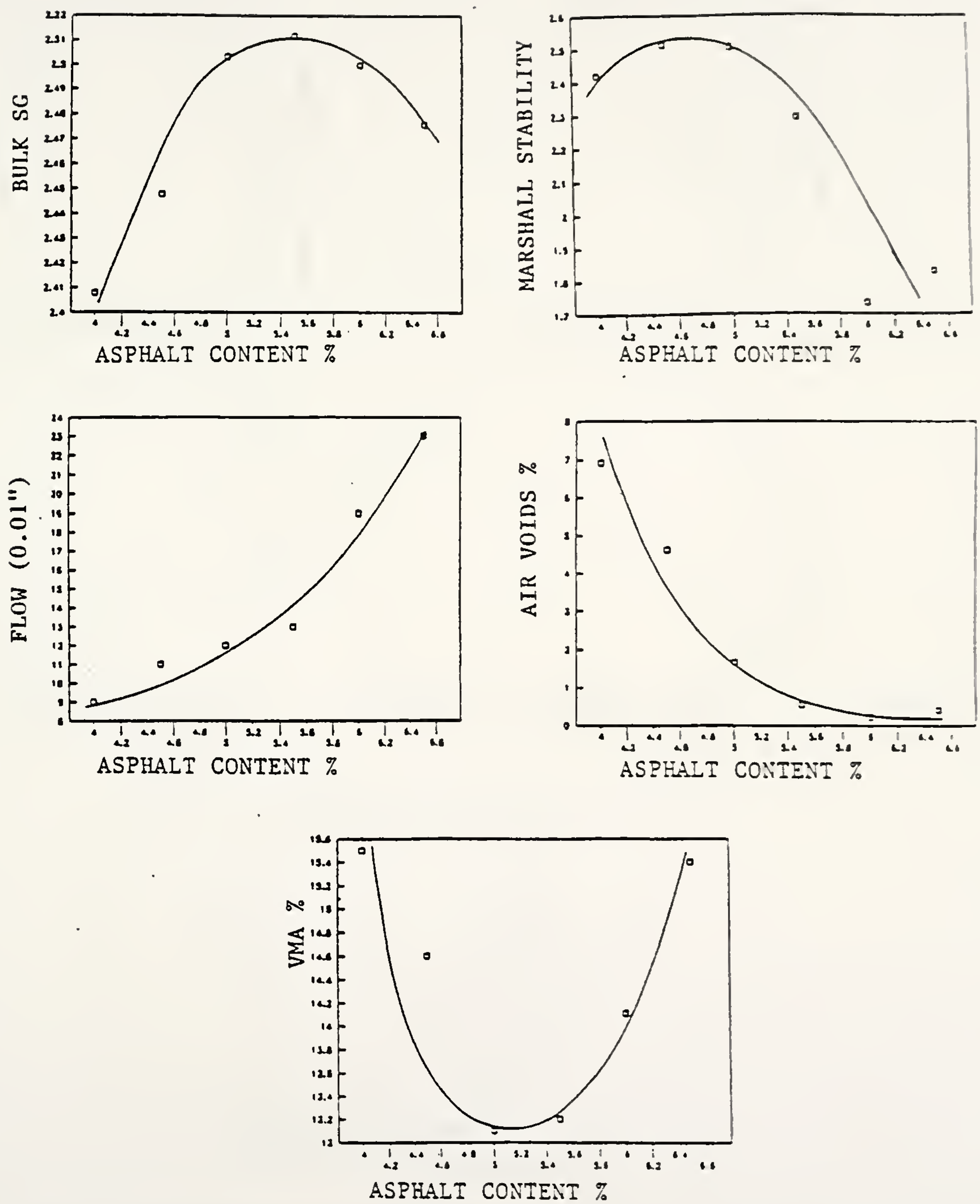

Figure 3.2. Mix Design Using Mechanical Marshall Compactor

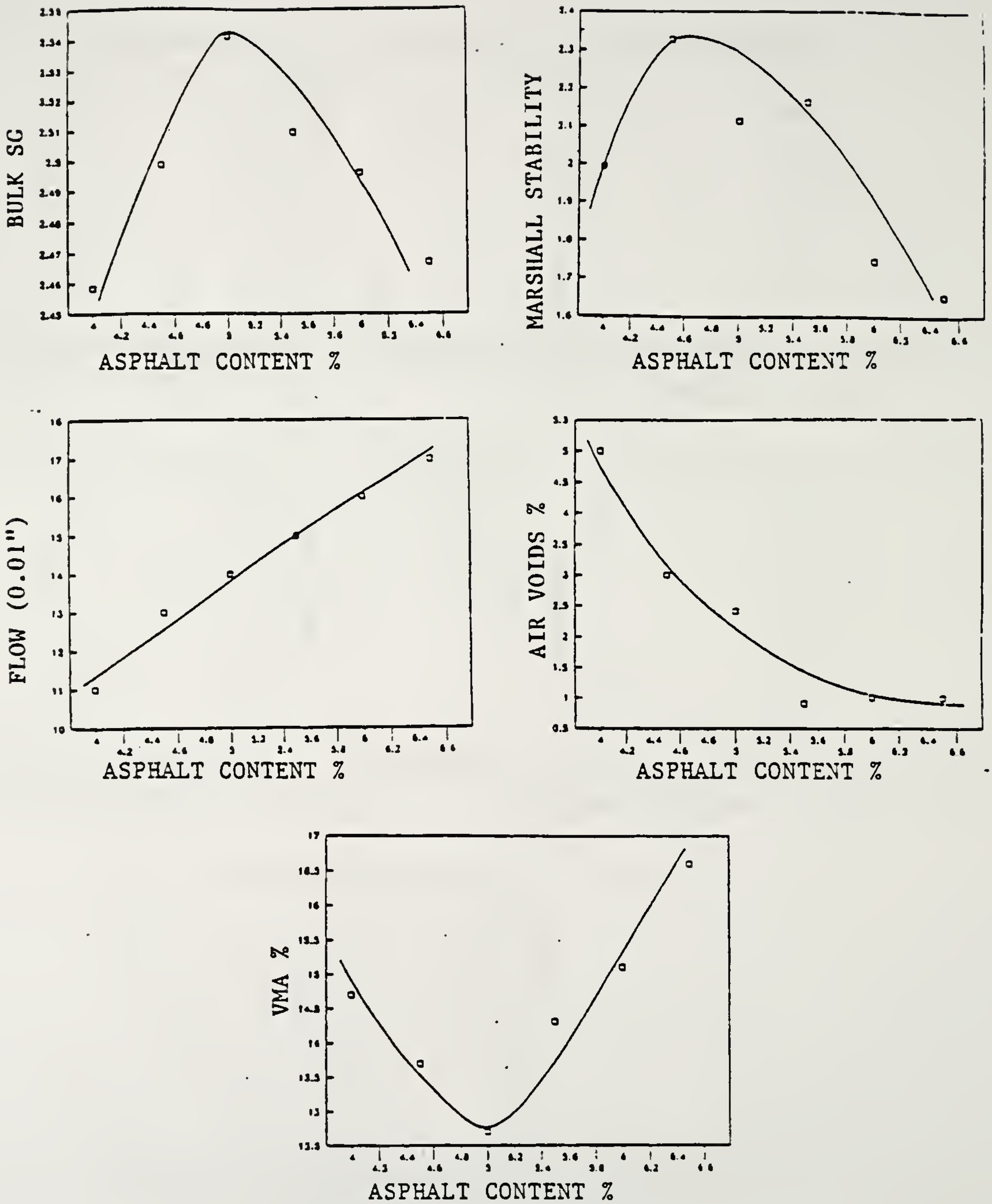

Figure 3.3. Mix Design Using Slanted Foot Rotating Base Marshall

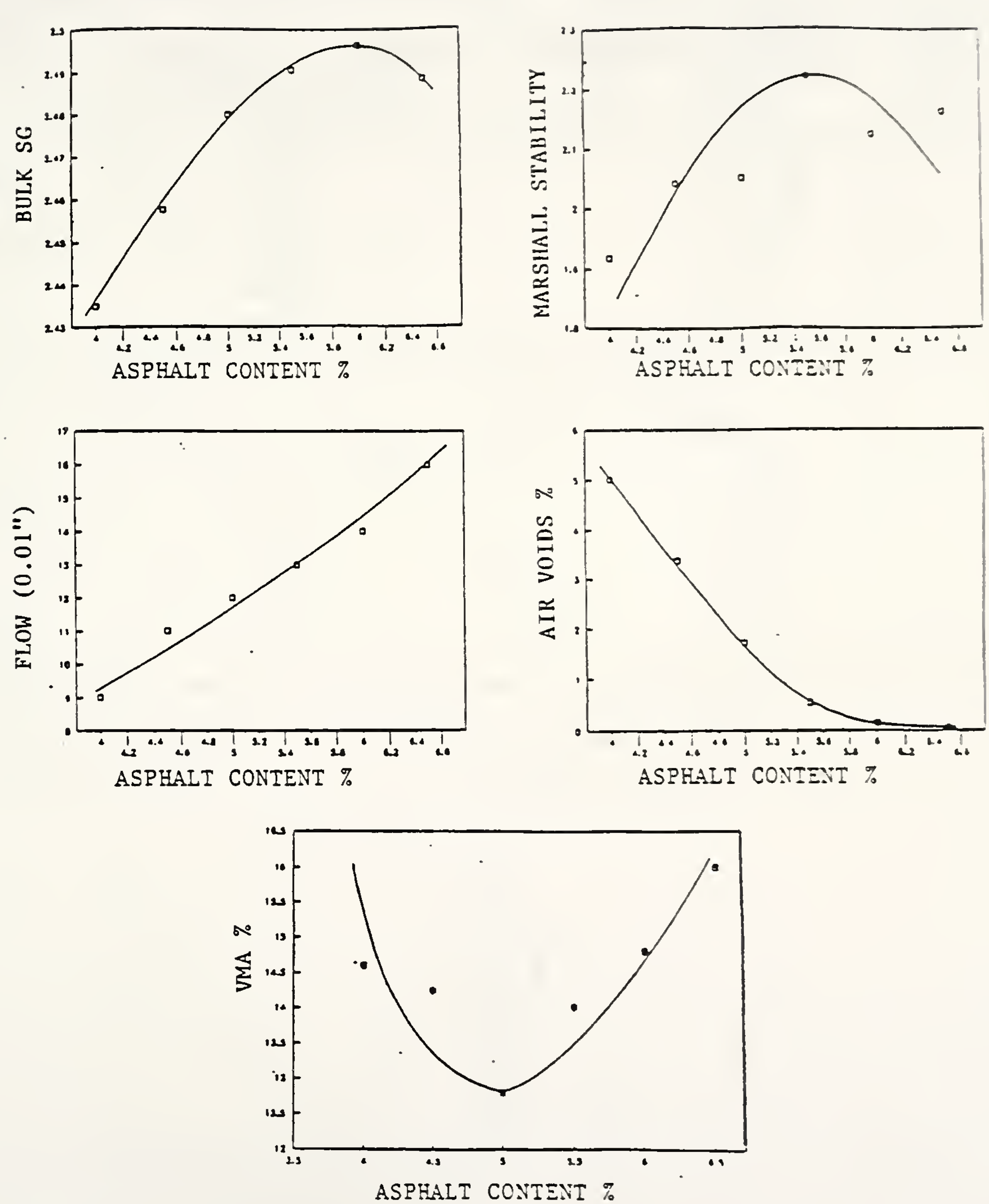

Figure 3.4. Mix Design Using Modified California Kneading Compactor

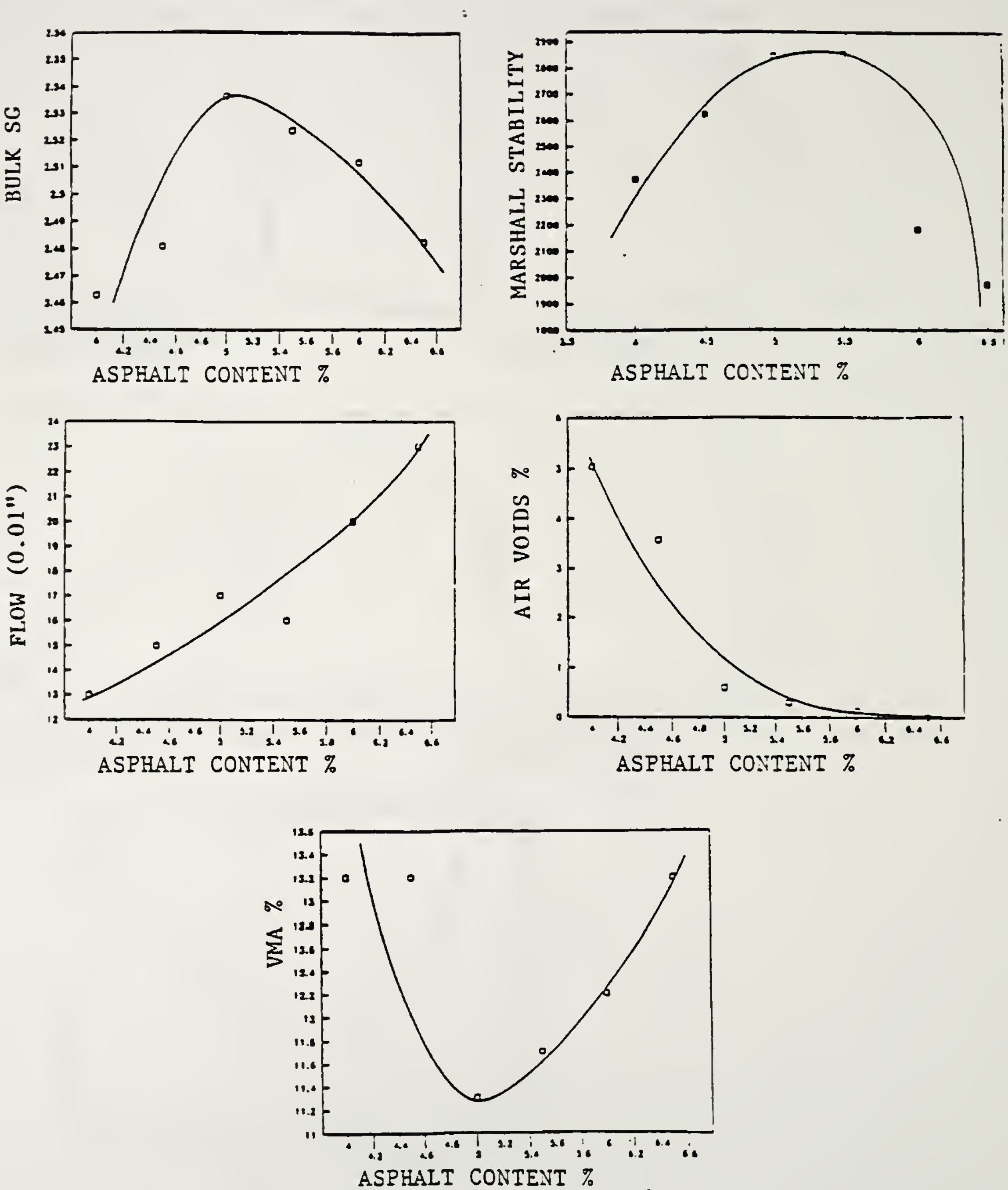

Figure 3.5. Mix Design Using Gyratory Testing Machine Compactor

Table 3.2. Summary of Mix Design Asphalt Contents For Various Compactors

COMPACTION METHOD	ASPHALT CONTENTS FROM FIGURES 3.1 - 3.5			DESIGN OPTIMUM ASPHALT CONTENT	ASPHALT CONTENT AT 6% AIR VOIDS
	MARSHALL STABILITY	BULK SPECIFIC GRAVITY	PERCENT AIR VOIDS		
MANUAL MARSHALL	4.7	5.8	4.8	5.1	4.1
MECHANICAL MARSHALL	4.7	5.5	4.4	4.9	4.2
SLANTED FOOT ROTATING BASE	4.6	5.0	4.2	4.6	3.7
MODIFIED CALIFORNIA KNEADING COMPACTOR	5.5	5.9	4.3	5.2	3.8
GYRATORY TESTING MACHINE	5.3	5.1	4.2	4.9	3.9

Table 3.3 Summary of Mix Design at Optimum Asphalt Content

COMPACTION METHOD	COMPACTION EFFORT	AVERAGE OPTIMUM ASPHALT CONTENT	MARSH. STABILITY (LBS.)	FLOW (0.01")	BULK SPECIFIC GRAVITY	PERCENT AIR VOIDS	VMA PERCENT
MANUAL MARSHALL	75	5.1	2280	12	2.476	3.2	12.9
MECHANICAL MARSHALL	75	4.9	2520	11	2.499	1.9	13.2
SLANTED FOOT ROTATING BASE	75	4.6	2330	13	2.571	2.9	13.3
MODIFIED CALIFORNIA KNEADING COMPACTOR	150 [ONE FACE]	5.2	2210	12	2.485	1.2	13.0
GYRATORY TESTING MACHINE	1° ANGLE 120 PSI 60 REV.	4.9	2820	16	2.533	1.4	11.4

these figures and tabulated results clearly show the effect of compactive effort on mixture properties.

3.6.1 Evaluation of Compaction Technique

The summary in Table 3.3 shows results of the mix designs (according to MS-2 Asphalt Institute Mix Design Method). In general, the air voids and VMA are too low. The gradation of the aggregate used in the study (No.9 Surface, Indiana Specifications 1988), as shown in Appendix A, does seem to show dense packing when plotted on a 0.45 power graph. Dense packing and low air voids are detrimental to pavement performance.

Brown and Cross (1991) indicated that the Marshall 75 blow manual compaction effort is equivalent to 6 million ESALs. In this sense, the mix designs with the various compactive efforts in this current study suggest that the air voids are unacceptably low at the optimum asphalt content using the Asphalt Institute mix design criteria.

Indiana has recently implemented a mix design procedure that selects an optimum asphalt content at a specific air void. Optimum asphalt content at six percent air voids is compared with the optimum asphalt content for the Asphalt Institute mix design criteria in Table 3.2. The six percent air void criteria produces an optimum asphalt content 0.7 to 1.4 percent lower than the Asphalt Institute criteria.

The selection of an optimum asphalt content is predicated on achieving a stable but durable mixture. Stability can be achieved with lower asphalt content and durability with higher asphalt content. The crux of the problem then is to balance these opposing factors in arriving at the optimum. A review of Tables 3.2 and 3.3 suggests that the slanted foot, rotating base Marshall hammer in combination with the Asphalt Institute mix design criteria would result in the lowest optimum asphalt content of 4.6 percent using the Asphalt Institute criteria. The air voids at this asphalt content are 2.9 percent which is marginally low. For this same compactive effort the optimum asphalt content using the six percent air void criteria is 3.7 percent which is quite low. Using only the six percent air voids criteria, the highest optimum asphalt contents are 4.1 and 4.2 percent for the manual and mechanical Marshall compactive efforts. These are low but reasonable for the dense aggregate grading.

3.6.2 Discussion of Compactors

From the laboratory study, a number of comments can be stated. Using the Asphalt Institute mix design criteria results in the following ranking of compactors based on a reasonable asphalt content.

1. Slanted Foot, Rotating Base
2. Mechanical Marshall*
3. Gyratory Testing Machine (1° angle, 120 psi, 60 rev.)*
4. Manual Marshall
5. Modified California Kneading Compactor

* tied

Using the six percent air voids criteria results in the following ranking based on a reasonable asphalt content.

1. Mechanical Marshall
2. Manual Marshall
3. Gyratory Testing Machine (1° angle, 120 psi, 60 rev.)
4. Modified California Kneading Compactor
5. Slanted Foot, Rotating Base

In the above ranking, the slanted foot rotating base Marshall hammer would produce a more acceptable optimum asphalt content using the Asphalt Institute mix design criteria. Using the six percent air void criteria indicates the Mechanical or Manual Marshall compactive efforts would produce a more acceptable optimum asphalt content.

Using the above evaluation still results in a 0.4 percent different in the optimum asphalt content. The effect of this difference is only going to be resolved by observations of field performance or accelerated pavement testing. There is further information in the following chapters on the acceptability of the range of 4.2 to 4.6 percent asphalt content. This information is provided in the discussion of the physical properties of in situ and laboratory recompacted samples from in service pavements.

3.7 Concluding Summary

The mix design study was successful in showing the effect of each type of compactor on determining optimum asphalt content. These values were utilized to create two rankings of the compactors based on different mix design criteria. The slanted foot, rotating base Marshall compactor produced the most reasonable asphalt content using the Asphalt Institute mix design criteria. It was shown that the Mechanical and Manual Marshall compactors produced mix designs with an acceptable asphalt content using a six percent air voids mix design criteria.

This study indicates that the asphalt mixture physical properties vary with both compactive effort and asphalt content. A major goal of asphalt mixture design is to select an optimum asphalt content for stability and durability. Consequently, compaction effort and criterion for selection of optimum asphalt content have to be considered concurrently. It is also likely that different asphalt mixtures may require adjustments in the criterion.

CHAPTER 4 DESIGN OF EXPERIMENT AND ANALYSIS

4.1 Introduction

There are a number of factors that affect asphalt mix performance. From a general consideration of these factors those that seem to be most significant to pavement performance include truck traffic, climate, underlying pavement base type and wheel path. Among the major distresses on Indiana pavements are rutting, thermal cracking, and stripping. To investigate the relationship of the factors affecting these distresses, an experimental design was developed to identify and possibly rank the effect of the major factors on these distresses. In addition, the relationship between factors and in situ physical properties of the asphalt mixtures were considered for identifying desirable mix design criteria.

A discussion is presented in the following sections on the application of design of experiment in planning the study. Also, statistical technique are described that are applied in later chapters.

4.2 Factors In Study

A number of factors were initially considered in development of the design of experiment. However, after careful consideration of resources and the potential significance of each factor, those used in developing the design of experiment were distress type, truck traffic, climate, underlying pavement type and wheel path. Pavement sections studied include asphalt surfaced pavement with little or no distress, control sections, as well as pavements with distresses such as rutting, thermal cracking and stripping. These distresses are related to several important factors such as truck traffic, climate and pavement base type. Two levels of truck traffic, high and low, were set at less than or greater than 1450. This determination was based on data presented by Lindly, 1987. Two levels of underlying pavement type were selected: flexible or rigid. The wheel path factor relates to samples taken from the wheel path, and those taken from between the wheel path. The climate factor was taken as either North or South based on the classification by Yoder et al., 1980.

Thus for the design of experiment there are four factors, each at two levels, giving a total of sixteen treatment combinations as shown in Table 4.1. Pavement distresses evaluated were rutting, thermal cracking, stripping and no distress. Thus there are four distresses in each treatment combination giving a total of 64 minor cells. This is a relatively large factorial when applied to field observations and sampling.

If only one pavement is selected for each cell of the full factorial with no replication there would be complete confounding between factors and site. A factorial analysis requires a replicate in each cell to remove the confounding. Since the climate factor has shown limited significance (Lindly, 1987, Pumphrey, 1989) in distress formation on asphalt surfaced pavements in Indiana, it was dropped. This would provide the needed replication in each cell. Excluding

Table 4.1 Layout of Factorial Design

CLIMATE		NORTH								SOUTH							
TRUCK TRAFFIC		HIGH				LOW				HIGH				LOW			
BASE TYPE	WHEELPATH	4 DISTRESSES*				4 DISTRESSES*				4 DISTRESSES*				4 DISTRESSES*			
FLEXIBLE	WP																
	BWP																
RIGID	WP																
	BWP																

Distresses: 1. ZERO 3. THERMAL CRACKING
2. RUTTING 4. STRIPPING

climate reduces the experimental design from 64 to 32. A layout of the factorial design is shown in Table 4.2.

4.3 Complete Factorial Design

The factorial design shown in Table 4.2 has four different pavement sections in each of the eight treatment combinations. From a sampled pavement section, seven 4" diameter cores were to be taken from the wheel path and seven more from outside the wheel path. The total number of core samples required for the full factorial totals 32 x 7 x 2 = 448. For each set of seven cores from a site, a testing plan was devised to test four cores for physical properties; the remainder were tested first in dynamic creep (discussed in Chapter 7), and then used in a recompaction study (discussed in Chapter 9).

An appropriate model for the factorial analysis would be:

$$Y_{ijkl} = \mu + T_i + B_j + TB_{ij} + W_k + TW_{ik} + BW_{jk} + TBW_{ijk} + \varepsilon_{(ijk)l} \qquad \text{......Equation 4.1}$$

Where

Y_{ijkl} = Dependant Variable (measured laboratory data)

μ = Common Effect

T_i = Truck Effect

B_j = Base Type

W_k = Wheel Path

$\varepsilon_{(ijk)l}$ = Error

Table 4.2 Layout Showing the Reduced Factorial Design

BASE TYPE	WHEELPATH	TRUCK TRAFFIC: HIGH				LOW			
		4 DISTRESSES*				4 DISTRESSES*			
FLEXIBLE	WP								
	BWP								
RIGID	WP								
	BWP								

Distresses: 1. ZERO 2. RUTTING 3. THERMAL CRACKING 4. STRIPPING

The EMS table for this analysis is shown in Table 4.3

Table 4.3 EMS Table for Factorial Design

EFFECTS	2	2	2	5	TESTS
	F	F	F	R	
	i	j	k	m	
T_i	0	2	2	5	$\sigma_\epsilon^2 + 20\ \sigma_T^2$
B_j	2	0	2	5	$\sigma_\epsilon^2 + 20\ \sigma_B^2$
W_k	2	2	0	5	$\sigma_\epsilon^2 + 20\ \sigma_W^2$
TB_{ij}	0	0	2	5	$\sigma_\epsilon^2 + 10\ \sigma_{TW}^2$
TW_{ik}	0	2	0	5	$\sigma_\epsilon^2 + 10\ \sigma_{TW}^2$
BW_{jk}	2	0	0	5	$\sigma_\epsilon^2 + 10\ \sigma_{BW}^2$
TBW_{ijk}	0	0	0	5	$\sigma_\epsilon^2 + 5\ \sigma_{TBW}^2$
$\varepsilon_{(ijk)l}$	1	1	1	1	σ_ϵ^2

An analysis was made using the SAS General Linear Model, GLM (Little et. al., 1991). GLM is capable of handling a data set with missing observations (unbalanced design of experiment).

4.4 Discriminant Analysis

In the analysis a multivariate statistical procedure known as discriminant analysis was performed on the laboratory data in order to identify the characteristic mixture group tending to cause a certain kind of distress. For example, a given bituminous mixture would develop a certain type of distress if it had a certain combination of mixture characteristics. The discriminant analysis would identify these critical mixture characteristics for each of the distresses studied, rutting, thermal cracking, stripping and no distress. The Mahalanobis Minimum Distant Method (Morrison, 1976) was used in the analysis. A prediction criteria was formed to characterize the distress potential of a given bituminous mixture based on its laboratory physical properties. This characterization could be possible before the mixture is placed in the field.

4.5 CP and Regression Procedures

The CP procedure (Little et. al., 1991) for determining the minimum number of variables needed to explain a regression was used in developing prediction equations between distress and mixture characteristics. The objective of the CP procedure is to analyze the entire data set and identify the minimum number of independent variables that would explain the dependant variable in a linear regression. The independent variables are the laboratory mixture characteristics such as dynamic modulus and kinematic viscosity, and the dependant variables are the measured distresses in the field such as rut depth and crack length. Once this objective is fulfilled, it is necessary to determine which mixture characteristics among the independent variables should be selected to fit into the distress model.

The Forward Stepwise Regression was used to determine the independent variables which are significant in affecting the measured variable at a given alpha value. These significant independent variables are then matched against the minimum number of variables from the CP procedure for constructing predictive models. Linear Regression was used to develop models to predict rutting, cracking and stripping.

CHAPTER 5 FIELD DATA COLLECTION AND PAVEMENT CONDITION SURVEY AND EVALUATION

5.1 Introduction

Identification of pavements with various distress types to satisfy the experimental design required a great deal of effort. An extensive search was made of all available data sources at Purdue University and at INDOT for candidate sections. Despite the extensive search to fulfill the requirements of the experimental design, there were cells that still could not be filled. However, sufficient cells were filled to enable an effective analysis to be carried out as will be shown in Chapters 6, 7 and 8.

5.2 Site Selection Method

Two main database sources were used in selecting candidate test highway sections. The first was the database developed by Lindly, 1987 and Pumphrey, 1989 which contained data on 1748 highway sections throughout the state of Indiana. Although the database did not yield many sections for this study it provided useful insight as to the criteria for selecting the rest of the test sections. The other important source was the Contract Proposals and Record of Construction at the INDOT Division of Research. These documents were the source for a majority of the test sections in the study. Also, these documents provided most of the information regarding the pavement sections such as binder and aggregate type, aggregate gradation, truck traffic, thickness, age and location. However, to ensure accuracy of these data a verification check was made at the INDOT Drawing Office. This office keeps details of all work on every highway section in Indiana. The information dates to the time the original pavement was laid out. This exercise proved useful as several sections did not match the records and they were eliminated from the study. New sections were found to replace them. The locations of the pavement sections sampled are shown in Figure 5.1.

5.2.1 Site Visit For Verification And New Test Sections

Apart from the two main data base sources, visiting the test sites which had been short-listed for the study was the most important step in verifying that what was described in the records matched with what was in the field. Several new sections were identified by field inspections to fill some of the remaining cells of the study. All sections are shown in Table 5.1. These cells represent unique pavement sections from which cores were obtained. These cores plus the pavement conditions are the main source of results presented in this report.

5.3 Field Sampling Procedure

Before pavement cores could be taken it was necessary to determine the quantity of material required for planned laboratory tests. The tests can be broadly divided into two categories, destructive testing and non-destructive testing.

Figure 5.1. Sampling Locations and North-South Dividing Line

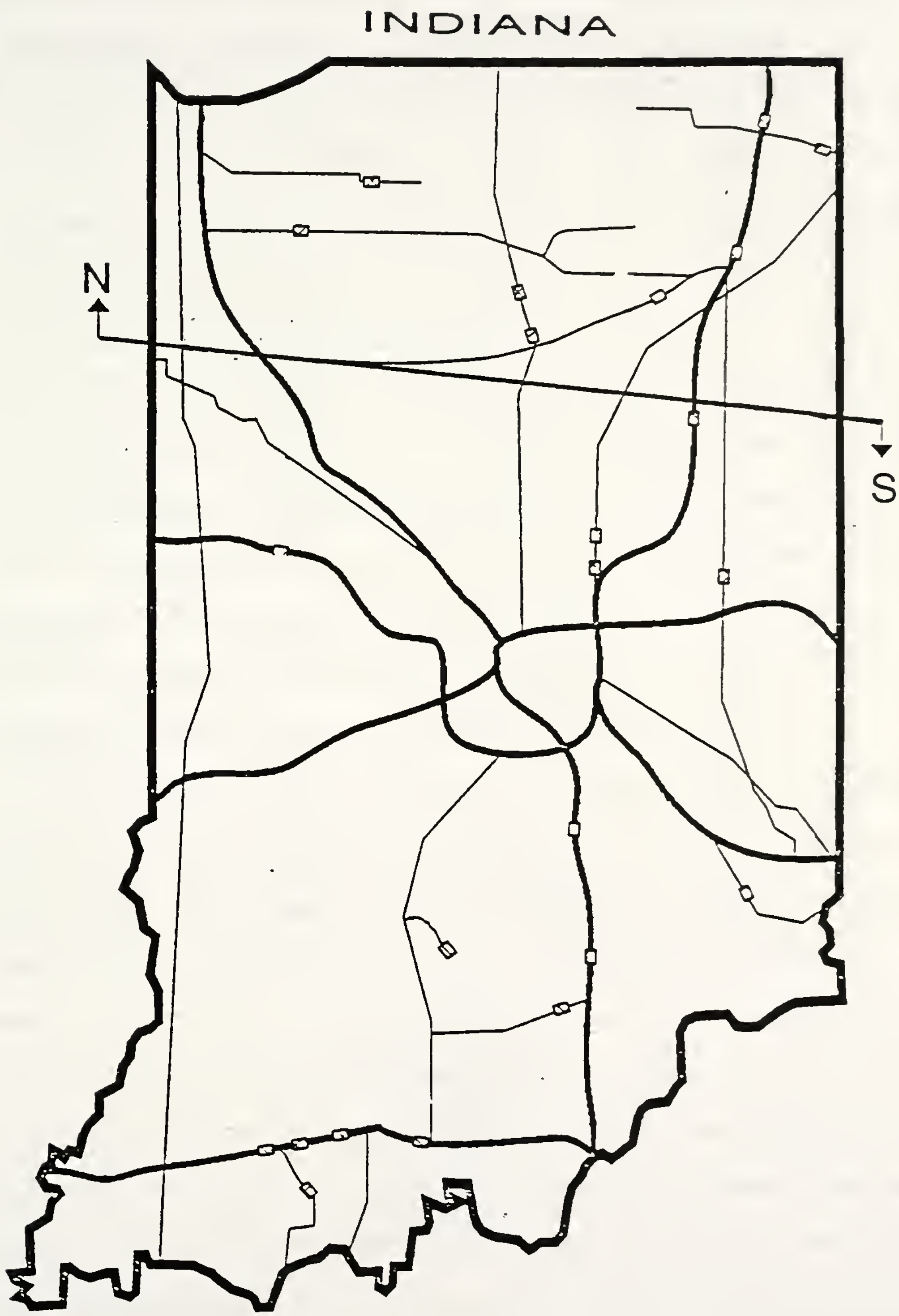

Table 5.1. Highway Pavements That Were Cored For Samples

SECTION #	DESCRIPTION (see below)	ROAD	CONTRACT #
1	Q H F C	SR 67	R-16912
2	Q H F U		
3	Q H R C	I 65	R-16963
4	Q H R U	I 65	R-17024
5	Q L F C	US 31	RS-16580
6	Q L F U	US 136	R-16885
7	Q L R C	US 41	RS-16690
8	Q L R U	US 41	RS-16692
9	NQ H F C	US 41	R-16442
10	NQ H F U		
11	NQ H R C	US 41	R-16685
12	NQ H R U		
13	NQ L F C	SR 38	RS-16667
14	NQ L F U	SR 1	RS-16080
15	NQ L R C	SR 18	R-15995
16	NQ L R U	SR 1	RS-16263

Q- QA
NQ- NON-QA
L- LOW
H- HIGH
F- FLEXIBLE
R- RIGID
C- CRUSHED
U- UNCRUSHED

The former includes laboratory tests on field cores, discussed in Chapter 6. The latter tests include dynamic creep testing.

5.3.1 Sample Requirement For Laboratory Testing

In order to determine the minimum number of samples required, 48 field cores were taken from a bituminous overlay on the east bound driving lanes of Indiana Interstate 74 between mileposts 10 and 16. The cores were taken in four sets (at four different subsection locations) of twelve cores within a 5.4 mile section. Within each subsection the spacing between cores was 100 feet. Of the twelve cores in a set, six were taken from the wheel path and six from between the wheel path. Tests conducted on the cores included bulk specific gravity (ASTM D-2726), Marshall stability (D-1559), Rice specific gravity (ASTM 2041), extraction (ASTM D-2172), Abson recovery (ASTM 1856) and penetration (ASTM D-5).

A statistical analysis was made as shown in Appendix B to determine the minimum number of samples required for a test. The test result most readily available and which was used in the analysis was the bulk specific gravity. These results could also be used to investigate the core homogeneity to determine if they are similar or different. By setting the α and β error at 10% it was found that the number of cores required was between 10 and 11 for every pavement subsection, half of the cores from the wheel path and the other half from between the wheel path. Thus since seven cores were needed to provide adequate material for planned tests, a decision was made to take seven each for in and between the wheel path.

The analysis also showed that the effect of location was insignificant, i.e. the cores were from the same population or batch. This means that the location of the cores within the test section does not matter. This result is important because it allows greater flexibility in sampling.

5.3.2 Sample Requirements For Dynamic Creep

The proposed ASTM method for conducting static creep test recommends the use of 3 cores for laboratory fabricated samples and 6 cores for field samples. There is no standard test method for conducting dynamic creep test. The recommendations of six field cores for static creep tests presumably resulted from assumptions of inherent variability in the field. However it has been quantitatively proven in Section 5.3.1 that field cores for a pavement section are relatively homogeneous. As a result, only 3 cores were tested for dynamic creep.

5.3.3 Field Sampling

The total number of wheel path core samples per section in this study is 14 (7 * 2 wheel paths). The total number of cores for the whole study for the number of cells filled in the Design of Experiment, Table 5.1, is 434. However, additional samples were taken to serve as backup should any cores be damaged. Cores were obtained from the field by INDOT District personnel. Highway sections cored are shown in Figure 5.1 and in Appendix C. Each section was visited and marked with yellow paint, and visited again after coring for verification.

5.3.4 Sample Coding System

A simple coding procedure was employed to mark and identify the samples. Each pavement core was sliced into layers namely surface, binder and base as shown in Figure 5.2. The coding scheme followed a numbering sequence shown in Table 5.2. The design of experiment table was divided into major cells and minor cells. Each major cell was numbered 1 - 8 and then sub-divided into 4 cells each for the 4 distress types considered in the study. This results in 32 minor cells or treatment combinations, each representing a highway section to be cored. From each section fourteen cores were taken, seven from the wheel path and seven from between the path. The cores were numbered 1 - 7 in sequence for wheel path and 8 - 14 for between the wheel path. To uniquely identify a particular core, a three digit numbering scheme was devised, where the first digit indicates the major cell of the experimental design table, the second digit indicates distress type between 1 - 4 and the last digit is the core number 1 - 14. A core bearing the number 326 for example represents a pavement with high truck traffic and from a flexible overlay on a rigid pavement having rutting distress.

Layer designation was made by assigning A for surface, B for binder and C for base. A schematic layout of a typically sliced and coded core is shown in Figure 5.2. This method of identification reduced confusion and unnecessary sorting

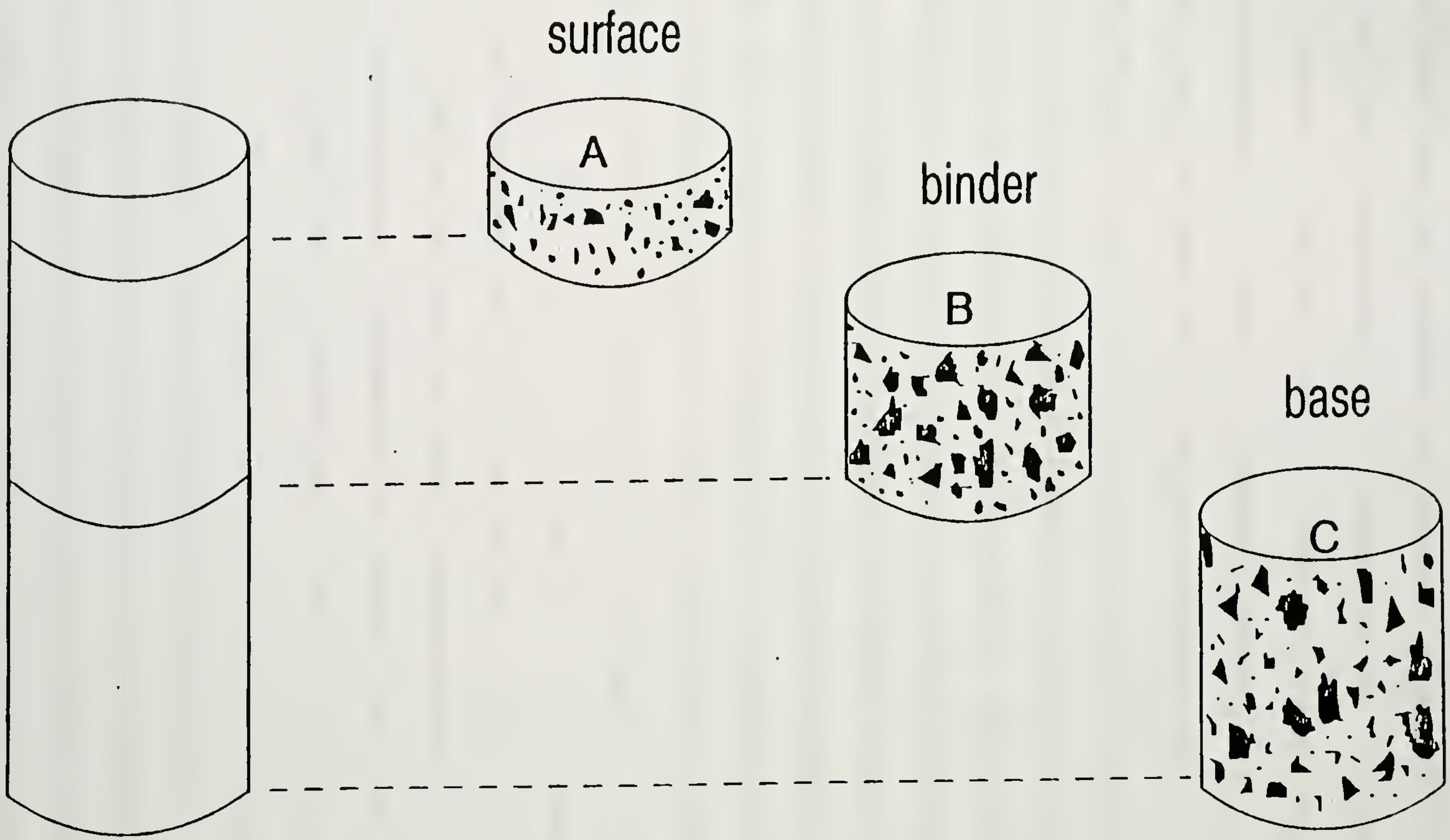

Figure 5.2. Typical Field Core Shown Sliced Into Component Layers

Table 5.2. Coding Scheme Used In Study

<table>
<tr><th colspan="2">TRUCK TRAFFIC</th><th colspan="4">HIGH</th><th colspan="4">LOW</th><th colspan="4">HIGH</th><th colspan="4">LOW</th></tr>
<tr><th>BASE TYPE</th><th>WHEELPATH</th><th>1</th><th>2</th><th>3</th><th>4</th><th>1</th><th>2</th><th>3</th><th>4</th><th>1</th><th>2</th><th>3</th><th>4</th><th>1</th><th>2</th><th>3</th><th>4</th></tr>
<tr><td rowspan="2">FLEXIBLE</td><td>WP</td><td></td><td colspan="2" rowspan="2">1</td><td></td><td></td><td colspan="2" rowspan="2">2</td><td></td><td></td><td colspan="2" rowspan="2">5</td><td></td><td></td><td colspan="2" rowspan="2">6</td><td></td></tr>
<tr><td>BWP</td><td></td><td></td><td></td><td></td><td></td><td></td><td></td><td></td></tr>
<tr><td rowspan="2">RIGID</td><td>WP</td><td></td><td colspan="2" rowspan="2">3</td><td></td><td></td><td colspan="2" rowspan="2">4</td><td></td><td></td><td colspan="2" rowspan="2">7</td><td></td><td></td><td colspan="2" rowspan="2">8</td><td></td></tr>
<tr><td>BWP</td><td></td><td></td><td></td><td></td><td></td><td></td><td></td><td></td></tr>
</table>

Distresses: 1. ZERO 3. THERMAL CRACKING
2. RUTTING 4. STRIPPING

between the various layers of each core once they were separated.

5.4 Pavement Condition Survey And Evaluation

The pavement condition survey carried out on all the test sections in this study employed the Paver (Department of the Army, 1982) method. It is a quantitative method of assigning a condition index (PCI) to a pavement that has qualitative distress.

The purpose of doing this survey is to obtain an index of the pavement condition and evaluate how that index corresponded to the other test parameters such as physical and material properties of the pavement mixture and age. The PCI values have served to indicate pavement performance [Lindly and White, 1988, and Badaruddin and McDaniel, 1992].

In this study, the cores were taken from uniquely identified test sections that exhibited the worst distress. As such the condition survey was conducted only within that one test section. Thus no averaging of the PCI values as is done when multiple samples are obtained from a pavement. So the condition index values shown in Appendix B represent results from a modified survey where only one section was surveyed.

The samples were stored in controlled laboratory conditions with room temperature not exceeding 70 degrees fahrenheit until needed for testing.

CHAPTER 6. LABORATORY ANALYSIS OF FIELD CORES

6.1 Introduction

Cores obtained from the field were tested to determine their physical as well as material properties. Each layer of the core as shown in the Chapter 5, Figure 5.2, were laid out individually. The surface layer which is largely a wearing course or sand mix was not tested because in most of the cores it's thickness was no more than half an inch. The binder layers were tested for all the cores. The surface and base layers (where applicable) were not used in this study.

6.2 Testing Procedure

Testing was intended to determine the physical as well as material properties of the cores. All physical testing was completed before destructive testing for component material properties was initiated.

6.2.1 Test Methods

After the cores were weighed and height measured, the following tests were carried out:

Bulk Specific Gravity (ASTM D-2726)

Marshall Stability and Flow (ASTM D-1559)

Maximum (Rice) Specific Gravity (ASTM D-2041)

Air Void Content (ASTM D-3203)

Extraction of Asphalt from Mixture (ASTM D-2171)

Abson Recovery (ASTM D-1856)

Penetration (ASTM D-5)

Absolute Viscosity (ASTM D-2171)

Kinematic Viscosity (ASTM D-2170)

Gradation of Aggregate (ASTM C-136)

The bulk specific gravity was conducted on each of the seven core samples from the wheel path. A schematic showing the entire test procedure on a set of field cores is given in Figure 6.1. The cores were then divided into two groups of four and three. The group containing four cores were analyzed by the test methods listed above. The remaining three cores were reserved for dynamic creep testing described in Chapter 7. Marshall stability and flow were determined for each of the four cores. These cores were then heated in a oven at 140°F and broken down so that they could be formed into two groups. The mixture was visually inspected and all aggregates with cut face(s) from coring or sawing were removed.

Aggregates with cut face(s) were removed in order to remove bias when determining the asphalt content as well as gradation of the recovered aggregate. When the aggregates with cut faces were not removed, the percent recovered asphalt content was lower than when they were removed. The reverse was true for the maximum specific gravity.

The maximum (Rice) specific gravity was then determined for the two groups. They were then placed separately in an oven at 140° F until completely dried. The asphalt binder was extracted and recovered using the rotorex and Abson Recovery methods, respectively. For each of the two groups above, two ointment cans of asphalt was recovered. Thus for each set of seven cores, four cores were tested to yield four Marshall

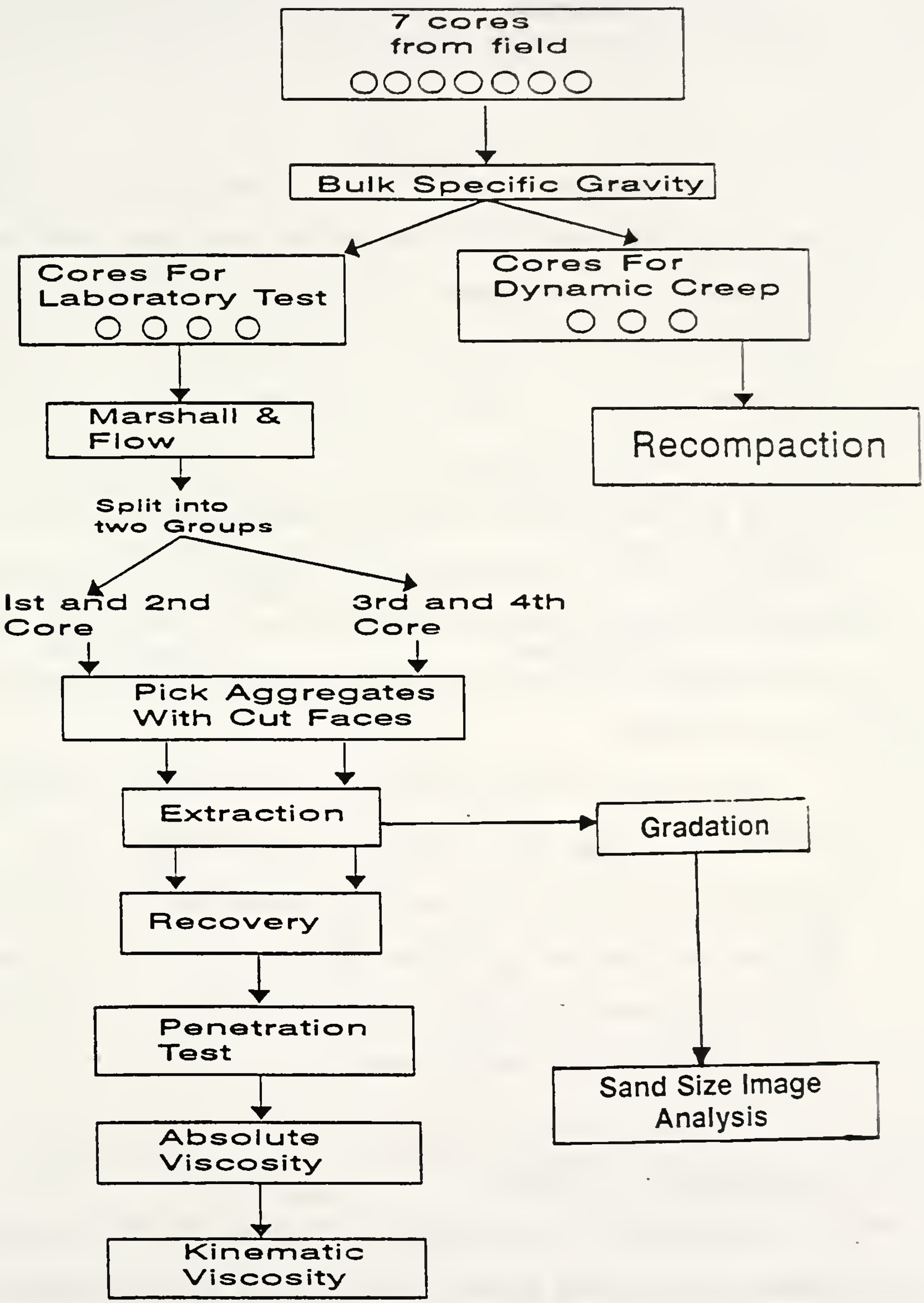

Figure 6.1. Schematic Layout for Testing in the Laboratory

stabilities and flow, two maximum (Rice) specific gravities, two asphalt contents and four ointment cans of recovered asphalt.

6.2.2 Data

Data generated from the tests were systematically recorded. The complete data set is combined together as shown in Appendix C. The data is arranged according to distress. There are some empty cells in the design of experiment where pavement sites could not be located. Also, in some cases the result is missing because no test was carried due to thin, broken or completely stripped sample. For example, no Marshall stability could be conducted on samples thinner than one inch. Similarly, some samples were broken at the time of sampling and neither bulk specific gravity nor Marshall stability could be determined.

The core coding system identifies the pavement, sample location, layer and design of experiment cell. Details regarding the coding scheme was presented in Chapter 5. A list showing the key to the abbreviations used in the data table is given in Appendix C. This data will be used in Chapters 7 and 8 for analysis and evaluation.

6.3 Gradation Analysis

Aggregates from cores in the wheel path and between the wheel path groups were combined into their respective group. The gradations of these combined samples were then determined and compared against construction specifications. Plots of the gradations are given in Figures 6.2 to 6.4. Gradations

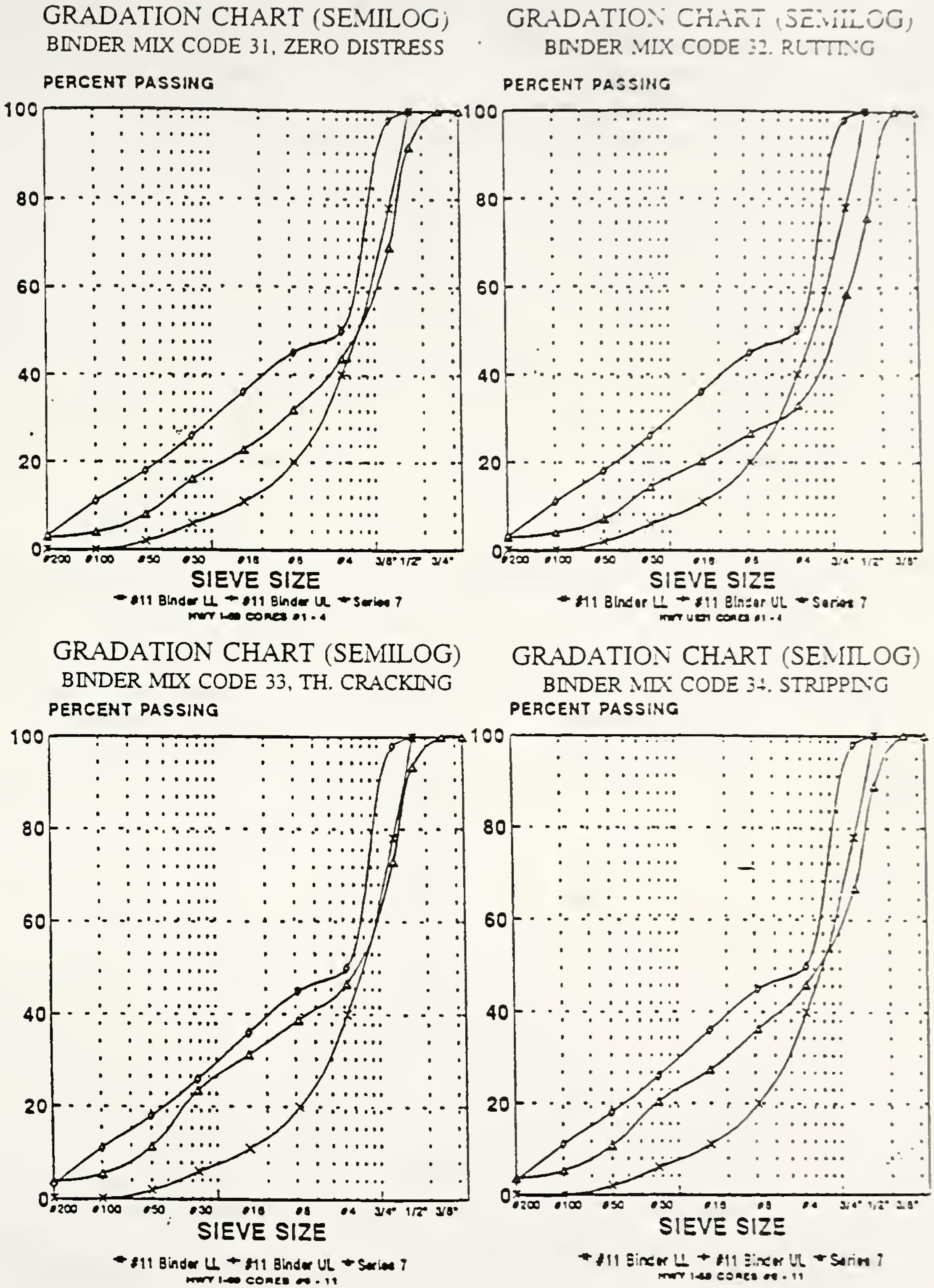

Figure 6.2. Gradation of Recovered Aggregate From Pavements With High Truck Traffic and Rigid Base

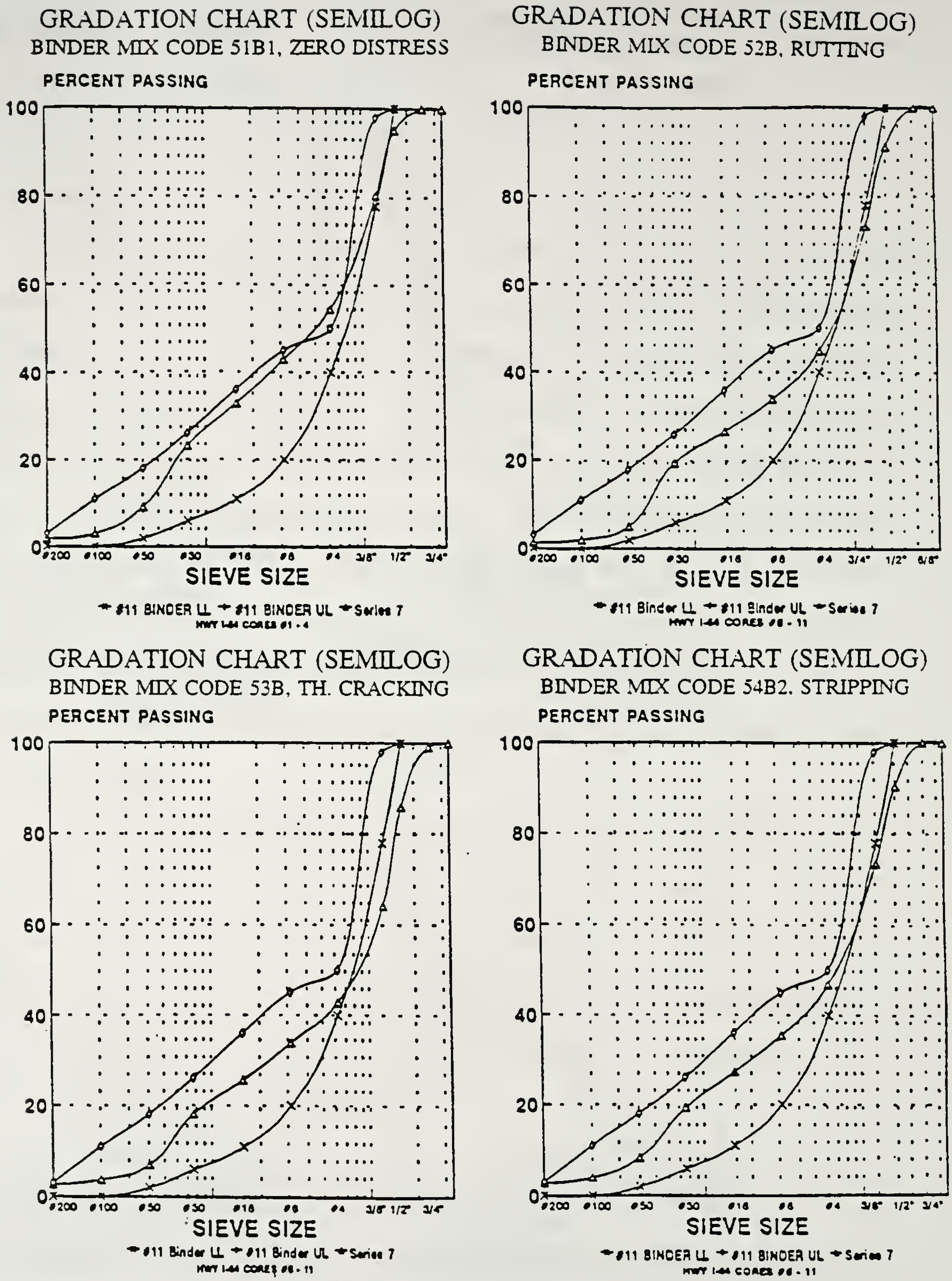

Figure 6.3. Gradation of Recovered Aggregate From Full Depth Bituminous Pavements With High Truck Traffic

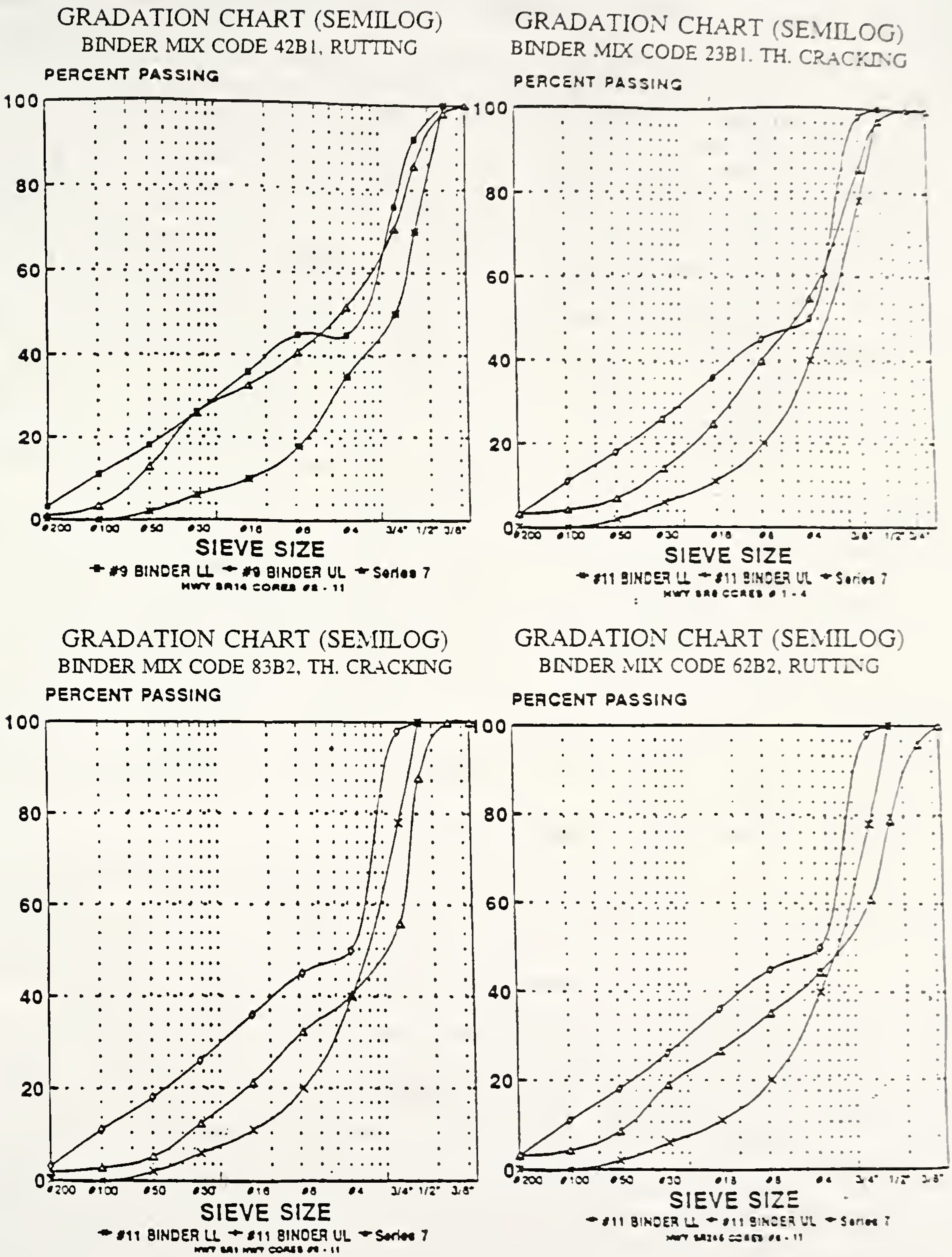

Figure 6.4. Gradation of Recovered Aggregate From Bituminous Pavements With Low Truck Traffic

generally fall within the limits of the Indiana Specification, INDOT, 1988, except at the coarser end where it appears that the recovered gradation has larger top size aggregates. This could be attributed to inaccuracies during mix proportioning in the field where the aggregate sieves are not as precise as those in the laboratory. However, more importantly, the recovered gradation of the finer sizes (minus #4 sieve and smaller) all fell within the specification limits. This shows for the pavements studied, minimal fracturing of the aggregates under traffic load. Consequently, the hardness of the aggregate in combination with the aggregate matrix determined by the gradation are adequate to withstand processing and traffic imposed loads. Figure 6.2 shows gradations of samples from high volume truck traffic pavements on rigid bases. In this figure the zero distress pavement has a gradation approximating the specification limits. However, the rutted section departs from the specification limits and shows a gap grading trend.

Figure 6.3 shows gradations for full depth flexible pavements with high truck traffic. The characteristic of the plots are the same as in Figure 6.2 with no apparent secondary crushing of the aggregates under traffic loading. Figure 6.4 shows gradations of aggregates from pavements with low truck traffic, the pavements consisting of full depth as well as flexible overlays on rigid bases. There is no definite trend in the gradation of these low truck trafficked pavements.

CHAPTER 7 DYNAMIC CREEP TESTING OF FIELD CORES TO EVALUATE PAVEMENT CHARACTERISTICS

7.1 Introduction

Dynamic creep or repeated loading tests have been shown to identify mixtures that are stable from those that have a potential to rut (Valkering et al., 1990). The various dynamic creep methods that are used show some degree of correlation between laboratory prediction and field measurement. However, the variations between test procedures make the result suitable only for those test conditions. A general test procedure for dynamic creep is yet to be formulated.

In this study, a dynamic creep test was used to evaluate samples from in service pavements. In particular, the dynamic modulus, phase angle, test temperature effect, and loading frequency effect were investigated. Tests were conducted on 4 inch diameter field cores at temperatures of 20, 30 and 40 degrees centigrade, and at three loading frequencies of 1, 4 and 8 cycles per second. The loading frequencies simulate vehicle speeds of about 4, 17 and 33 miles per hour (Yeager and Wood, 1974), assuming a tire with an inflation pressure of 100 psi moving at 55 miles per hour.

Although the ideal setup would be to simulate field loading conditions in terms of load magnitude and frequency, it was not feasible to do so because at temperatures over 30 degrees centigrade and stresses above 70 psi (880 pounds on 4" diameter cores) the test specimens failed prematurely. The testing frequency was limited by the resolution of the 2501 A-D Data Translation Board used to capture data from the LVDT

(Linear Variable Differential Transducer) that was used to measure sample deformation. This hardware could only handle test frequencies of up to 10 hertz without truncating the data.

7.2 Testing

Samples tested in dynamic creep were 4 inch diameter field cores that had been separated into their respective layers as described in Chapter 5. Only the binder layers were tested for dynamic creep. The ends of the cylindrical cores were capped using a sulphur capping compound that produced smooth ended surfaces as shown in Figure 7.1. A special device shown in Figure 7.2 was used to complement the standard capping equipment in order to obtain perpendicularity of the capped ends with respect to the cylindrical axis of the core.

Deformation was measured using a set of LVDT's mounted in holders shown in Figures 7.3 and 7.4. These holders were clamped in place with elastic bands. A vertical section through a sample ready for testing is shown in Figure 7.5. Care was required to insure the holders were stable because of the LVDT's sensitivity. The top loading platen was held up by a set of three springs with the platen resting on a metal ball to permit it to rotate and seat uniformly on top of the sample during testing.

Prior to testing the samples were conditioned for each test temperature for at least 24 hours inside a temperature control chamber.

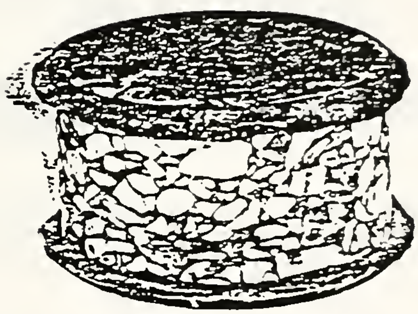

Figure 7.1. Typical Capped Sample Ready For Testing

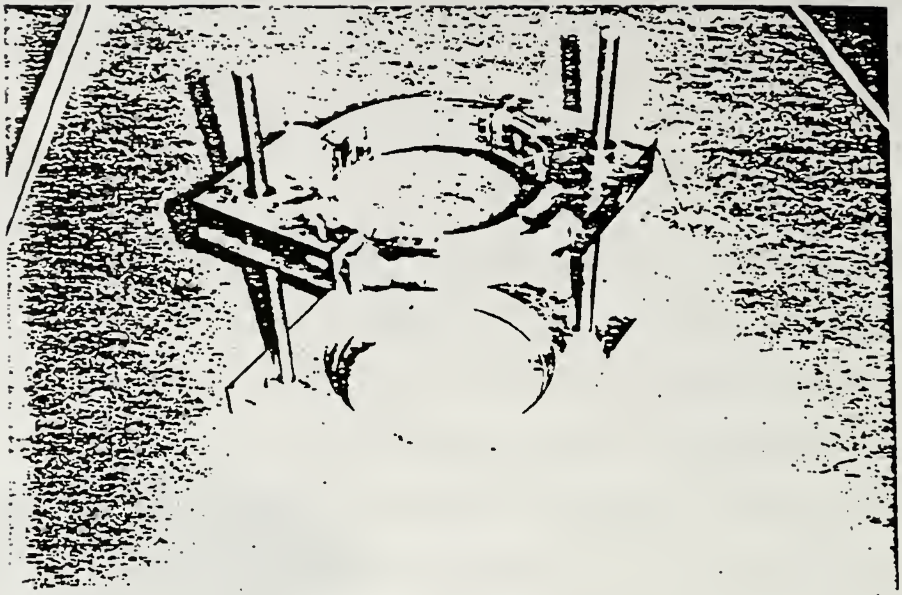

Figure 7.2. Capping Devices To Ensure Perpendicularity

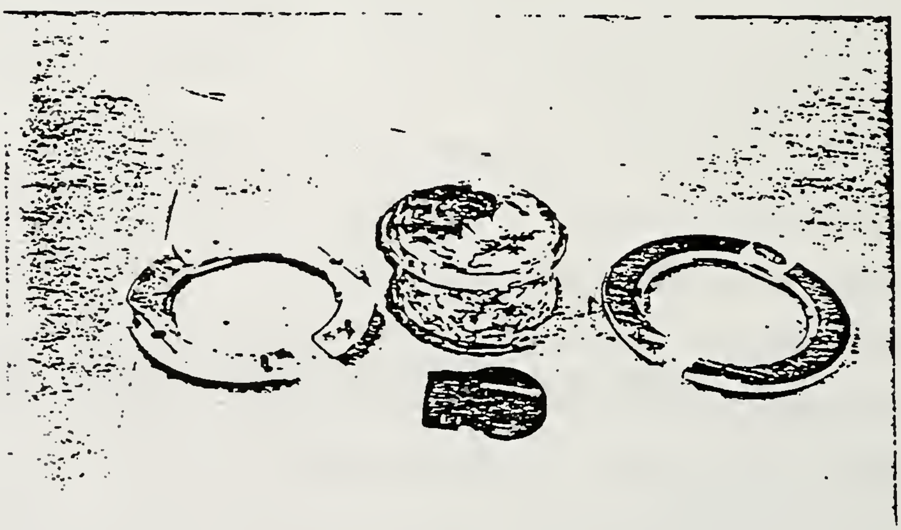

Figure 7.3. Custom Designed LVDT Holders

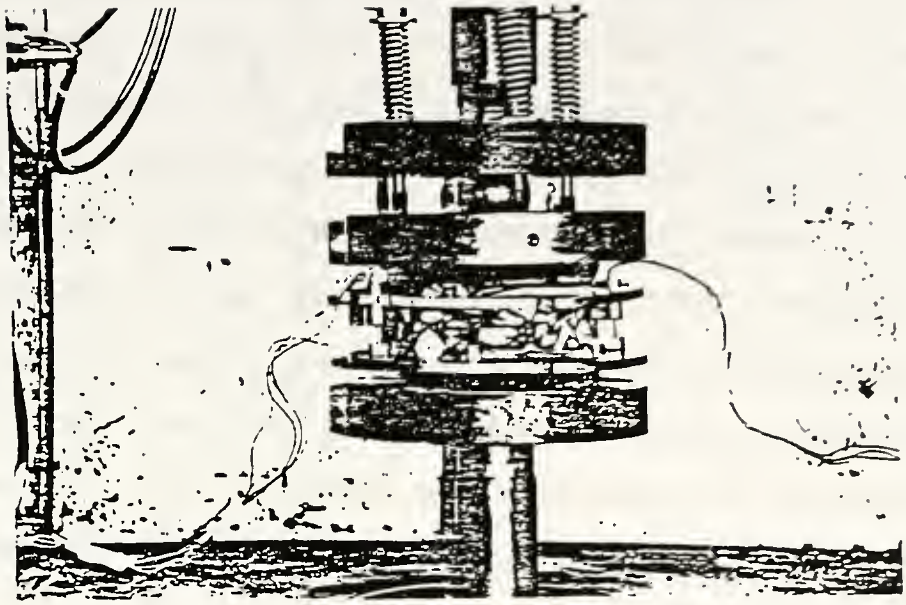

Figure 7.4. Sample With Attached LVDTs Ready for Testing

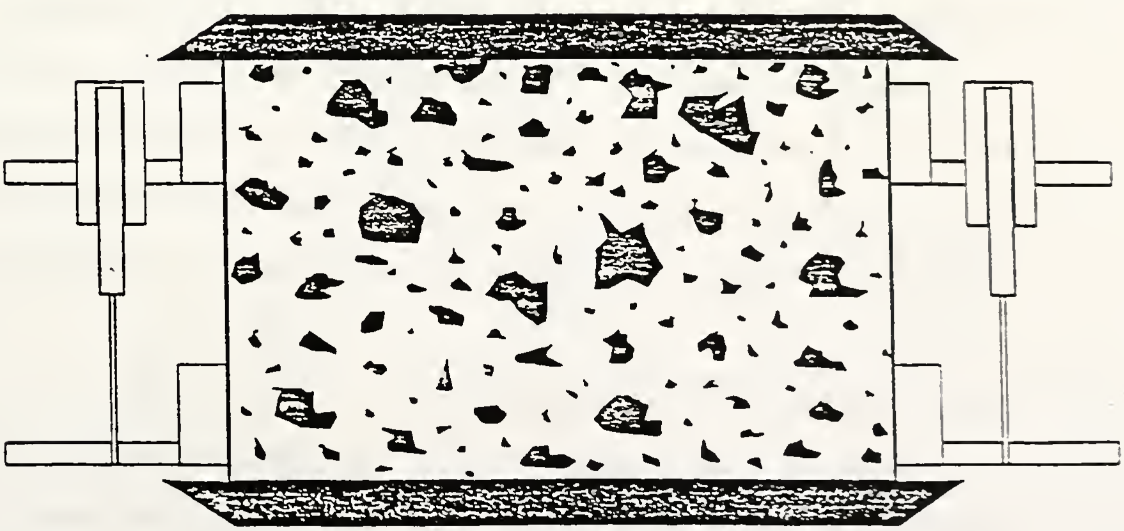

Figure 7.5. Section Showing Core Sample Ready for Dynamic Creep Testing

In the dynamic creep testing each sample was tested at three temperatures (20, 30 and 40 degrees centigrade) and three frequencies (1, 4, and 8 cycles per second). As a result, each sample was tested nine times. It has been shown that applying repeated, short duration dynamic loading on the same sample does not affect subsequent test results (Soussa, 1987). Seven field cores were available for testing from each location. Four of the cores were tested for their physical properties as described in Chapter 6 and the remaining three were reserved for dynamic creep testing. Some of the cores reserved for dynamic creep were too thin and could not be tested. As a result, testing was done on available cores as shown in Table 7.1.

7.2.1 Test Limitations

In the dynamic creep test, the sample is subjected to a dynamic, periodic loading. In the field, the pavement section is loaded intermittently depending upon the rate of truck arrival. Also, in the field the loaded section is confined by an all around continuous medium of asphalt concrete while in this study testing was carried out on an unconfined core.

7.2.3 Dynamic Testing Procedure

Testing was carried out using a Model 483.01 MTS servo controller and function generator. A haversine loading function was used to ensure that there was always a contact load for the entire loading and unloading period. A contact preload of about 20 pounds was applied at the 20 and 30

Table 7.1. Layout Showing Core Samples Used For Dynamic Creep

CLIMATE		NORTH								SOUTH							
TRUCK TRAFFIC		HIGH				LOW				HIGH				LOW			
BASE TYPE	WHEELPATH	ZERO	RUT	STRIP	T.CR.	ZERO	RUT	T.CR.	STRIP	ZERO	RUT	T.CR.	STRIP	ZERO	RUT	T.CR.	STRIP
FLEXIBLE	WP		121 125 126			216 217		235		514	527	535 537		6112 6114			
RIGID	BWP		325 326	335 336	345		4213			7112 7114	7213 7214		7413 7414	815 817	826 827	836 837	845 846

degree centigrade tests temperature while a 10 pound preload was used for the 40 degree centigrade test. Before starting the test, the LVDT voltage reading was zeroed using a hand-held digital volt meter. Configurations for data collection in each test involved setting the load duration, test frequency, data file name, and response display parameters in the Notebook software (LabTech Notebook, 1986). An internal verification test confirmed that all test and data acquisition parameters were compatible. This was important to ensure success of the test and data collection. An oscilloscope was connected to the output load function generator which recorded the haversine trace of the applied load. The oscilloscope provided a visual check of the test frequency.

Applied loads ranged between 400 to 700 pounds depending on test temperature and also on the sample response displayed on the computer monitor. For the 20 degree centigrade test temperature, the maximum applied load was 400 pounds for the 1 Hz test frequency; if the response exhibited a sinusoidal trace as shown in Figure 7.6, the test results were accepted. For flat or irregular traces the test was repeated by increasing the load in 100 pound increments. If the trace remained the same, the LVDT housing and holder assembly were dismantled and reassembled and the test repeated. This step was taken because preliminary testing indicated that when there was no free travel between the LVDT and its core, the deformation response would always be flat or damped.

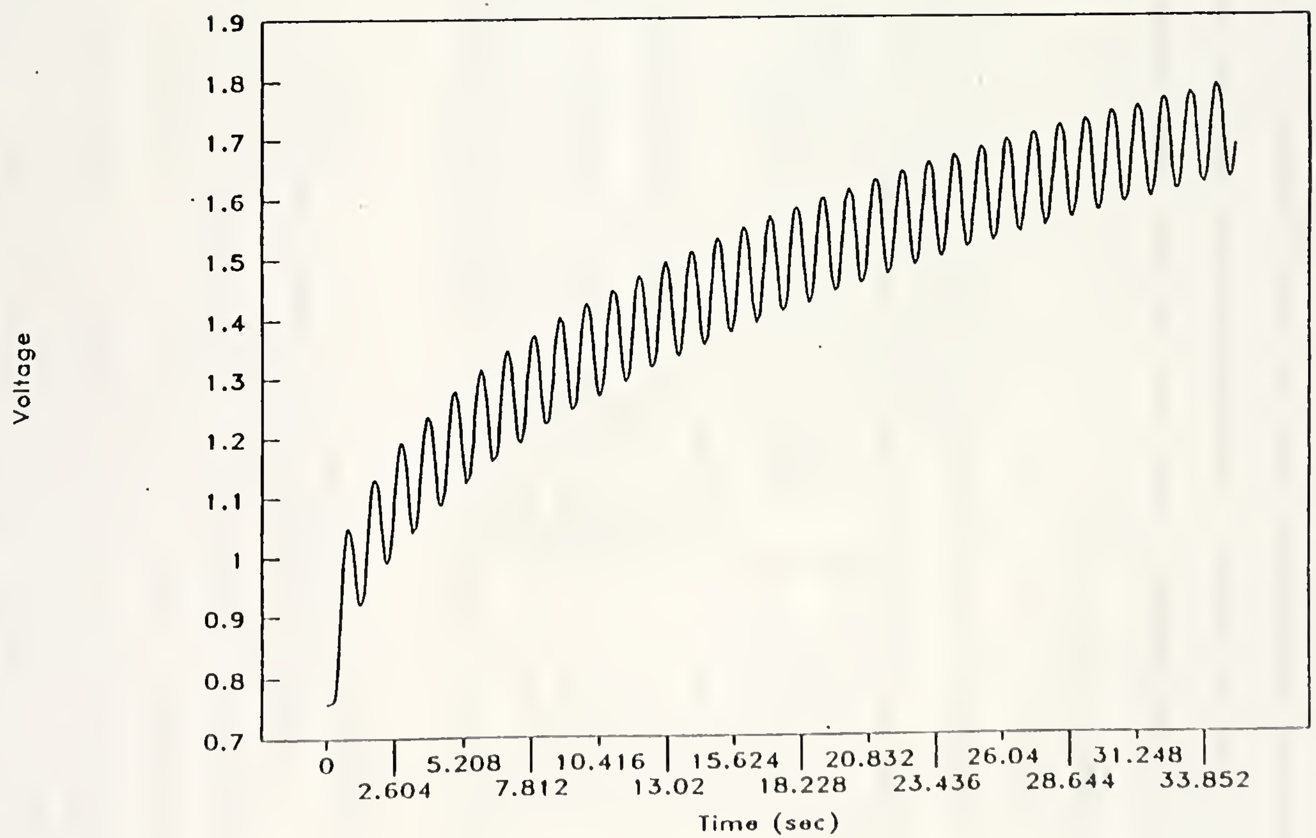

Figure 7.6. Typical Sample Response Display

The applied loads used for the various test temperatures and frequencies are shown in Table 7.2. Once testing at one frequency was completed, the test conditions were reset on the computer template for the next higher frequency without removing the sample from the test chamber or from the preload. As discussed above, repeating short duration dynamic tests on the same sample does not affect subsequent test results (Soussa et al., 1987).

Table 7.2. Preload And Test Load Values For Different Frequencies And Test Temperatures

TEMPERATURE ^{0}C (^{0}F)	LOAD (LBS)	FREQUENCY (Cycles per Second), Hz		
		1	4	8
20 (68)	PRELOAD TEST LOAD	20 400 - 600	20 500 - 700	20 600 - 700
30 (86)	PRE LOAD TEST LOAD	20 300 - 400	20 400 - 500	20 500 - 600
40 (104)	PRE LOAD TEST LOAD	10 150 - 250	10 200 - 300	10 200 - 300

7.3 Data

Dynamic response data were recorded via the two LVDT's attached to each side of the sample. This represented two independent sets of data for evaluating the dynamic characteristics for each sample at each loading condition. The dynamic load signal was also recorded on the same time base as the deformation response. The voltage outputs of the LVDTs measuring the sample response were recorded and stored in ASCII format. Due to the visco-elastic nature of the samples, the Nyquist theory suggests that data be acquired at a rate of at least twice the rate of load excitation to avoid signal interference (Labtech Notebook Manual, 1986). Two sampling rates were used in this study; a sampling rate of 10 per second was used for the 1 and 4 Hz loading while 20 per second was used for the 8 Hz loading.

A replicate sample was tested in several cells, where samples were available, as shown in Table 7.1. Since the samples in each cell were taken from the same stretch of highway, and it has been shown in Chapter 5 that there is no significant difference between such samples, the results from the two samples can be pooled when appropriate. As a result, a better measure of the error term is provided.

7.3.1 Data Handling

Data gathered from each test were in the form of voltage and had to be converted into deformation and load according to the following factors:

LVDT #1	1"	= 996.364 Volts
LDVT #2	1"	= 985.909 Volts
LOAD	100 lbs.	= 1 Volt

A least squares method was used to fit a sinusoidal curve to the data. The resulting function aided interpolation and data analysis. Figure 7.6 shows the deformation amplitude of a sample under load in the thirty-five second loading period. This is the same display that was observed on the computer screen during testing. The curve fit program was tailored to use the last 60 data points (about 3 seconds per data point) of sample response. The peak deformation and load were converted to strain and stress on the basis of LVDT gage length and core loaded area. These peak values were used to compute dynamic modulus and determine the phase angle between load and deformation. A summary of the dynamic modulus and phase angle of the samples tested is given in Table 7.3.

7.4 Evaluation

Data from Table 7.3 was used to plot dynamic modulus for each distress type against frequency. The plots are shown in Figure 7.7. They are coded according to the cells in the design of experiment in Table 7.1. Two immediate trends that appear from these graphs are the positive slopes of each plot indicating higher dynamic modulus (E^*) values at higher frequencies, and lower E^* values at higher test temperatures. At 20 to 30 degrees centigrade the plots generally show a positive slope, but from 30 to 40 degrees centigrade the frequency effect tends to diminish. This can be attributed to the softening of the asphalt hence the increasing dominance of the viscous component where the sample response is delayed due to an increase in phase angle, ϕ. This increase in phase angle tends to nullify the effect of frequency, thus the drop in

Table 7.3. Summary of Dynamic Creep Data

Distress	Sample Number	Freq. Hz	Age Years	E @20C PSI	Ave. Phase Angle @20 C	E @30C PSI	Ave. Phase Angle @30 C	E @40C PSI	Ave. Phase Angle @40 C
	815	4	5	5.55E+06	27	3.42E+06	28	6.30E+05	*
	815	8	5	5.93E+06	27	4.54E+06	25	1.18E+06	26
	817	1	5	2.49E+06	30	1.27E+06	38	6.20E+05	*
	817	4	5	3.36E+06	19	2.50E+06	22	1.90E+06	26
	817	8	5	3640000	19	2950000	20	2330000	*
	235	1	9	1.28E+06	33	1.01E+06	36	2.60E+05	54
Thermal	235	4	9	1.65E+06	21	1.19E+06	21	7.80E+05	51
Cracking	235	8	9	1.69E+06	16	1.58E+06	17	9.73E+05	51
	335	1	11	2.83E+06	26	5.18E+05	38	5.12E+05	58
	335	4	11	3.91E+06	23	6.62E+05	30	5.46E+05	41
Thermal	335	8	11	5.20E+06	35	7.36E+05	40	6.53E+05	38
Cracking	336	1	11	5.40E+06	13	3.30E+06	18	1.40E+06	23
	336	4	11	9.20E+06	20	6.40E+06	26	1.26E+06	31
	336	8	11	1.15E+07	14	8.12E+06	27	1.76E+06	29
	535	1	15	5.38E+06	40	2.06E+06	44	7.24E+05	57
	535	4	15	9.15E+06	34	4.63E+06	23	9.81E+05	38
Thermal	535	8	15	1.41E+07	36	5.05E+06	19	1.34E+06	30
Cracking	537	1	15	2.50E+06	36	2.50E+06	*	9.00E+05	45
	537	4	15	4.52E+06	29	3.20E+06	*	1.17E+06	39
	537	8	15	5.75E+06	16	3.68E+06	*	1.16E+06	23
	836	1	12	2.80E+05	31	1.31E+05	32	7.34E+04	33
	836	4	12	4.09E+05	28	1.93E+05	32	1.14E+05	30
	836	8	12	4.75E+05	*	2.28E+05	*	1.51E+05	22
Thermal	837	1	12	1.46E+07	26	1.67E+06	33	2.17E+05	34
Cracking	837	4	12	1.98E+07	16	4.24E+06	16	3.32E+05	32
	837	8	12	2.14E+07	*	7.62E+06	*	4.85E+05	26
	345	1	10	3.80E+06	37	2.50E+06	42	6.10E+05	47
Stripping	345	4	10	4.80E+06	36	3.20E+06	36	1.36E+06	41
	345	8	10	6.30E+06	21	3.61E+06	30	2.03E+06	33
	7413	1	12	2.22E+05	31	1.30E+05	45	3.20E+05	57
	7413	4	12	3.87E+05	30	2.65E+05	31	3.40E+05	43
Stripping	7413	8	12	4.34E+05	31	8.50E+05	28	1.30E+06	33
	7414	1	12	2.18E+06	26	1.76E+05	40	1.96E+05	42
	7414	4	12	3.28E+06	20	4.69E+05	31	3.16E+05	33
	7414	8	12	3.73E+06	21	7.09E+05	24	4.95E+05	27
	846	1	10	4.36E+06	14	1.97E+06	21	5.29E+05	*
	846	4	10	4.95E+06	*	2.10E+06	17	6.75E+05	26
Stripping	846	8	10	5.10E+06	8	2.30E+06	17	7.56E+05	18
	847	1	10	3.47E+06	21	2.06E+06	22	1.64E+06	28
	847	4	10	4.93E+06	17	2.76E+06	20	1.70E+06	27
	847	8	10	6.59E+06	*	3.05E+06	13	2.80E+06	22

* Not Available

Table 7.3 Continued

Distress	Sample Number	Freq. Hz	Age Years	E @20C PSI	Ave. Phase Angle @20 C	E @30C PSI	Ave. Phase Angle @30 C	E @40C PSI	Ave. Phase Angle @40 C
	121	1	15	1.49E+06	29	4.34E+05	32	1.71E+05	49
	121	4	15	1.88E+06	22	6.87E+05	28	4.64E+05	36
	121	8	15	2.17E+06	20	8.35E+05	19	6.16E+05	31
Rutting	125	1	15	2.50E+06	31	1.62E+06	33	3.20E+05	42
	125	4	15	3.40E+06	17	2.40E+06	22	5.86E+05	32
	125	8	15	3.50E+06	18	2.70E+06	18	7.14E+05	28
Rutting	527	1	14	3.13E+06	37	9.33E+05	38	6.58E+05	41
	527	4	14	3.24E+06	31	1.58E+06	32	1.44E+06	34
	527	8	14	4.03E+06	23	1.92E+06	24	1.45E+06	31
	326	1	15	2.39E+06	30	3.95E+05	45	1.76E+05	*
Rutting	326	4	15	2.53E+06	28	1.28E+06	29	9.90E+05	32
	326	8	15	2.64E+06	*	2.14E+06	22	9.90E+05	29
	7213	1	3	1.54E+06	*	1.03E+06	34	6.22E+05	50
Rutting	7213	4	3	2.34E+06	20	1.74E+06	22	6.30E+05	41
	7213	8	3	2.94E+06	*	2.22E+06	16	6.35E+05	38
	4213	1	12	1.92E+06	32	8.36E+05	41	5.29E+05	35
	4213	4	12	1.92E+06	23	1.00E+06	25	8.36E+05	32
	4213	8	12	1.92E+06	23	1.40E+06	25	1.06E+06	27
	826	1	9	2.93E+06	24	1.32E+06	28	4.57E+05	34
	826	4	9	3.80E+06	16	1.51E+06	20	6.78E+05	31
	826	8	9	4.52E+06	12	2.03E+06	12	8.11E+05	24
Rutting	827	1	9	5.50E+06	32	2.06E+06	33	1.50E+06	54
	827	4	9	5.60E+06	12	2.90E+06	27	1.45E+06	33
	827	8	9	5.70E+06	11	3.50E+06	*	1.53E+06	14
	216	1	16	4.22E+05	35	4.00E+05	36	1.62E+05	58
	216	4	16	1.13E+06	24	6.42E+05	32	2.55E+05	52
Control	216	8	16	2.43E+06	24	7.73E+05	31	3.38E+05	42
	217	1	16	7.55E+06	20	3.33E+06	59	2.70E+05	65
	217	4	16	9.68E+06	14	3.70E+06	27	7.80E+05	47
	217	8	16	1.15E+07	11	3.86E+06	16	1.30E+06	30
	6112	1	2	4.08E+06	34	2.30E+06	*	6.54E+04	44
	6112	4	2	4.50E+06	32	2.70E+06	33	1.30E+05	42
	6112	8	2	1.07E+07	*	5.06E+06	21	2.56E+05	39
	6114	1	2	3.31E+06	32	2.08E+06	34	1.97E+05	35
	6114	4	2	3.77E+06	12	2.41E+06	19	1.00E+06	34
Control	6114	8	2	4.38E+06	17	2.30E+06	14	1.05E+06	30
	7112	1	4	1.46E+06	24	5.20E+05	35	2.36E+05	45
	7112	4	4	2.02E+06	19	1.32E+06	23	4.32E+05	35
	7112	8	4	2.17E+06	*	1.61E+06	14	5.50E+05	27
	7114	1	4	1.75E+06	*	5.46E+05	31	6.32E+05	43
	7114	4	4	3.15E+06	30	1.04E+06	31	1.28E+06	*
	7114	8	4	3.36E+06	23	1.26E+06	27	1.94E+06	28
	815	1	5	4.13E+06	40	1.88E+06	47	4.74E+05	33

* Not Available

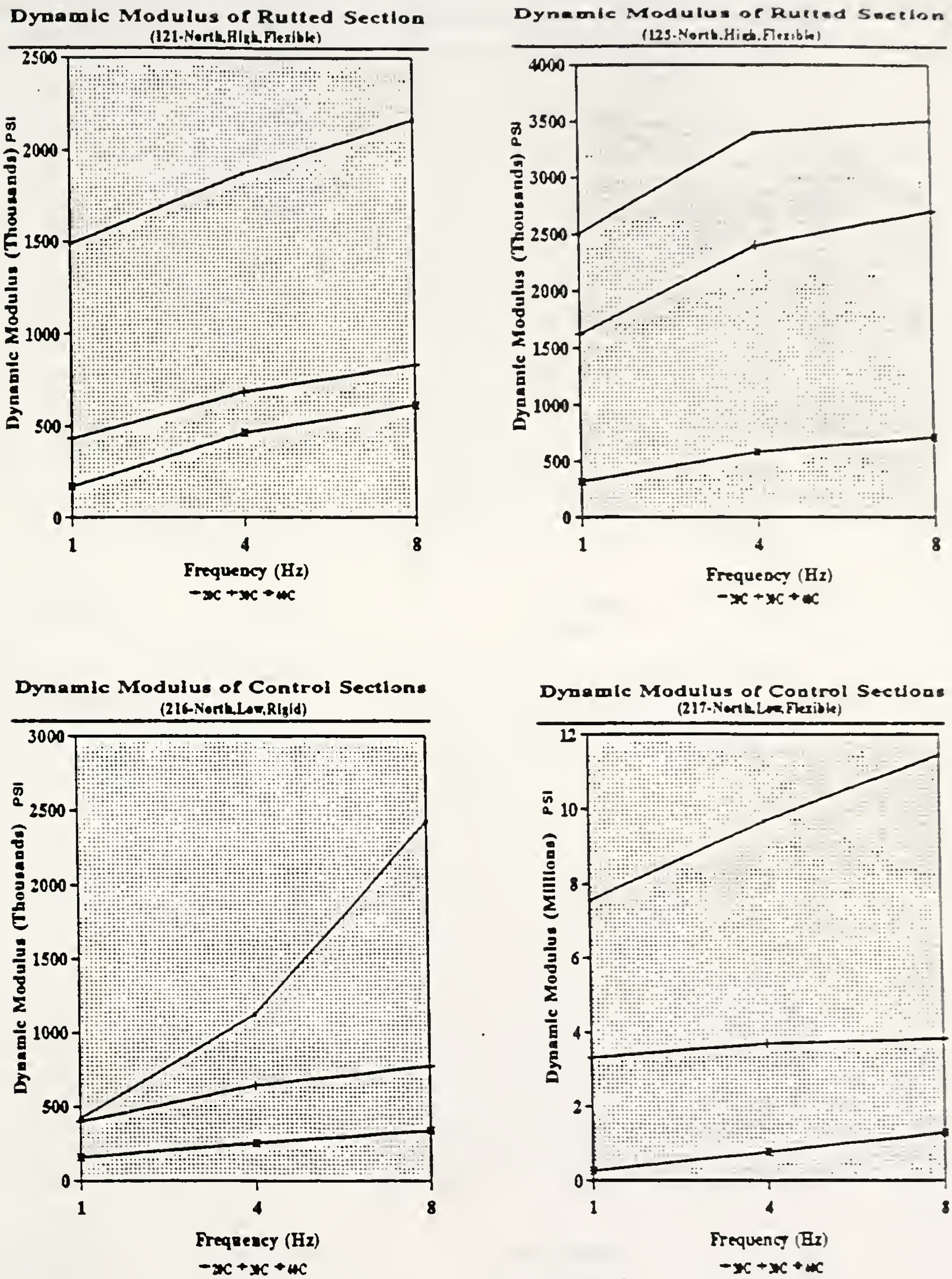

Figure 7.7. Dynamic Modulus Plots At Various Frequencies and Test Temperatures

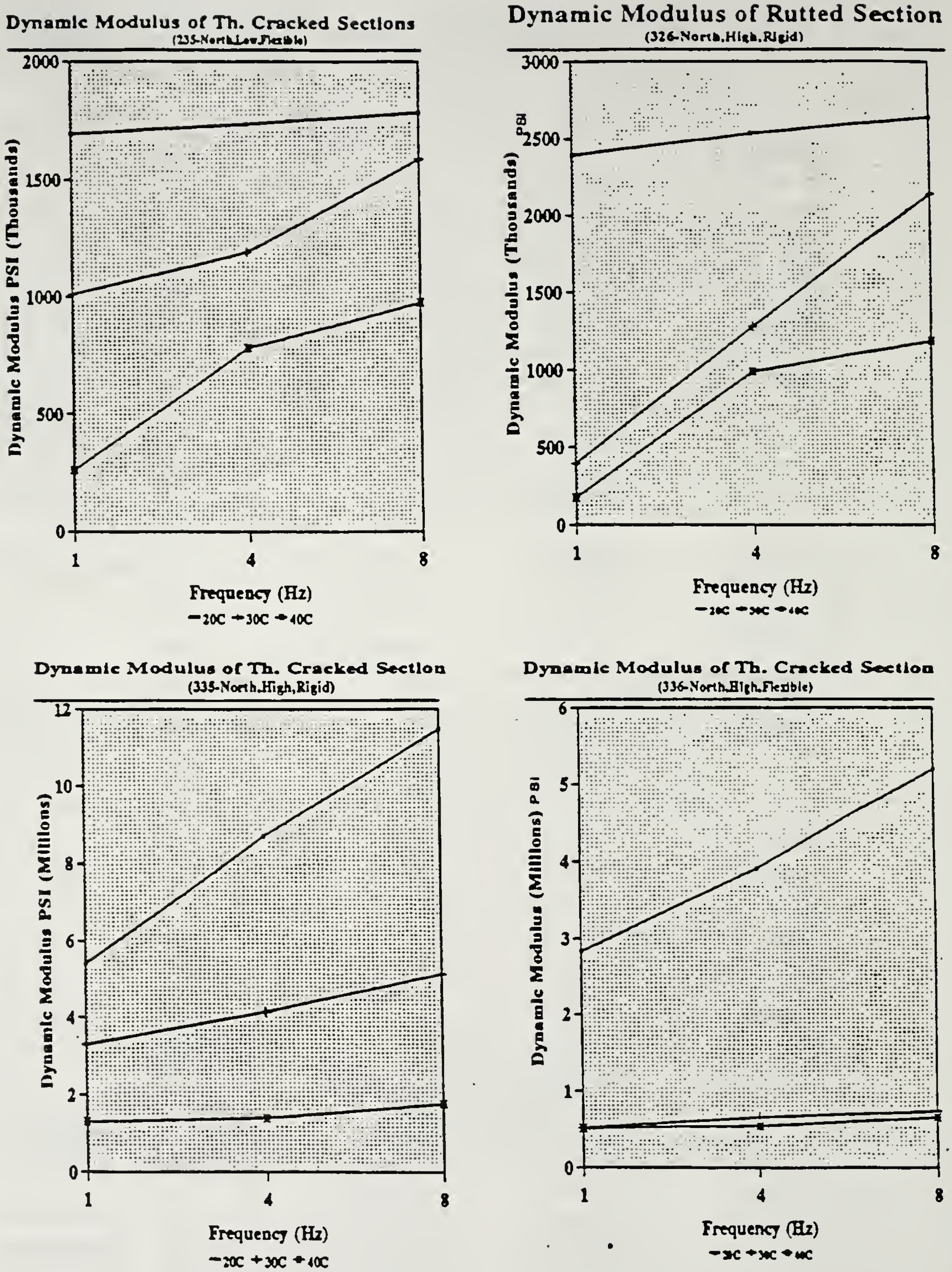

Figure 7.7. (continued)

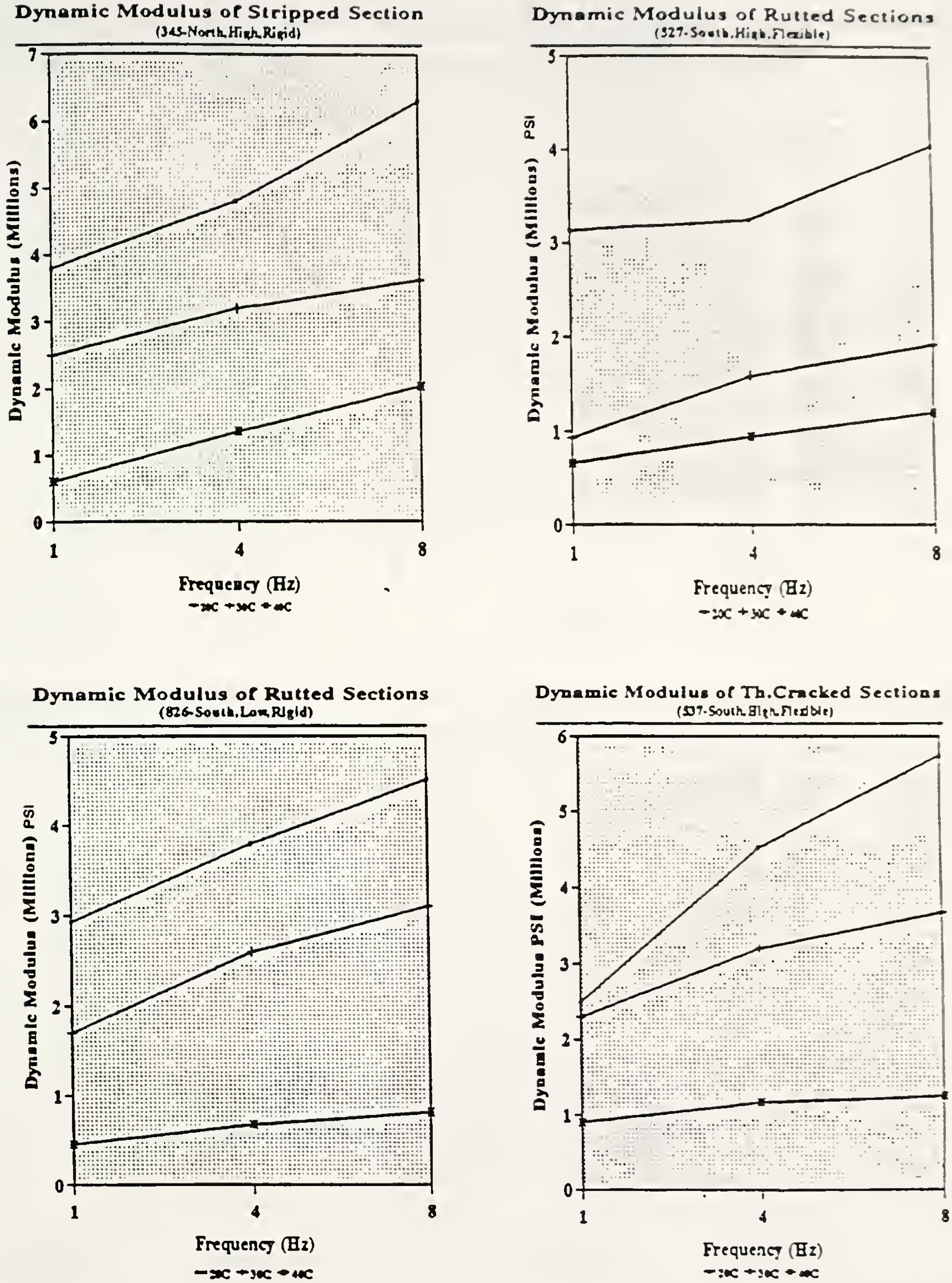

Figure 7.7. (continued)

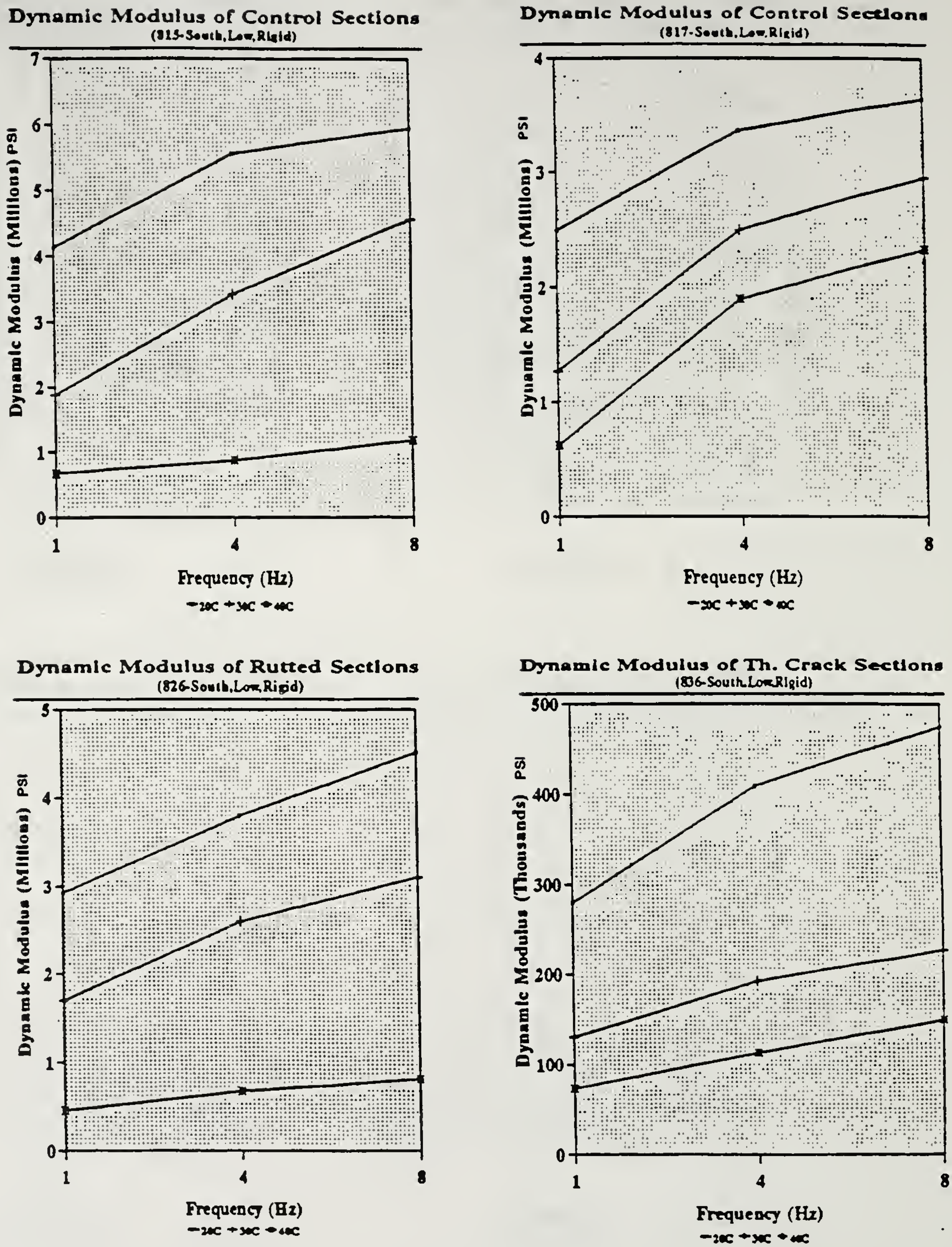

Figure 7.7. (continued)

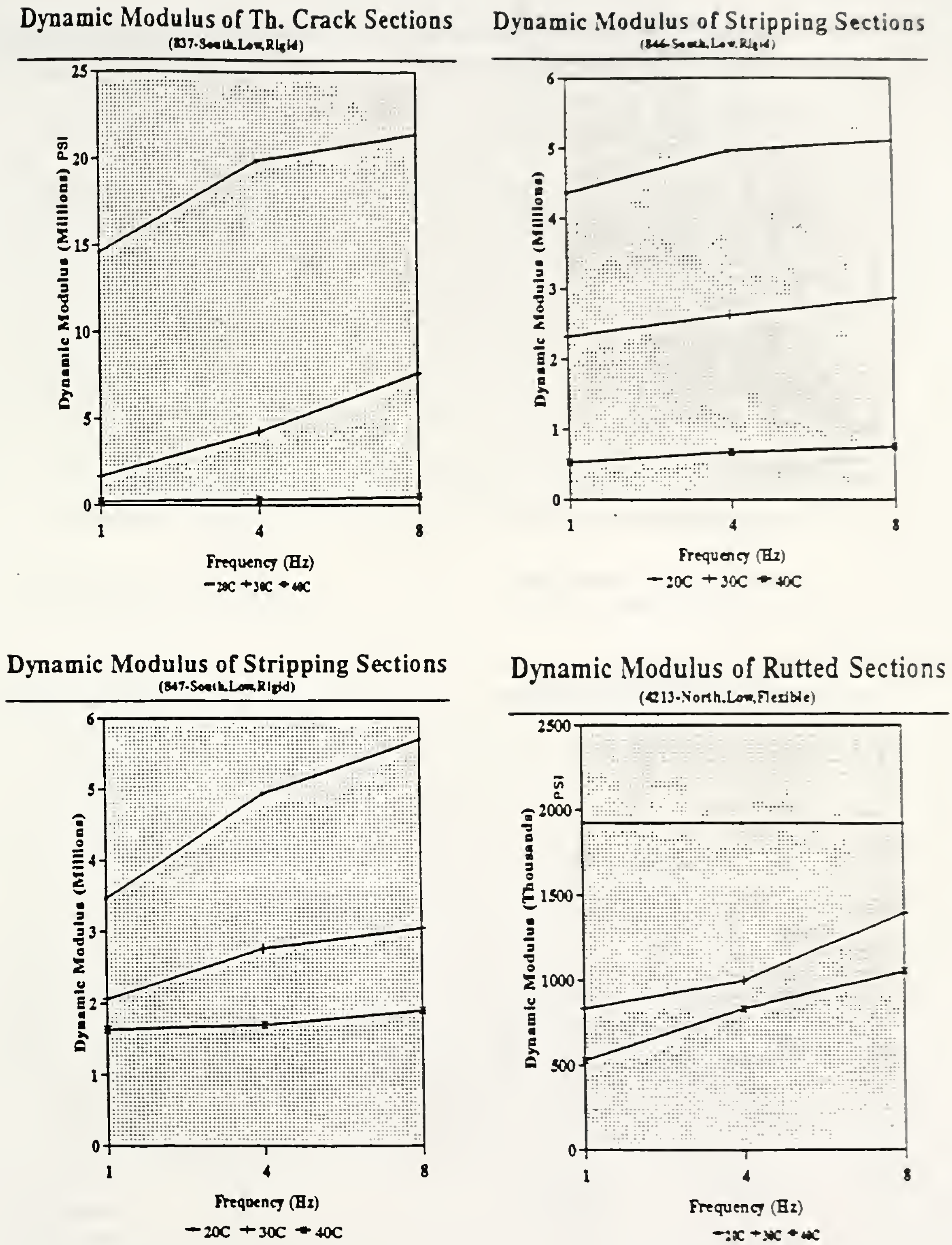

Figure 7.7. (continued)

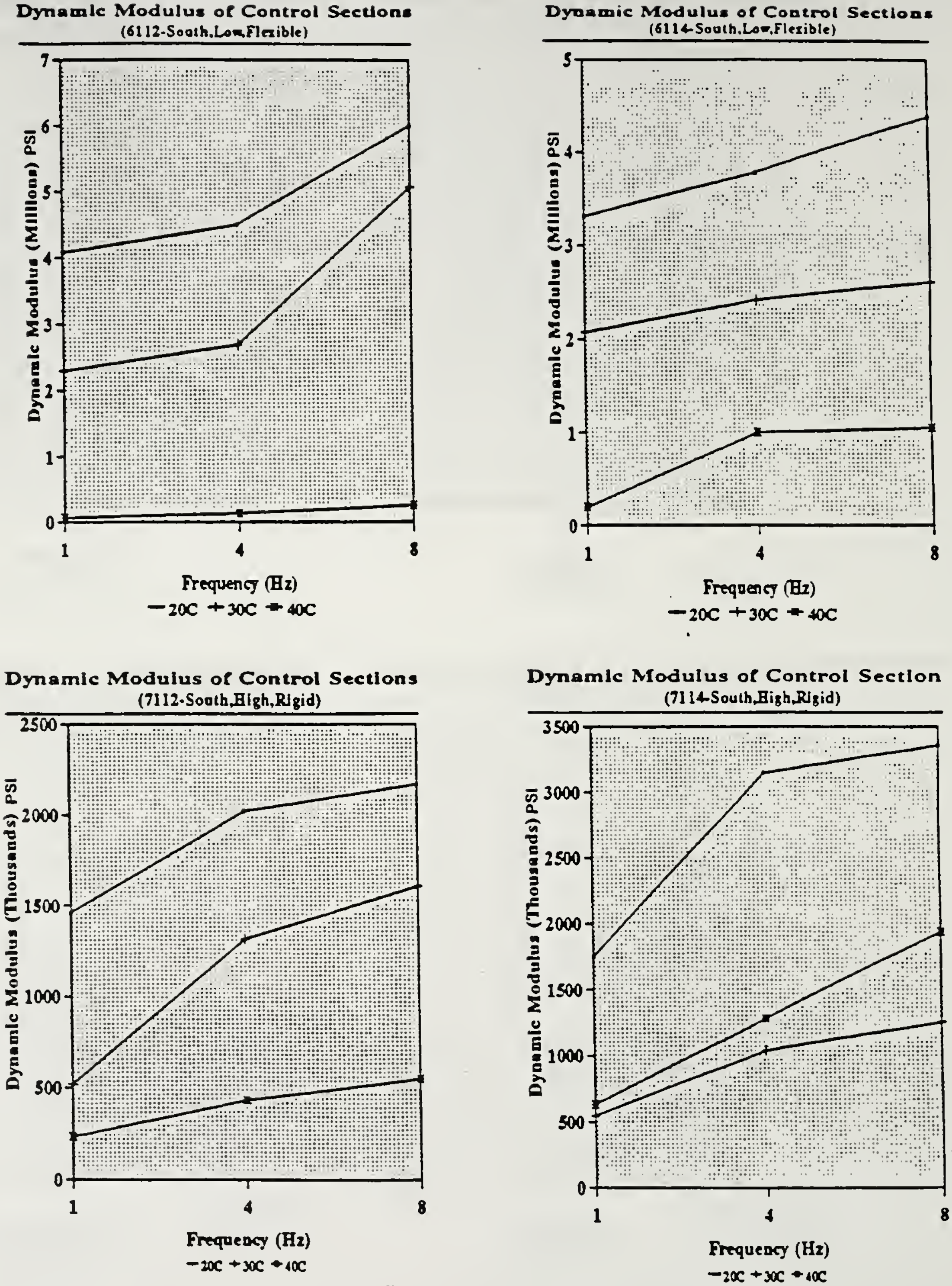

Figure 7.7. (continued)

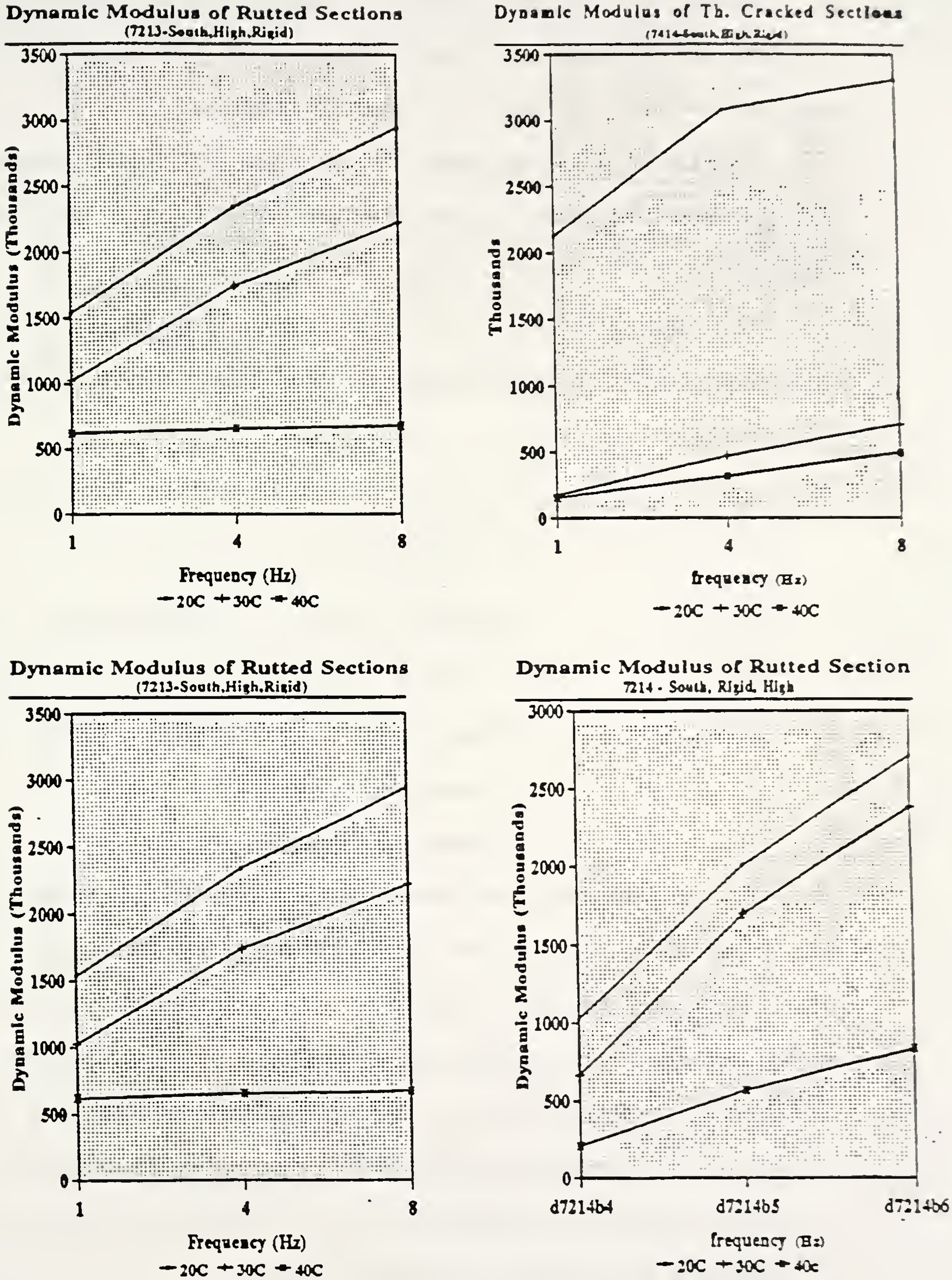

Figure 7.7. (continued)

gradient of the plot. This observation is generally the case in most of the plots shown. In some cases, however, when the binder stiffness is very high, as in thermally cracked sections, this effect is less pronounced.

These plots represent a measure of the E^* values of the bituminous concrete cores tested. They will be compared to theoretical E^* values later.

The dynamic modulus, also called the complex modulus, has been mathematically reduced to the form shown in Equation 7.1 [Bonnaure, 1977]:

$$E^* = E\,e^{i\varphi} = E\,(\cos\varphi + i\sin\varphi) \qquad \text{Equation 7.1}$$

Where E^* = Dynamic Modulus of Bituminous Concrete

E = Elastic Modulus of Bituminous Concrete

ϕ = Phase Angle, a measure of the viscous response

i = Imaginary Number

Since the samples were from pavements with different ages and traffic counts, the relationship of average E^* with Age was graphed for each temperature in Figure 7.8. This figure shows no definite relationship between the E^* and age, but the effect of temperature on E^* is quite obvious. A regression relationship between Age and E^* for the data in Table 7.3 gave a correlation coefficient of 0.22, 0.03 and 0.06 at 20, 30 and 40 degrees centigrade, respectively.

In Figure 7.9, a plot is shown of average E^* against distress types at 20, 30 and 40 degrees centigrade. A

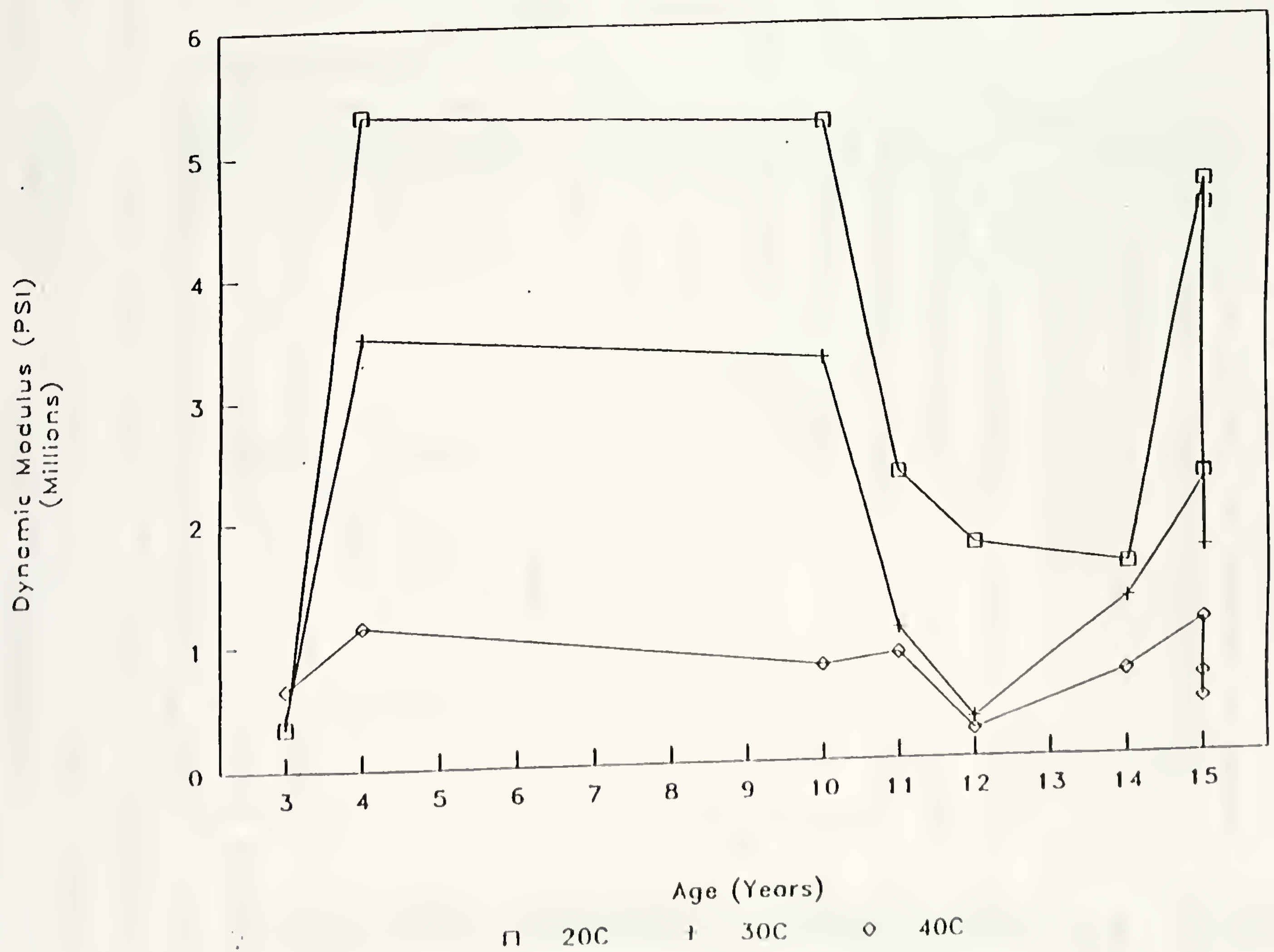

Figure 7.8. Dynamic Modulus Vs. Age of Core Samples (High Truck Traffic)

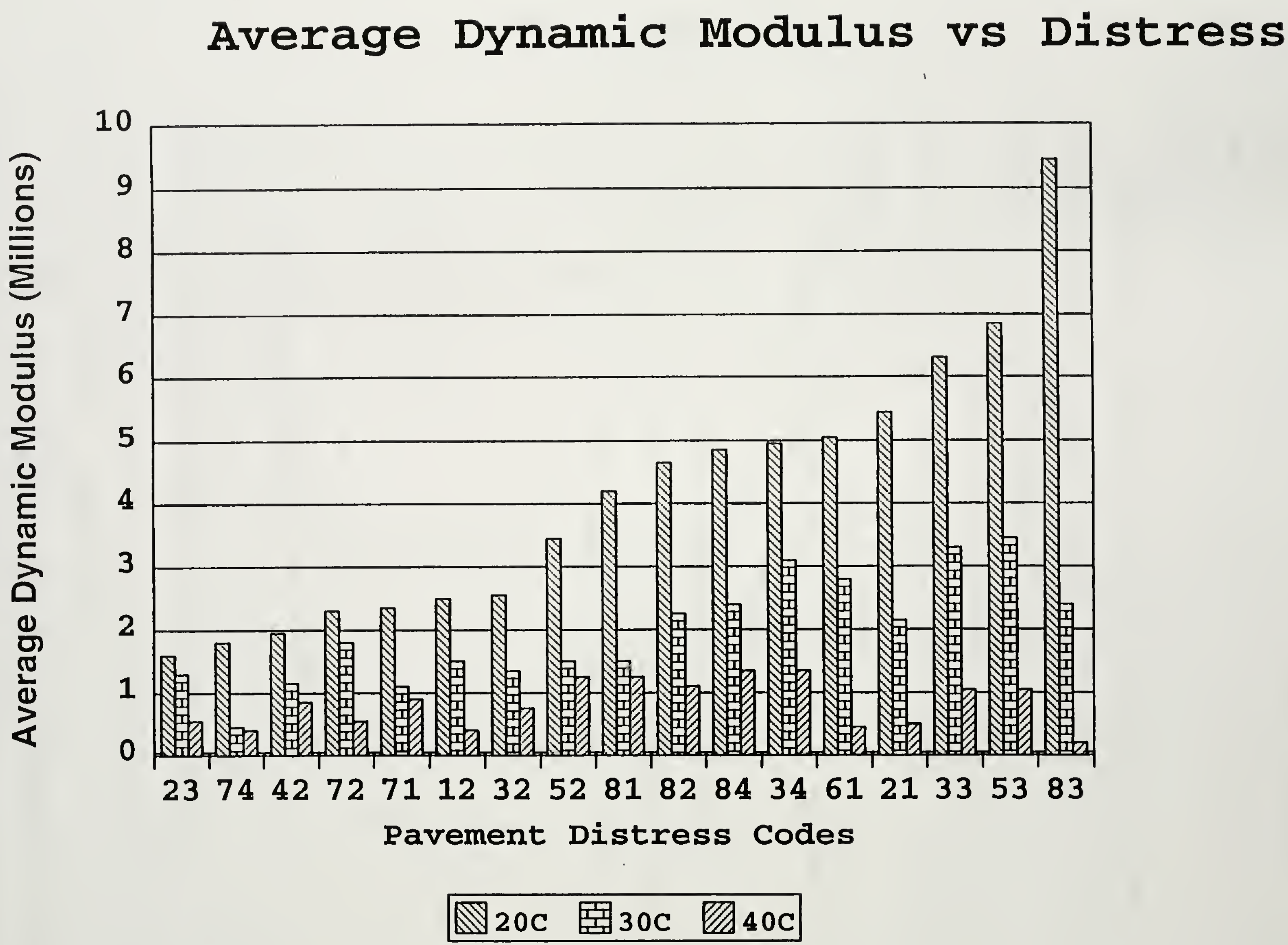

Figure 7.9. Average Dynamic Modulus Vs. Distress Type

distinct pattern emerges in that all thermal cracked sections have very high modulus values and all the rutting sections have lower values. Some of the control sections (no distress) have low truck traffic. With low truck traffic pavement distress would be expected to be minimal.

At 30 degrees centigrade, the thermal cracked sections still show high E^* values followed by the control and the rutted sections. Results from stripped sections do not show any definite trend, perhaps due to the small sample number.

Sample response at 40 degrees centigrade shows the effect of temperature susceptibility of the asphalt binder in the bituminous concrete where all the thermal cracked sections have lower E^* values. All of the control sections except one had higher E^* values, showing that these sections were indeed stable. The rutting sections still had relatively low E^* values compared to samples from pavements with other distress.

Dynamic creep test results at various temperatures identify pavement sections that are performing well, have high temperature susceptibilities and have rutting potential. There is, however, no trend to link dynamic creep to stripping potential. Figure 7.10 show clearly the effect of test temperature on dynamic modulus values, and summarizes their variations by distress type. Again thermally cracked sections stand out distinctly from other distresses, while rutting sections have low modulus values. In Table 7.3 it was shown that the phase angle, ϕ, increases with test temperature and decreases as the test frequency increases. This is in agreement with dynamic tests on bituminous concrete carried

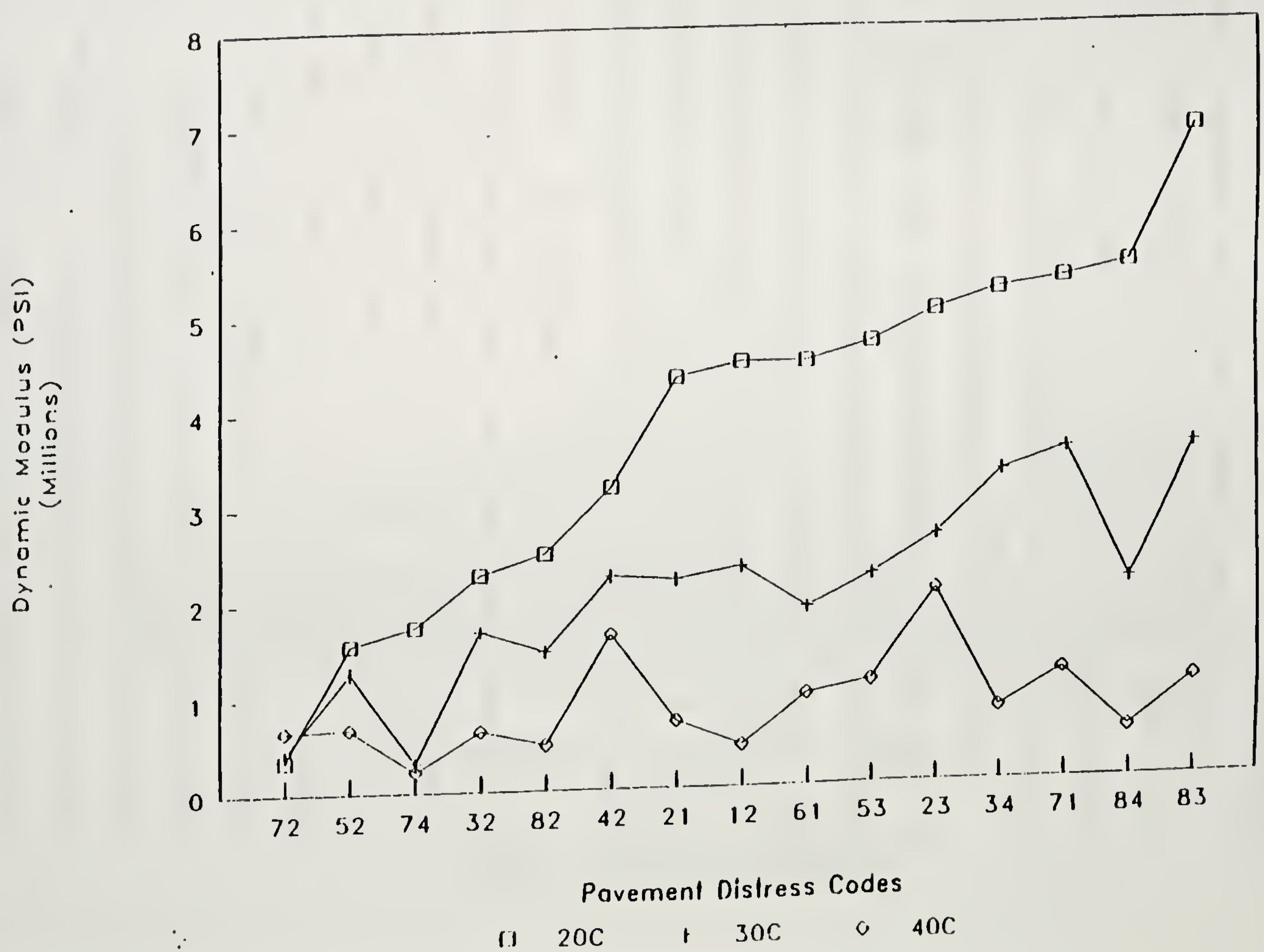

Figure 7.10. Dynamic Modulus at Different Test Temperatures

out by Bonnaure et al., 1977.

Table 7.4 shows the minimum and maximum E^* values at each test temperature for each distress type. This was done to see if a range of values could be related to a tendency towards certain distress types. The material properties of the samples are given in Table 7.5 where the penetration-viscosity number (PVN) indicates a variability in the temperature susceptibility of the asphalt cement (Mcleod, 1989). For the rutting distress type, three pavement sections 12, 32 and 72 have large negative PVN values. These sections represent high truck traffic with rut depths of over 1.5 inches. Section 12 is a full depth asphalt pavement while sections 32 and 73 are asphalt overlays on a rigid base.

There is an overlap in the range of E^* for the distresses. For example, a rutted section could also be identified as a control section if the higher bound is considered. This overlap is due to the way the minimum and maximum values were evaluated where the entire data for one distress was used in order to observe the actual variations in E^*.

7.5 Theoretical Dynamic Modulus

The dynamic modulus of bituminous concrete, as shown by Coree and White, 1989, can be evaluated if five physical characteristics of the mixture are known, namely, initial binder penetration, volume concentration of binder, volume concentration of aggregate, time of loading and test temperature. They used an equation presented by Ullidtz, 1979

Table 7.4. Range of Dynamic Modulus Values for Each Test Location

Distress Type	Traffic Condition	Base Type	Range of Dynamic Modulus Values (PSI) 20 C	30 C	40 C
Control	High	Rigid	1.46E+06 3.36E+06	5.20E+05 1.61E+06	2.36E+05 1.94E+06
Control	Low	Flexible	4.22E+05 1.15E+07	4.00E+05 5.06E+06	1.62E+05 1.30E+06
Control	Low	Rigid	2.49E+06 5.93E+06	1.27E+06 4.54E+06	4.74E+05 2.33E+06
Rutting	High	Flexible	1.49E+06 4.03E+06	4.34E+05 2.70E+06	1.71E+05 1.45E+06
Rutting	High	Rigid	1.54E+06 2.94E+06	3.95E+05 2.22E+06	1.76E+05 9.90E+05
Rutting	Low	Flexible	1.63E+05 2.79E+06	1.86E+05 2.73E+05	1.74E+05 4.32E+05
Rutting	Low	Rigid	1.92E+06 5.70E+06	8.36E+05 3.50E+06	4.57E+05 1.53E+06
Thermal Cracking	High	Flexible	2.50E+06 1.41E+07	2.06E+06 5.05E+06	7.24E+05 1.34E+06
Thermal Cracking	High	Rigid	2.83E+06 1.15E+07	5.18E+05 8.12E+06	5.12E+05 1.76E+06
Thermal Cracking	Low	Flexible	1.28E+06 1.69E+06	1.01E+06 1.58E+06	2.60E+05 9.73E+05
Thermal Cracking	Low	Rigid	2.80E+05 2.14E+07	1.31E+05 7.62E+06	7.34E+04 4.85E+05
Stripping	High	Rigid	3.80E+06 6.30E+06	2.50E+06 3.61E+06	6.10E+05 2.03E+06
Stripping	Low	Rigid	3.47E+06 6.59E+06	1.97E+06 3.05E+06	5.29E+05 2.80E+06

Table 7.5. Material Properties of Core Samples Used For Dynamic Creep Testing

Distress Code	Age	Air Voids	Kin. Visc.	Abs. Visc.	Asp%	Pen 77F	PVN
21	16	16	902	20408	4.7	28	−0.42708
61	2	2	656		5.9	27	−0.85237
71	4	4	1026		5.2	25	−0.37292
81	5	5	835	6415	4.6	16	−0.98959
12	15	15	547	9045	5.4	32	−0.93361
32	15	15	719	14110	5.6	18	−1.07094
42	12	12	496	4759	5.8	44	−0.77532
52	14	14	812	18332	5.8	29	−0.52541
72	3	3	563	7815	5.3	26	−1.07141
82	9	9	1151	63886	4.8	20	−0.43473
23	9	9	657	12577	5.5	33	−0.67433
33	11	11	1266	8405	5.4	15	−0.56857
53	15	15	785	16295	5.6	21	−0.84546
83	12	12	545	6415	5.8	36	−0.83505
34	10	34	775	16489	5.1	29	−0.58345
74	12	74	471	3859	5.2	33	−1.09695
84	10	84	1420	33956	4	12	−0.62036

to estimate the binder stiffness from the nomograph developed by Heukelom and Klomp, 1964. Asphalt mixture stiffness was determined using the relations developed by Bonnaure et al., 1977 as shown in Equation 7.2.

$$\log_{10}(S_m) = \left[\frac{S_v + S_x}{2}\right]\left[\log_{10}(S_b) - 8\right] + \left[\frac{S_v - S_x}{2}\right]\left|\log_{10}(S_b) - 8\right| + S_y \quad \text{... Equation 7.2}$$

where;

S_m = Theoretical Stiffness Modulus of Bituminous Concrete

$$S_z = 10.82 - 1.342\left[\frac{100 - V_b}{V_a + V_b}\right]$$

$$S_y = 8.0 + 5.68 * 10^{-3} V_a + 2.135 * 10^{-4} V_a^2$$

$$S_x = 0.6 \log_{10}\left[\frac{1.37 V_b^2 - 1}{1.33 V_b - 1}\right]$$

$$S_v = 0.76 \; (S_z - S_y)$$

S_b = Stiffness of the Binder [Ullidtz,1979]

V_a = Percent Volume of Binder

V_b = Percent Volume of Aggegate

This relationship was used to evaluate the theoretical E^* for all the cores which were tested for dynamic creep above. However, this evaluation was only possible for test temperatures up to about 30 degrees centigrade due to the limitations of the original nomograph by Heukelom and Klomp, 1964. Thus, while the experimental dynamic modulus was conducted at 20, 30 and 40 degrees centigrade, comparison with the theoretical E* could be carried out only at 20 and 30 degrees centigrade as shown in Figures 7.11 to 7.16. These plots all show that the theoretical E^* values generally agree with the experimental E^* values and could be used as an approximation when the measured E^* is not available.

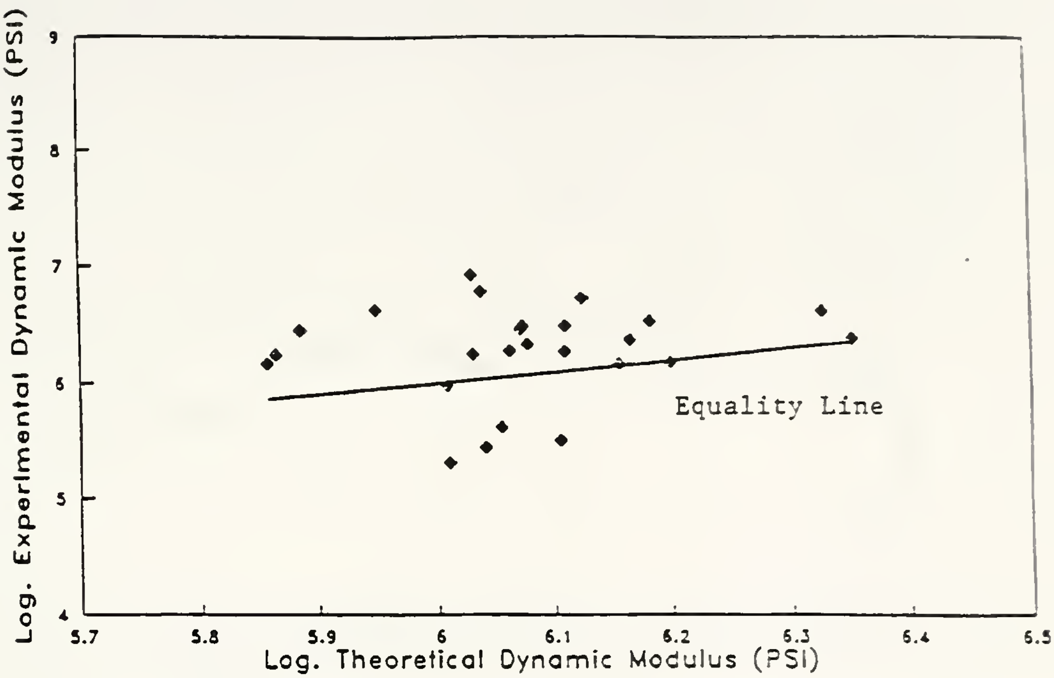

Figure 7.11. Theoretical Vs. Experimental Dynamic Modulus (20 C @ 1 Hz)

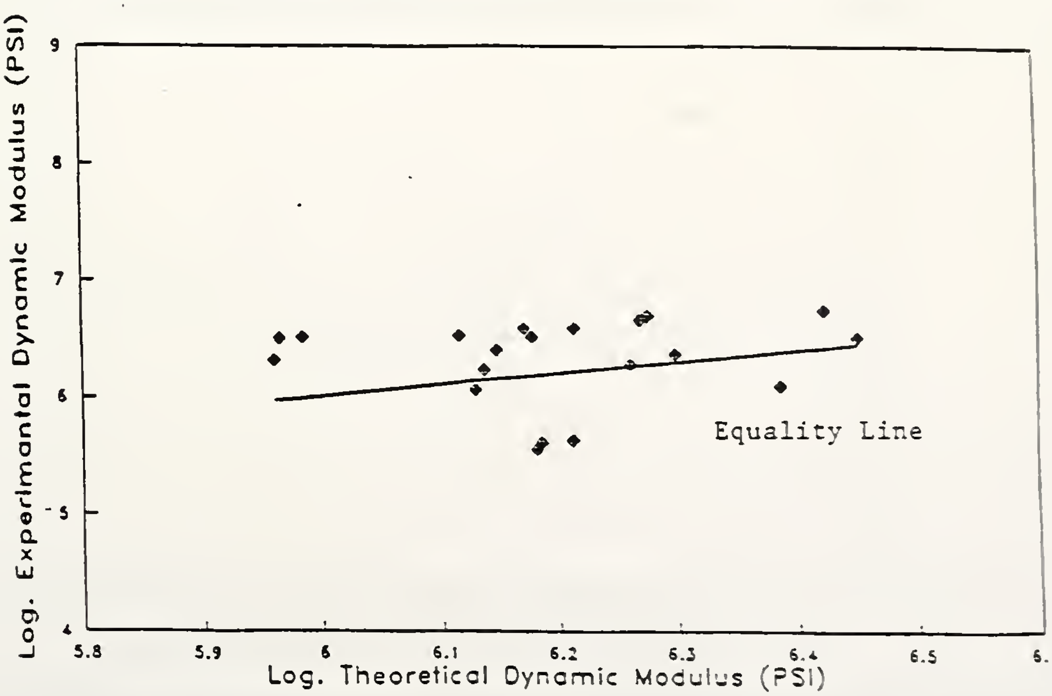

Figure 7.12. Theoretical Vs. Experimental Dynamic Modulus (20 C @ 4 Hz)

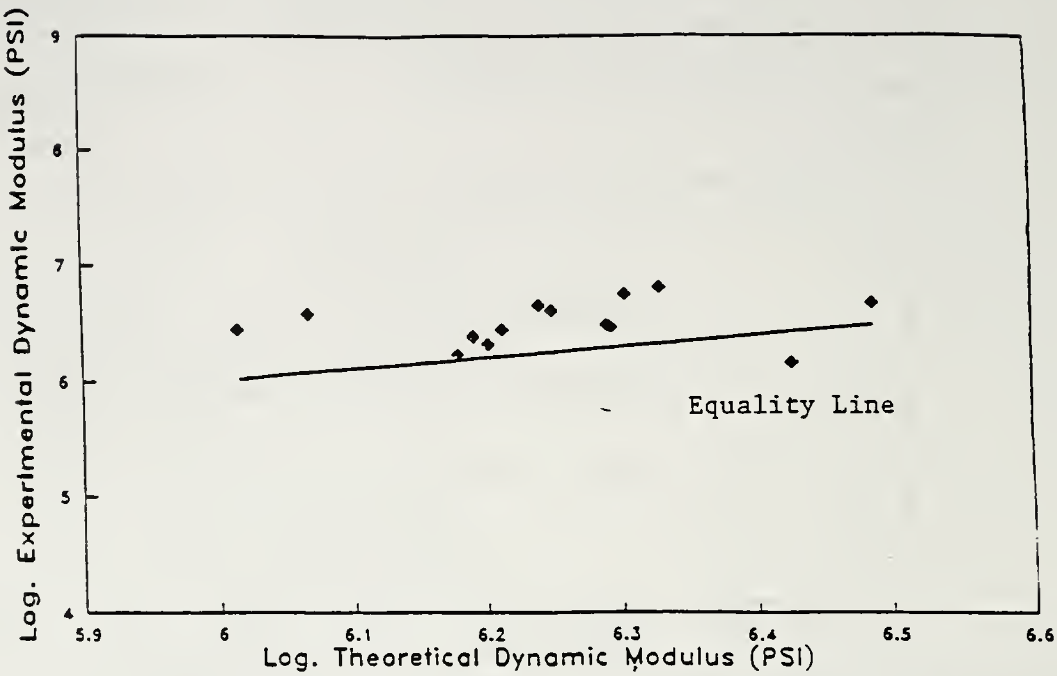

Figure 7.13. Theoretical Vs. Experimental Dynamic Modulus (20 C @ 8 Hz)

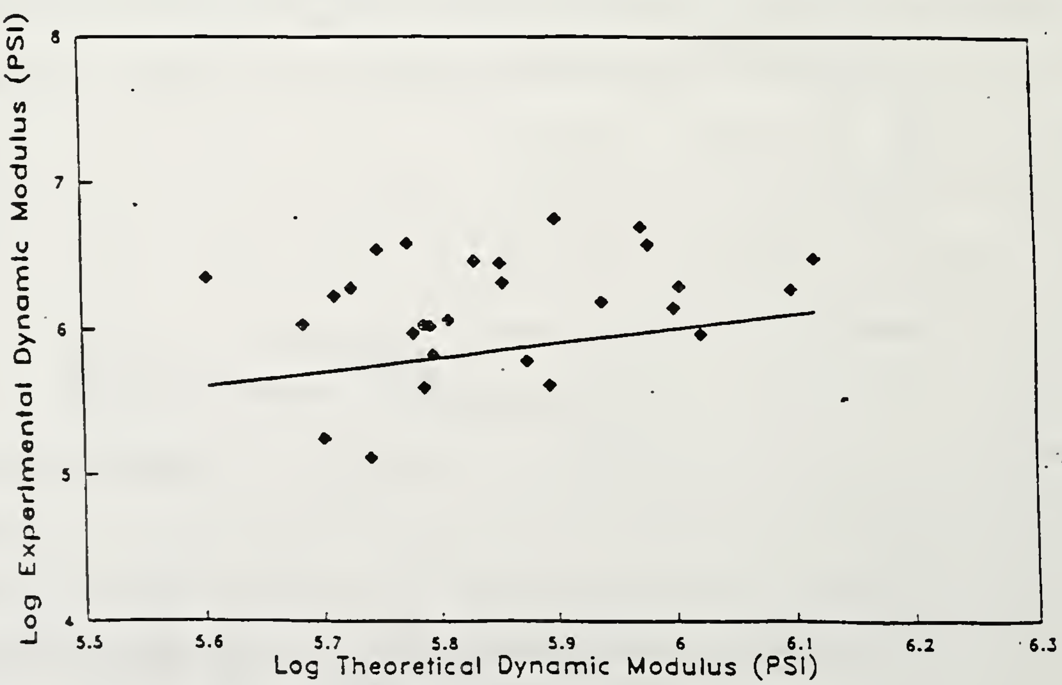

Figure 7.14. Theoretical Vs. Experimental Dynamic Modulus (30 C @ 1 Hz)

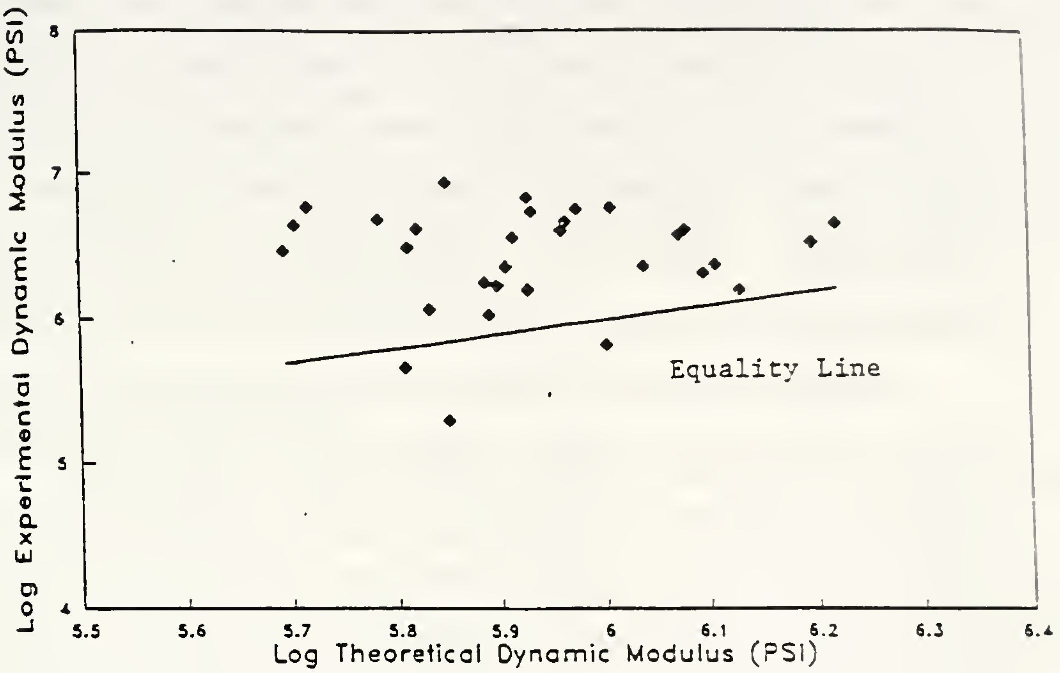

Figure 7.15. Theoretical Vs. Experimental Dynamic Modulus (30 C @ 4 Hz)

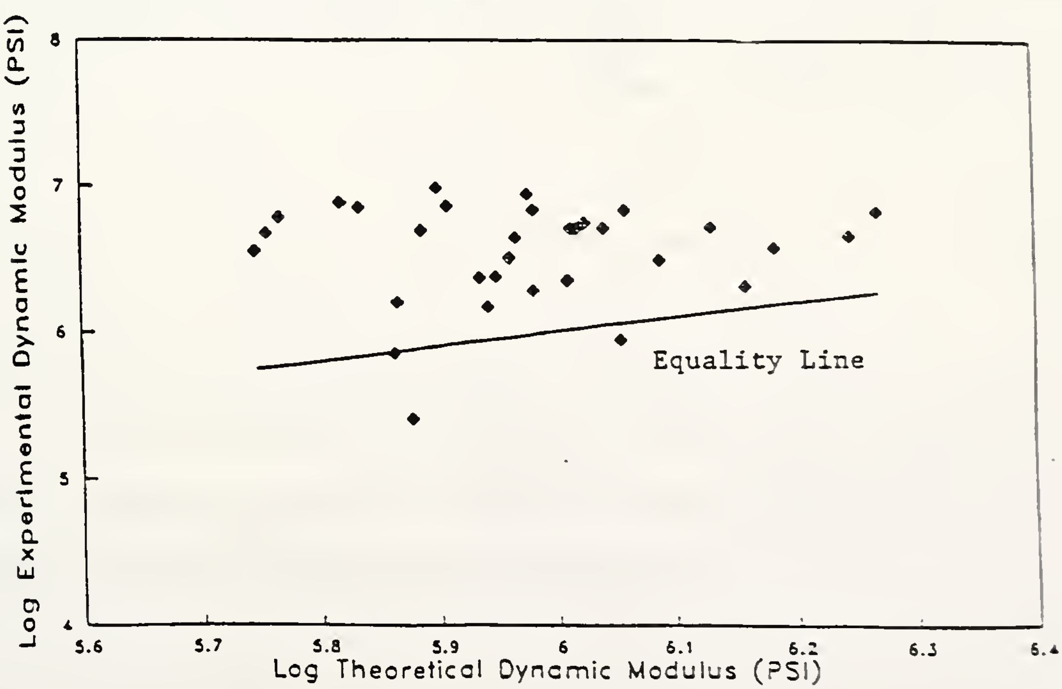

Figure 7.16. Theoretical Vs. Experimental Dynamic Modulus (30 C @ 8 Hz)

7.6 Conclusion

The dynamic creep test results from this study confirmed several characteristics of bituminous concrete. Also, the results have shown the potential of using E^* to identify those mixtures that would exhibit various types of distress. The increase of E^* values with test frequency and decrease at higher test temperatures has also been observed by other researchers. Phase angle variations with test frequency and temperature also agreed with results from other research.

Pavement sections exhibiting rutting were shown to have low E* values at all test temperatures and frequencies while pavement sections exhibiting thermal cracking had very high values. The worst rutting sections with low E* values were also shown to have large negative PVN numbers. There was no apparent indication of stripping potential from the E* values. Theoretical E^* values were shown to compare well with experimental E^* values.

CHAPTER 8. ANALYSIS OF RESULTS AND PERFORMANCE EVALUATION

Test results from Chapters 6 and 7 are analyzed in this chapter. It became obvious that although a large number of cores were obtained from the field and tested, the results would have benefitted from replication in order to remove confounding. However, the data generated in the study provides an indication of pavement performance and satisfactory categorization of distress.

8.1 ANOVA of Factors

The four factors in the study; Climate (C), Truck Traffic (T), Base Type (B) and Wheel Path (W); were to be tested for significance based on the design of experiment shown in Table 8.1. Core samples were obtained from only one pavement for each treatment combination. Thus analyzing the original design of experiment would in effect have ignored the complete confounding between factors and site. The only way to avoid this confounding is to obtain replicates in each cell. By dropping one factor the replication could be achieved. Climate was dropped as a factor because of limited significance in previous studies (Lindly, 1987 and Pumphrey, 1989) and also since the remaining factors were considered to have a logical influence on the distresses. The model shown in Equation 8.1 was used in this analysis.

$$Y_{ijkl} = \mu + T_i + B_j + W_k + TB_{ij} + TW_{ik} + BW_{jk} + TBW_{ijk} + \varepsilon_{(ijk)l} \quad \text{...Equation 8.1}$$

where:

Y_{ijkl} = dependant variable (measured laboratory data)

μ = Common Effect

T_i = Truck Traffic

B_j = Base Type

W_k = Wheelpath

$\varepsilon_{(ijk)l}$ = Error .

Table 8.1 Design of Experiment Layout For Asphalt Mix Design Study

BASE TYPE	WHEELPATH	NORTH HIGH	NORTH LOW	SOUTH HIGH	SOUTH LOW
CLIMATE / TRUCK TRAFFIC		4 DISTRESSES*	4 DISTRESSES*	4 DISTRESSES*	4 DISTRESSES*
FLEXIBLE	IN				
FLEXIBLE	OUT				
RIGID	IN				
RIGID	OUT				

The dependent variables consisted of laboratory measured data that would be most affected by these four factors. Bulk specific gravity (BSG) measurements was used in the analysis because it is directly affected by the factors T, B and W. Also BSG values were available for almost all seven cores in each cell thus enabling sufficient degrees of freedom for significance testing. The other dependant variable considered was kinematic viscosity.

The GLM procedure in SAS (Little et. al., 1991) was used for the analyses due to the presence of some empty cells. A full 2^3 factorial analysis was carried out and the results are shown in Table 8.2. This analyses indicated that all major factors and most of their one way and two way interactions are insignificant for the selected dependent variables. Base type (B) and wheel path (W) were found to be significant for bulk specific gravity measurements on rutted pavements. These results are not unexpected since on rutted sections bulk specific gravity is affected by wheel track and by underlying base pavement type.

Table 8.2. Factors and Their Interactions That Were Significant

Dependant Variable	Distress Type	Factors Included	Factors And Interactions Significant
Bulk Specific Gravity, Kinematic Viscosity	ZERO, THERMAL CRACKING	B, T, W	None
Bulk Specific Gravity	RUTTING	B, T, W	B, T

8.2 Discriminant Analysis

A statistical procedure called discriminant analysis (Morrison, 1976) was performed to identify groups of laboratory measured data that would fall under a particular distress category. A layout of the procedure is shown in Figure 8.1. Data shown in Table 8.3 was used in the analysis. This data set includes laboratory measured data as well as calculated values of dynamic moduli at various temperatures and test frequencies. Initially the entire data set shown in Table 8.3 was used as input with 25 observations and 19 variables in each observation. The discriminant analysis automatically excluded any observation that had a missing variable, thus only 13 observations were classified. The result shown in Figure 8.2 gives a perfect classification with zero error for rutting and zero distresses.

As another approach, an analysis was conducted by dropping variables with missing data. For example, data (Thomas, 1993) for the variables N30, N50 and N100 (see Appendix C for key to variables) were not available for the thermal cracking and stripping observations. Dropping variables with missing test results leaves 14 input variables for the analysis. The analysis produced a successful zero classification error for the 21 observations as shown in Figure 8.3. Four of the 25 observations were dropped automatically because of missing data for some of the remaining variables. (These variables were retained because they were important and had non-missing data for the remaining 21 observations). Consideration was given to whether or not

Figure 8.1. Discriminant Analysis Procedure

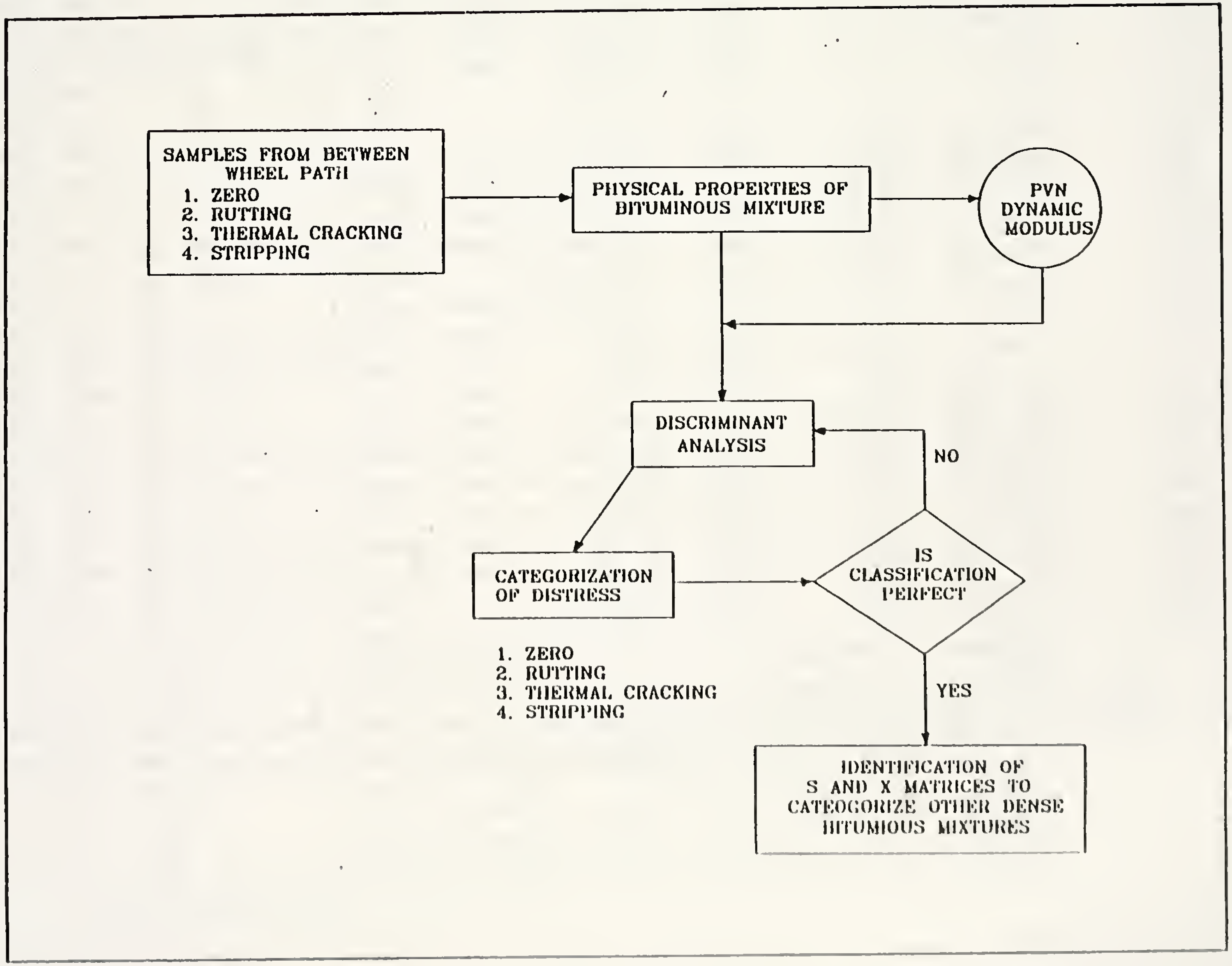

Table 8.3. Data For Discriminant Analysis (Outside Wheel Path)

CODE	DISTRESS	N30	N50	N100	KIN. VISC. CSt.	ABS. VISC. Poise	PVN	BULK SG	MAX SG	MARSHALL STABILITY LBS	FLOW (0.01")	PEN (0.1 MM)	ASPHALT CONTENT %	AIR VOID %
118	zero	9	32	25	1282	.	−0.37	2.2290	2.4950	1125	14.3	18	6.1	9.9
128	rut	17	56	63	554	8894	−1.11	2.3756	2.4611	1484	13.3	25	5.3	3.1
218	zero	20	43	46	903	20489	−0.49	2.3555	2.5158	2606	15.5	26.5	4.9	7.3
238	tc	.	.	.	627	12435	−0.81	2.3934	2.4783	.	.	30.5	5.3	3.4
318	zero	.	48	56	664	25794	−0.94	2.3723	2.4680	1438	16.3	24	4.9	3.2
328	rut	18	48	53	717	14151	−0.98	2.4309	2.4680	2068	16.3	20.5	5.4	1.8
338	tc	.	.	.	1582	41580	−0.33	2.3628	2.4807	2598	17.0	14.5	5.3	4.8
348	strip	.	.	.	776	17360	−0.78	2.3551	2.5021	1833	19.0	23	5.4	6.4
418	zero	23	57	73	800	.	.	2.4084	2.5315	1733	12.3	.	.	4.6
428	rut	15	52	68	604	8448	−0.74	2.4974	2.5189	1929	11.0	35	5.6	0.6
438	tc	.	.	.	1374	65886	−0.42	2.2231	2.4629	.	.	16	5.4	8.8
518	zero	30	59	63	816	.	−0.40	2.3977	2.4296	2316	9.0	33	4.9	0.8
528	rut	42	76	65	799	18220	−0.48	2.2960	2.4452	1221	8.3	31	5.1	5.5
538	tc	.	.	.	707	15652	−1.04	2.3400	2.4445	1592	15.3	19	5.1	4.4
548	strip	.	.	.	691	12030	−0.51	2.3251	2.4763	1297	15.7	36.5	5.4	5.6
618	zero	25	46	50	673	.	−0.85	2.2501	2.4569	386	14.0	26.5	4.8	8.1
628	rut	29	60	56	920	29643	−0.73	2.1631	2.4684	1610	14.3	19.5	4.9	9.5
718	zero	14	41	42	1026	.	−0.44	2.2137	2.4523	1438	15.7	23.5	5.1	9.6
728	rut	19	53	69	558	6870	−1.09	2.3860	2.4738	1490	13.8	27.5	5	2.9
738	tc	.	.	.	1124	41195	−0.44	2.3102	2.4909	.	.	20.5	4.9	6.4
748	strip	.	.	.	463	4125	−1.14	2.3828	2.4580	2004	12.3	31.5	5.4	3.1
818	zero	27	50	50	843	.	−0.99	2.4218	2.4868	2119	18.3	16	4.8	2.3
828	rut	15	36	39	1303	63965	−0.52	2.3069	2.4969	2069	16.3	15.5	4.5	7.3
838	tc	.	.	.	548	.	−0.83	2.4093	2.4649	1256	15.0	36	5.8	2.4
848	strip	.	.	.	1420	.	−0.31	2.3622	2.4946	1952	14.0	17.5	4.6	6.2

See Appendix C For Key To Variables

Table 8.3. Continued

CODE	DISTRESS	E1HZ20 (PSI)	E1HZ30 (PSI)	E4HZ20 (PSI)	E4HZ30 (PSI)	E8HZ20 (PSI)	E8HZ30 (PSI)
118	zero	6.85E+05	3.69E+05	8.86E+05	4.77E+05	1.01E+06	5.42E+05
128	rut	1.28E+06	6.76E+05	1.63E+06	8.61E+05	1.84E+06	9.71E+05
218	zero	8.85E+05	4.77E+05	1.11E+06	6.00E+05	1.25E+06	6.73E+05
238	tc	1.12E+06	5.69E+05	1.42E+06	7.23E+05	1.60E+06	8.15E+05
318	zero	1.41E+06	7.71E+05	1.77E+06	9.71E+05	1.99E+06	1.09E+06
328	rut	1.62E+06	8.85E+05	2.06E+06	1.13E+06	2.33E+06	1.27E+06
338	tc	1.44E+06	8.31E+05	1.83E+06	1.06E+06	2.06E+06	1.19E+06
348	strip	9.35E+05	4.98E+05	1.19E+06	6.36E+05	1.35E+06	7.18E+05
418	zero	.		.	.	.	.
428	rut	1.30E+06	6.26E+05	1.66E+06	8.02E+05	1.88E+06	9.07E+05
438	tc	9.21E+05	5.25E+05	1.17E+06	6.69E+05	1.33E+06	7.56E+05
518	zero	1.50E+06	7.68E+05	1.89E+06	9.68E+05	2.12E+06	1.09E+06
528	rut	9.22E+05	4.74E+05	1.17E+06	6.00E+05	1.32E+06	6.75E+05
538	tc	1.34E+06	7.50E+05	1.69E+06	9.50E+05	1.91E+06	1.07E+06
548	strip	7.71E+05	3.72E+05	9.84E+05	4.74E+05	1.11E+06	5.36E+05
618	zero	8.30E+05	4.50E+05	1.04E+06	5.65E+05	1.17E+06	6.34E+05
628	rut	8.38E+05	4.75E+05	1.06E+06	5.99E+05	1.19E+06	6.73E+05
718	zero	7.28E+05	3.96E+05	9.21E+05	5.01E+05	1.04E+06	5.64E+05
728	rut	1.39E+06	7.48E+05	1.75E+06	9.44E+05	1.97E+06	1.06E+06
738	tc	1.10E+06	6.22E+05	1.39E+06	7.84E+05	1.56E+06	8.79E+05
748	strip	1.11E+06	5.58E+05	1.41E+06	7.11E+05	1.60E+06	8.02E+05
818	zero	1.95E+06	1.15E+06	2.45E+06	1.44E+06	2.75E+06	1.62E+06
828	rut	1.25E+06	7.52E+05	1.56E+06	9.39E+05	1.74E+06	1.05E+06
838	tc	1.00E+06	4.73E+05	1.29E+06	6.08E+05	1.46E+06	6.90E+05
848	strip	1.29E+06	7.60E+05	1.62E+06	9.50E+05	1.81E+06	1.06E+06

See Appendix C For Key To Variables

The SAS System

Discriminant Analysis   Classification Summary for Calibration Data: WORK.ASPMIX

Resubstitution Summary using Linear Discriminant Function

Generalized Squared Distance Function:

$$D_j^2(X) = (X-\bar{X}_j)' \, COV^{-1} (X-\bar{X}_j)$$

Posterior Probability of Membership in each DISTRESS:

$$Pr(j|X) = \exp(-.5 \, D_j^2(X)) \, / \, \sum_k \exp(-.5 \, D_k^2(X))$$

Number of Observations and Percent Classified into DISTRESS:

From DISTRESS	RUT	ZERO	Total
RUT	7 100.00	0 0.00	7 100.00
ZERO	0 0.00	6 100.00	6 100.00
Total Percent	7 53.85	6 46.15	13 100.00
Priors	0.5000	0.5000	

Error Count Estimates for DISTRESS:

	RUT	ZERO	Total
Rate	0.0000	0.0000	0.0000
Priors	0.5000	0.5000	

Figure 8.2. Discriminant Analysis of Entire Data Set Showing Zero Classification Error.

The SAS System

Discriminant Analysis

Classification Summary for Calibration Data: WORK.NEW

Resubstitution Summary using Linear Discriminant Function

Generalized Squared Distance Function:

$$D_j^2(x) = (x-\bar{x}_j)\ \mathrm{cov}^{-1}(x-\bar{x}_j)$$

Posterior Probability of Membership in each DISTRESS:

$$Pr(j|x) = \exp(-.5\ D_j^2(x)) \ /\ SUM_k \exp(-.5\ D_k^2(x))$$

Number of Observations and Percent Classified into DISTRESS:

From DISTRESS	rut	strip	tc	zero	Total
rut	7 100.00	0 0.00	0 0.00	0 0.00	7 100.00
strip	0 0.00	4 100.00	0 0.00	0 0.00	4 100.00
tc	0 0.00	0 0.00	3 100.00	0 0.00	3 100.00
zero	0 0.00	0 0.00	0 0.00	7 100.00	7 100.00
Total Percent	7 33.33	4 19.04	3 14.29	7 33.33	21 100.00
Priors	0.2500	0.2500	0.2500..	0.2500	

Error Count Estimates for DISTRESS:

	rut	strip	to	zero	Total
Rate	0.0000	0.0000	0.0000	0.0000	0.0000
Priors	0.2500	0.2500	0.2500	0.2500	

Figure 8.3. Discriminant Analysis of Reduced Data Set Showing Zero Classification Error

all 14 variables were needed in the analysis in order to obtain zero error classification. By selectively dropping the variables while maintaining a zero error requirement, the analysis showed that only 12 of the initial 14 variables were necessary to obtain perfect classification of distresses as shown in Figure 8.4.

A further analysis was carried out using eight selected laboratory measured variables and age. This reduced the input variables to 9 for each of the 25 observations. The analysis dropped 5 observation due to the same reasons as before and produced a classification for the remaining 20 observations with an error of 0.119 as shown in Figure 8.5. Two of the observations were misclassified as given in Figure 8.6.

These results indicate that for the selected list of measured variables, the discriminant analysis method was able to correctly identify and categorize the pavements into appropriate distress categories. When the number of variables were reduced a small error in classification occurred, but the method still correctly classified 18 of the observations.

The discriminant analysis uses the method of minimum distance or the Mahalanobis Distance (Little et. al., 1991) criterion given in Equation 8.2. This equation can be used to classify observations into one of the four distress categories investigated in this study, using the classification rule shown in Equation 8.3.

The SAS System

Discriminant Analysis   Linear Discriminant Function

Constant $= -.5\ \bar{X}_j'\ COV^{-1}\ \bar{X}_j$ Coefficient Vector $= COV^{-1}\ \bar{X}_j$

DISTRESS

	RUT	STRIP	TC	ZERO
CONSTANT	-16345	-16171	-15908	-16587
PVN	-519.17537	-515.01742	*-509.53675	-518.71704
BSG	6702	6663	6635	8732
MARSH	-0.10910	-0.10670	-0.10845	-0.11063
FLOW	-47.52783	-46.55438	-48.86463	-46.88894
PEN	89.05072	98.41[illegible]48	87.84743	99.40878
ASP	718.45969	721.79378	709.31787	727.53423
AIR	889.39677	882.13277	873.81278	897.34780
E1HZ20	0.03885	0.03843	0.03858	0.03930
E1HZ30	-0.04716	-0.04601	-0.04741	-0.04689
E4HZ30	0.02555	0.02545	0.02517	0.02477
E8HZ20	-0.01752	-0.01730	-0.01757	-0.01767
E8HZ30	0.0000640	-0.0005766	0.0008988	0.0003503

Posterior Probability of Membership in DISTRESS:

Obs	From DISTRESS	Classified into DISTRESS	RUT	STRIP	TC	ZERO
1	ZERO	ZERO	0.0091	0.0003	0.0000	0.9906
2	RUT	RUT	0.6173	0.0515	0.3305	0.0006
3	ZERO	ZERO	0.1310	0.2245	0.0000	0.6445
5	ZERO	ZERO	0.2741	0.0997	0.0019	0.6243
6	RUT	RUT	0.0482	0.0379	0.0118	0.0022
7	TC	TC	0.0003	0.0002	0.0995	0.0000
8	STRIP	STRIP	0.0210	0.8062	0.1707	0.0021
10	RUT	RUT	0.6070	0.0073	0.0001	0.3858
12	ZERO	ZERO	0.0164	0.0000	0.0000	0.0836
13	RUT	RUT	0.7839	0.1443	0.0710	0.0007
14	TC	TC	0.0934	0.0086	0.8977	0.0003
15	STRIP	STRIP	0.0192	0.9255	0.0502	0.0052
16	ZERO	ZERO	0.1115	0.0002	0.0000	0.8883
17	RUT	RUT	0.6365	0.0230	0.0001	0.3405
18	ZERO	ZERO	0.0127	0.0007	0.0000	0.9866
19	RUT	RUT	0.5853	0.0059	0.0000	0.4088
21	STRIP	STRIP	0.2429	0.7501	0.0068	0.0002
22	ZERO	ZERO	0.0119	0.0005	0.0000	0.9875
23	RUT	RUT	0.4550	0.2897	0.0187	0.2367
24	TC	TC	0.0007	0.4658	0.5335	0.0000
25	STRIP	STRIP	0.0528	0.9439	0.0002	0.0031

Figure 8.4. Discriminant Analysis Showing Distresses Being Classified.

The SAS System

Discriminant Analysis   Classification Summary for Calibration Data: WORK.NEW

Resubstitution Summary using Linear Discriminant Function

Generalized Squared Distance Function:

$$D_j^2(X) = (X-\bar{X}_j)' \, COV^{-1} (X-\bar{X}_j)$$

Posterior Probability of Membership in each DISTRESS:

$$Pr(j|X) = \exp(-.5\, D_j^2(X)) \,/\, SUM_k \exp(-.5\, D_k^2(X))$$

Number of Observations and Percent Classified into DISTRESS:

From DISTRESS	RUT	STRIP	TC	ZERO	Total
RUT	6 85.71	0 0.00	0 0.00	1 14.29	7 100.00
STRIP	0 0.00	3 100.00	0 0.00	0 0.00	3 100.00
TC	1 33.33	0 0.00	2 66.67	0 0.00	3 100.00
ZERO	0 0.00	0 0.00	0 0.00	7 100.00	7 100.00
Total Percent	7 35.00	3 15.00	2 10.00	8 40.00	20 100.00
Priors	0.2500	0.2500	0.2500	0.2500	

Error Count Estimates for DISTRESS:

	RUT	STRIP	TC	ZERO	Total
Rate	0.1429	0.0000	0.3333	0.0000	0.1190
Priors	0.2500	0.2500	0.2500	0.2500	

Figure 8.5. Discriminant Analysis With Only Laboratory Measured Data Showing Distress Classification With Small Error

The SAS System

Discriminant Analysis   Linear Discriminant Function

Constant $= -.5\ \bar{X}_j'\ COV^{-1}\ \bar{X}_j$ Coefficient Vector $= COV^{-1}\ \bar{X}_j$

	DISTRESS			
	RUT	STRIP	TC	ZERO
CONSTANT	-6166	-5084	-6188	-6059
KINV	1.04342	1.02836	1.08172	1.00268
PVN	-739.21196	-734.71548	-760.73621	-710.16339
BSG	3876	3821	3847	3858
MARSH	-0.23897	-0.22999	-0.24370	-0.23251
FLOW	-6.70316	-7.88212	-7.18174	-8.00371
PEN	22.42843	22.67553	23.54798	21.45693
ASP	-164.55447	-158.08258	-164.97947	-160.42889
AIR	83.14518	83.07075	81.65915	83.28587
AGE	20.17437	19.56137	20.60098	19.32859

Obs	From DISTRESS	Classified into DISTRESS		Posterior Probability of Membership in DISTRESS: RUT	STRIP	TC	ZERO
1	ZERO	ZERO		0.1459	0.0191	0.0046	0.8305
2	RUT	RUT		0.7782	0.0020	0.2174	0.0023
3	ZERO	ZERO		0.0829	0.3582	0.0001	0.5588
5	ZERO	ZERO		0.1587	0.0410	0.0044	0.7959
6	RUT	RUT		0.6542	0.0182	0.2634	0.0643
7	TC	TC		0.0053	0.0001	0.9946	0.0000
8	STRIP	STRIP		0.0117	0.7460	0.0007	0.2416
10	RUT	RUT		0.8550	0.0370	0.0254	0.0826
12	ZERO	ZERO		0.1864	0.0043	0.0006	0.8087
13	RUT	RUT		0.7747	0.0002	0.0008	0.2244
14	TC	RUT	*	0.8746	0.0018	0.1022	0.0214
15	STRIP	STRIP		0.0015	0.9802	0.0022	0.0161
16	ZERO	ZERO		0.3466	0.0052	0.0008	0.6474
17	RUT	RUT		0.7583	0.0366	0.1840	0.0211
18	ZERO	ZERO		0.0004	0.0490	0.0000	0.9506
19	RUT	ZERO	*	0.2455	0.2347	0.0009	0.5189
21	STRIP	STRIP		0.0573	0.9360	0.0021	0.0046
22	ZERO	ZERO		0.0688	0.0111	0.0007	0.9194
23	RUT	RUT		0.8487	0.0005	0.1188	0.0320
24	TC	TC		0.0020	0.0044	0.9936	0.0000

* Misclassified observation

Figure 8.6 Discriminant Analysis Showing Distresses Being Classified

$D_i^2 = (x - \overline{x}_i)^T S^{-1} (x - \overline{x}_i)$ .... Equation 8.2

Where,

D_i^2 = Mahalanobis Distance

x = Sample Vector (laboratory measured data)

$\overline{x}_i$ = Sample Mean Vector (Appendix D)

S = Pooled within-class covariance matrix (Appendix D)

T = Transpose of a Matrix

Assign observation **X** to population **i** if,

$D_i^2 = \min \{ D_1^2, D_2^2, D_3^2, D_4^2 \}$ ..... Equation 8.3

The values in $\mathbf{X}_i$ and **S** matrices in Appendix D were obtained from analyzing 21 observations with 12 variables as explained previously. Twelve variables were the minimum required in this study to produce a perfect classification. Data in Table 8.3 were used to create the $\mathbf{X}_i$ and **S** matrices which could be used to classify any unknown dense bituminous concrete mixture into one of the four distress categories selected in this study. For example, to identify what distress may develop using a given asphalt mixture, the following steps need to be carried out. Compute ($\mathbf{X} - \mathbf{X}_i$) and the covariance matrix and use Equation 8.2 to compute $\mathbf{D}_i^2$. Finally using Equation 8.3, the sample belongs to distress i, {i=1(zero), 2(rutting), 3(thermal cracking), 4(stripping)} corresponding to the minimum D_i^2. An illustrated example is presented in Appendix D.

8.3 CP and STEPWISE Procedure

An effort was made to develop a model for predicting rutting using laboratory measured data only. As above, data from samples that were obtained from between the wheel path were used because the pavement in this location was considered to better represent the as built condition of the pavement.

The test data used is given in Table 8.4. Each data point represents an average of the test results in each cell. For example, there were seven measurements of bulk specific gravity for each cell, but only the average value was used in the analysis. Averaging the data to a single point in every cell created a problem in terms of degrees of freedom for the models to be developed within each distress category. For example, there is rut depth data available in every distress category, but developing rut depth models in each distress category would be difficult because of the limited degrees of freedom. But by taking the entire data and developing the same model for rutting would provide sufficient degrees of freedom for the analysis. Thus, the 18 laboratory measurements and enumerated values were used as independent variables in the model development. It was necessary to determine how many variables were required to fit a model.

A CP procedure (Little et. al., 1991) was used to obtain a plot indicating the minimum number of observations required to fit the model. This result is shown in Figure 8.7.

In conjunction with the CP procedure, a forward stepwise regression was performed to identify which variables were significant and should be used in the model construction. A

Table 8.4. Data Used In Model Development

CODE	DISTRESS	RUTD (in.)	TRUCKS (per day)	LONGTC (ft.)	BLOCKC (sq.ft.)	N30	N50	N100	KINV (CSt.)	ABSV (Poise)	PVN	BSG	MARSH (LBS.)
318	zero	0.2	4033	24	5	.	48.1	56.4	664	25794	−0.94	2.3723	1438
618	zero	0	66	0	0	24.9	46	50	673		−0.85	2.2501	386
818	zero	0	217	18	0	27	50.1	50.4	843		−0.99	2.4218	2119
118	zero	0	1480	0	0	8.8	32.1	25	1282		−0.37	2.2290	1125
718	zero	0.13	3765	0	0	13.9	41	41.7	1026		−0.44	2.2137	1438
218	zero	0	78	14	0	20	43	46	903	20489	−0.49	2.3555	2606
418	zero	0	67	12	3	23.2	57.2	73	800		.	2.4084	1733
518	zero	0.22	2880	0	0	29.8	59.3	62.8	816		−0.40	2.3977	2316
528	rut	0.75	2850	0	0	42.2	76.4	64.5	799	18220	−0.48	2.2960	1221
728	rut	0.8	3383	30	0	18.9	52.8	68.7	558	6870	−1.09	2.3860	1490
428	rut	0.25	67	214	0	15.4	52.1	68.4	604	8448	−0.74	2.4974	1929
828	rut	0.2	303	47	0	14.6	35.9	38.5	1303	63965	−0.52	2.3069	2069
328	rut	0.78	1563	82	0	18	47.5	53.1	717	14151	−0.98	2.4309	2068
128	rut	0.55	1621	5	0	16.9	56.4	63.2	554	8894	−1.11	2.3756	1484
628	rut	0.41	57	34	0	29.2	60	56.4	920	29643	−0.73	2.1631	1610
238	tc	0	95	129	456	.	.	.	627	12435	−0.81	2.3934	.
738	tc	0.63	5676	11	0	.	.	.	1124	41195	−0.44	2.3102	.
438	tc	0.3	164	85	259	.	.	.	1374	65886	−0.42	2.2231	.
338	tc	0	2243	0	1309	.	.	.	1582	41580	−0.33	2.3628	2598
538	tc	0	2890	86	16	.	.	.	707	15652	−1.04	2.3400	1592
838	tc	0	179	43	142	.	.	.	548		−0.83	2.4093	1256
748	strip	0.45	5786	4	0	.	.	.	463	4125	−1.14	2.3828	2004
348	strip	0.25	2356	54	0	.	.	.	776	17360	−0.78	2.3551	1833
548	strip	0.44	3001	0	0	.	.	.	691	12030	−0.51	2.3251	1297
848	strip	0	1056	89	20	.	.	.	1420		−0.31	2.3622	1952

Note: See Appendix C For Key

Table 8.4 Continued

CODE	DISTRESS	FLOW (0.01")	Q	PEN (MM.)	ASP CONTENT (%)	AIR VOID (%)	E1HZ20 (PSI)	E1HZ30 (PSI)	E4HZ20 (PSI)	E4HZ30 (PSI)	E8HZ20 (PSI)	E8HZ30 (PSI)
318	zero	16.3	88.5	24	4.9	3.2	1.41E+06	7.71E+05	1.77E+06	9.71E+05	1.99E+06	1.09E+06
618	zero	14.0	27.6	26.5	4.8	8.1	8.30E+05	4.50E+05	1.04E+06	5.65E+05	1.17E+06	6.34E+05
818	zero	18.3	116.1	16	4.8	2.3	1.95E+06	1.15E+06	2.45E+06	1.44E+06	2.75E+06	1.62E+06
118	zero	14.3	78.9	18	6.1	9.9	6.85E+05	3.69E+05	8.86E+05	4.77E+05	1.01E+06	5.42E+05
718	zero	15.7	91.8	23.5	5.1	9.6	7.28E+05	3.96E+05	9.21E+05	5.01E+05	1.04E+06	5.64E+05
218	zero	15.5	168.1	26.5	4.9	7.3	8.85E+05	4.77E+05	1.11E+06	6.00E+05	1.25E+06	6.73E+05
418	zero	12.3	140.5	.	.	4.6	.	6.50E+05	.	.	.	.
518	zero	9.0	257.3	33	4.9	0.8	1.50E+06	7.68E+05	1.89E+06	9.68E+05	2.12E+06	1.09E+06
528	rut	8.3	146.5	31	5.1	5.5	9.22E+05	4.74E+05	1.17E+06	6.00E+05	1.32E+06	6.75E+05
728	rut	13.8	108.4	27.5	5	2.9	1.39E+06	7.48E+05	1.75E+06	9.44E+05	1.97E+06	1.06E+06
428	rut	11.0	175.4	35	5.6	0.6	1.30E+06	6.26E+05	1.66E+06	8.02E+05	1.88E+06	9.07E+05
828	rut	16.3	127.3	15.5	4.5	7.3	1.25E+06	7.52E+05	1.56E+06	9.39E+05	1.74E+06	1.05E+06
328	rut	16.3	127.2	20.5	5.4	1.8	1.62E+06	8.85E+05	2.06E+06	1.13E+06	2.33E+06	1.27E+06
128	rut	13.3	111.3	25	5.3	3.1	1.28E+06	6.76E+05	1.63E+06	8.61E+05	1.84E+06	9.71E+05
628	rut	14.3	112.3	19.5	4.9	9.5	8.38E+05	4.75E+05	1.06E+06	5.99E+05	1.19E+06	6.73E+05
238	tc	.	.	30.5	5.3	3.4	1.12E+06	5.69E+05	1.42E+06	7.23E+05	1.60E+06	8.15E+05
738	tc	.	.	20.5	4.9	6.4	1.10E+06	6.22E+05	1.39E+06	7.84E+05	1.56E+06	8.79E+05
438	tc	.	.	16	5.4	8.8	9.21E+05	5.25E+05	1.17E+06	6.69E+05	1.33E+06	7.56E+05
338	tc	17.0	152.8	14.5	5.3	4.8	1.44E+06	8.31E+05	1.83E+06	1.06E+06	2.06E+06	1.19E+06
538	tc	15.3	103.8	19	5.1	4.4	1.34E+06	7.50E+05	1.69E+06	9.50E+05	1.91E+06	1.07E+06
838	tc	15.0	83.7	36	5.8	2.4	1.00E+06	4.73E+05	1.29E+06	6.08E+05	1.46E+06	6.90E+05
748	strip	12.3	163.6	31.5	5.4	3.1	1.11E+06	5.58E+05	1.41E+06	7.11E+05	1.60E+06	8.02E+05
348	strip	19.0	96.5	23	5.4	6.4	9.35E+05	4.98E+05	1.19E+06	6.36E+05	1.35E+06	7.18E+05
548	strip	15.7	82.8	36.5	5.4	5.6	7.71E+05	3.72E+05	9.84E+05	4.74E+05	1.11E+06	5.36E+05
848	strip	14.0	139.4	17.5	4.6	6.2	1.29E+06	7.60E+05	1.62E+06	9.50E+05	1.81E+06	1.06E+06

See Appendix C For Key

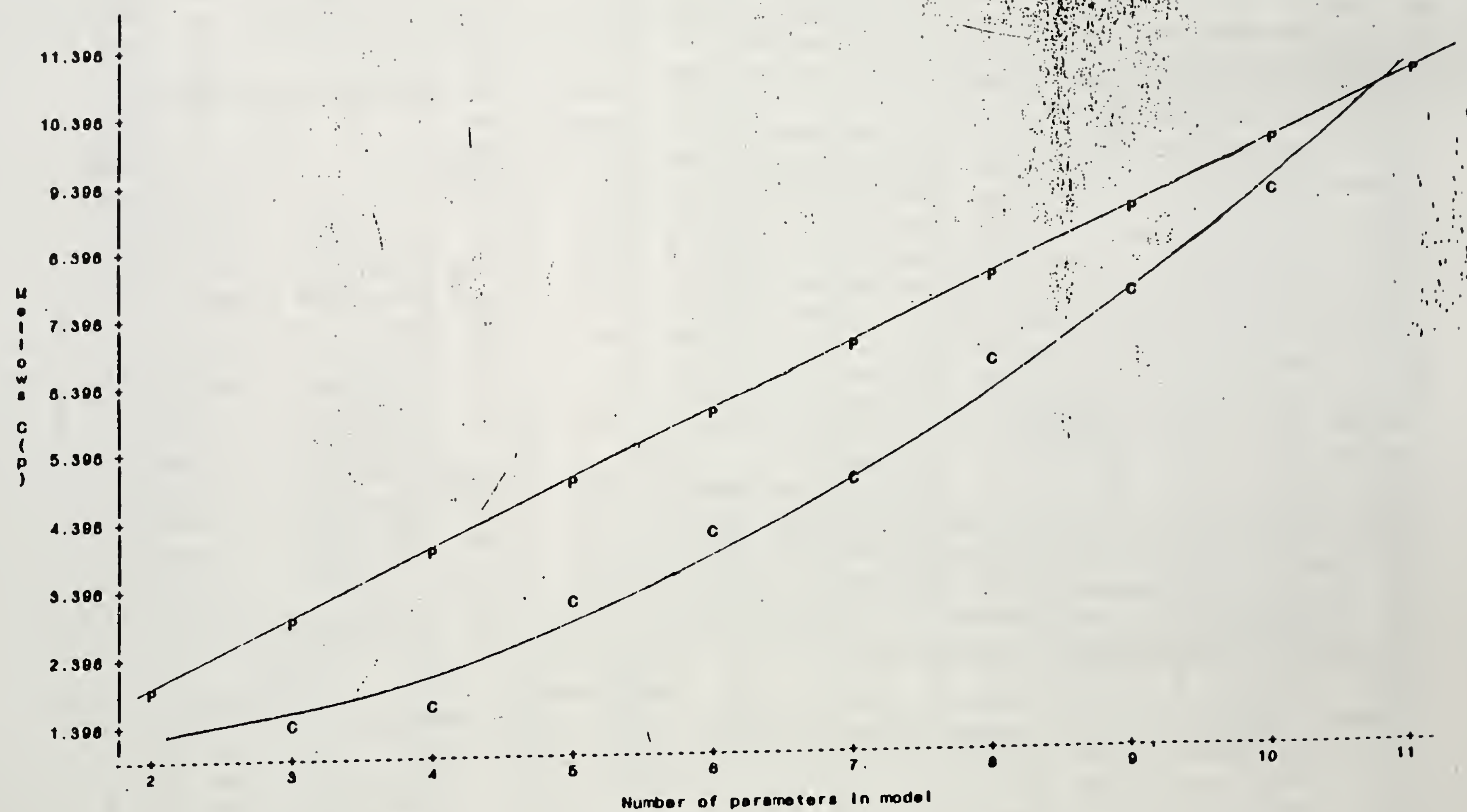

Figure 8.7. CP Plot Showing Minimum Number of Parameters Required in Rutting Model

summary of the SAS output is shown in Figure 8.9.

The final step in building the distress prediction model was to develop the regression model. Table 8.5 shows the rutting model with the adjusted R^2 value. The regression analysis output showing the parameter values in the model is presented in Figure 8.10. With an adjusted R^2 value of 0.61, this model would have to be categorized as a weak predictor of rutting distress. The model would need to be tested over a larger data set before being utilized for evaluating bituminous mixtures.

8.4 Conclusion

Statistical analysis of the data has permitted inferences to be made about asphalt mixture performance. ANOVA of factors in a 2^3 design of experiment showed that only Base Type and Wheel Path were significant in the performance of rutted pavement sections. All other effects were insignificant. A discriminant analysis successfully categorized all the pavements in the study into their respective distresses. As a result, criteria was established that could be used to assign an unknown bituminous mixture to a particular distress category based on laboratory test results. A combination of CP, stepwise regression and linear regression procedures was used to develop a model for predicting rutting distress. This model is suggested to be used during the mix design stage as an indicator of distresses that might occur in a pavement. The model needs to be tested on a larger data base before broad application to mix design specifications.

Summary of Forward Selection Procedure for Dependent Variable RUTD

Step	Variable Entered	Number In	Partial R**2	Model R**2	C(p)	F	Prob>F
1	N100	1	0.3843	0.3843	103.6325	8.8681	0.0236
2	TRUCKS	2	0.1193	0.5036	83.7235	2.4039	0.1521
3	PVN	3	0.0713	0.5749	72.6962	1.5090	0.2504
4	KINV	4	0.0689	0.6438	62.0981	1.6482	0.2488
5	E4HZ30	5	0.0415	0.6854	56.5059	0.9242	0.3684
6	AIR	6	0.0265	0.7119	53.6574	0.5525	0.4854
7	N30	7	0.0800	0.7919	41.0425	1.9209	0.2244
8	FLOW	8	0.1375	0.9294	17.9071	7.7897	0.0493
9	N50	9	0.0289	0.9583	14.6301	2.0748	0.2454
10	BSG	10	0.0224	0.9806	12.6377	2.3137	0.2678
11	E1HZ20	11	0.0139	0.9945	12.0000	2.5377	0.3569

Figure 8.9. Summary of Forward Stepwise Regression Procedure For Rutting Model

Table 8.5. Summary of Model for Predicting Rutting Distress

MEASURED DISTRESS	INDEPENDENT VARIABLES IN MODEL	ADJ. R^2
Rut Depth (in.)	1.4867 + 0.0047(KINV) + 0.000143(Trucks) + 0.0535(N30) + 0.0143(N100) - 2.8737(PVN) - 1.9077(BSG) + 0.2144(Flow) - 0.5503(Air) - 0.00000253(E1HZ20) - 0.00000237(E4HZ30)	0.61

Where:

- KINV = Kinematic Viscosity in Centi-Stokes of recovered asphalt cement.
- Trucks = Average annual daily trucks in one direction
- N30 = Percent of silicious material in aggregates retained on No.30 sieve and passing No.16 sieve.
- N100 = Percent of silicious materials retained on No.100 sieve and passing No.50 sieve.
- PVN = Pen-Vis Number of Asphalt Cement.
- BSG = Bulk specific gravity.
- Flow = Deformation measured in Marshall Testing of Cores.
- Air = Percent of air voids in compacted bituminous concrete.
- E1HZ20 = Dynamic Modulus of bituminous concrete tested at a frequency of 1 hz and temperature of 20° Centigrade.
- E4HZ30 = Dynamic Modulus of bituminous concrete tested at a frequency of 1 hz and temperature of 30° Centigrade.

Analysis of Variance

Source	DF	Sum of Squares	Mean Square	F Value	Prob>F
Model	10	1.08673	0.10867	2.868	0.2862
Error	2	0.07580	0.03790		
C Total	12	1.16252			

Root MSE	0.19467	R-square	0.9348
Dep Mean	0.31462	Adj R-sq	0.6088
C.V.	61.87664		

Parameter Estimates

Variable	DF	Parameter Estimate	Standard Error	T for H0: Parameter=0	Prob > |T|
INTERCEP	1	1.486695	18.66026046	0.080	0.9438
KINV	1	0.004668	0.00216223	2.159	0.1635
TRUCKS	1	0.000143	0.00006724	2.122	0.1679
N100	1	0.014281	0.01302943	1.096	0.3874
PVN	1	-2.873693	1.66335367	-1.728	0.2262
DSG	1	-1.907737	5.15118490	-0.370	0.7467
FLOW	1	0.214383	0.11456634	1.871	0.2022
E4HZ30	1	-000002374	0.00001451	-0.164	0.8851
AIR	1	-0.550254	0.44776513	-1.229	0.3441
N30	1	0.053496	0.03107906	1.721	0.2273
E1HZ20	1	-0.000002528	0.00001216	-0.208	0.8546

Figure 8.10. Parameter Estimates of the Rutting Model.

CHAPTER 9. RECOMPACTION STUDY OF FIELD CORES AND COMPARISON WITH LABORATORY COMPACTION

A study was undertaken to investigate the properties of recompacted bituminous field cores that were obtained from distressed pavement sections in Indiana and compare them with characteristics of laboratory compacted cores. The gyratory compactor was used to recompact the material from the field cores. As a result, data was generated for GCI (gyratory compactibility index), GSI (gyratory shear index), GSF (gyratory shear factor), and maximum shear strain. These gyratory characteristics provide indications about the condition and performance of the bituminous mixtures.

9.1 Sample Preparation

The field cores that were used for the dynamic creep study in Chapter 7 were reused for the recompaction study. Additional cores that could not be tested for dynamic creep were also used for recompaction. Table 9.1 shows the cores that were used in the recompaction. The samples were first stripped of their end caps and then heated to loosen the mixture. Aggregates with cut faces were removed to reduce bias in the test results for maximum specific gravity. Material was combined from cores with the same distress and compacted into cores 4" in diameter and about 2.5" high. A Model 4C gyratory testing machine was used for the recompaction.

Table 9.1. Core Samples in Recompaction Study

CLIMATE		NORTH								SOUTH							
TRUCK TRAFFIC		HIGH				LOW				HIGH				LOW			
BASE TYPE	WHEELPATH	ZERO	RUT	STRIP	T.CR.	ZERO	RUT	T.CR.	STRIP	ZERO	RUT	T.CR.	STRIP	ZERO	RUT	T.CR.	STRIP
FLEXIBLE	WP		121 125 126			214 216 217		235		514	525 527	535 537	546	6112 6113 6114	6213		
RIGID	BWP	314	325 326 327	335 336	345		4213			7112 7114	7213 7214	7312	7413 7414	815 816 817	825 826 827	835 836 837	845 846

9.2 Recompaction

A total of twenty-two cores were recompacted using the gyratory testing machine in accordance to ASTM D 3387-83. Compaction conditions are shown in Table 9.2.

Table 9.2 GTM Recompaction Conditions

DESCRIPTION	CRITERIA
Sample Size	4" Diameter, 2.5" High
Compaction Temperature	250° F
Ram Pressure	120 psi
Roller Type	Oil
Gyratory Angle	1°
Number of Revolutions	60

After compaction the samples were left in the molds to cool for an hour under a fan before being extracted for testing.

9.3 Testing

The recompacted cores were tested to obtain mixture characteristics according to the methods shown in Table 9.3.

Table 9.3. Test Methods To Obtain Recompacted Mixture Characteristics

MIXTURE CHARACTERISTICS	TEST METHOD
Bulk Specific Gravity (SSD)	D 2726-90
Marshall Stability & Flow	D 1559-89
Maximum Theoretical Specific Gravity	D 2041-91
Air Void Content	D 3203-91
Voids in Mineral Aggregate	Asphalt Institute MS-2

9.4 Results

A summary of the results of the recompaction study is given in Table 9.4. Data for the mixture characteristics of the original field cores before they were tested for dynamic creep are included in this table. As a result, a comparison can be made of the original and recompacted cores. A comparison of the results could indicate the effect of compaction and loading on distress type and binder properties.

9.5 Comparison With Laboratory Compaction

The data in Table 9.4 and those from Table 3.3 were used to make the comparison between the recompacted field mixture cores and laboratory mix design cores in terms of compaction density and void content. Since the recompaction of the field material cores was achieved using the GTM machine, results from the laboratory GTM mix design will be used in the comparison.

9.5.1 Bulk Specific Gravity and Air Void Comparison

The bulk specific gravity and air void content of the field cores before and after recompaction are plotted in Figures 9.1 and 9.2, respectively. Bulk specific gravities of in situ cores are plotted in Figure 9.1 against bulk specific gravities of laboratory compacted cores at both 30 and 60 revolutions of the GTM. The first obvious point is that the variation of the bulk specific gravities at 30 revolutions and

Table 9.4. Test Results of Recompacted Cores

CORE #	AGE YEARS	BULK SG (RECOMP. CORES, 60 REV.)	BULK SG (RECOMP. CORES, 30 REV.)	BULK SG (ORIG. CORES)	MAX. SG	MARSHALL STABILITY (LBS)	FLOW (0.01")	AIR VOIDS (RECOMP. CORES)	AIR VOIDS (ORIG. CORES)	ASPHALT CONTENT %	DISTRESS TYPE	VMA %	PCI
4213	12	2.5350	2.4712	2.5151	2.5369	3225	10	0.08	0.5	5.8	Rutting	10.73	61
124	15	2.4254	2.3221	2.4211	2.4378	2433	13	0.51	1.07	5.4	Rutting	14.23	34
7213	3	2.3840	2.3045	2.3871	2.4487	2197	10	2.64	1.1	4.8	Rutting	15.15	38
816	5	2.3370	2.2019	2.4315	2.4782	3639	10	5.70	1.28	4.6	Control	16.65	95
316	5	2.3947	2.3077	2.4211	2.4705	1554	11	3.07	1.51	4.7	Control	14.69	60
327	15	2.4122	2.3109	2.4312	2.4587	2137	10	1.89	2.06	5.3	Rutting	14.6	38
835	12	2.4196	2.3221	2.4059	2.4757	2535	11	2.27	2.39	5.8	Th. Cracking	14.79	57
525	14	2.3441	2.2468	2.3713	2.4475	2512	16	4.23	2.5	5.3	Rutting	17.02	38
7413	12	2.3823	2.2981	2.3808	2.4206	3060	10	1.58	2.79	5.4	Stripping	15.75	29
535	15	2.3841	2.3045	2.3587	2.4160	2819	11	1.32	3.58	5.3	Th. Cracking	15.6	79
235	9	2.3911	2.2933	2.3803	2.4506	2661	12	2.43	3.89	5.5	Th. Cracking	15.53	58
515	14	2.3931	2.3173	2.4013	2.4207	2571	9	1.14	3.99	5.8	Control	15.73	84
546	6	2.4267	2.3429	2.2499	2.4547	2812	12	1.14	5.07	4.9	Stripping	13.73	32
345	10	2.3862	2.2869	2.4172	2.5020	3263	11	4.63	5.21	5.1	Stripping	15.34	59
7312	13	2.3216	–	2.3314	2.3913	3444	11	2.92	5.79	4.7	Th. Cracking	17.29	45
214	16	2.4077	2.2949	2.3307	2.4786	2833	13	2.86	6.51	4.7	Control	14.22	94
335	11	2.3736	2.2901	2.3631	2.4651	3560	12	3.71	6.54	4.9	Th. Cracking	15.62	53
825	9	2.3988	2.2596	2.3301	2.4940	4340	11	3.82	6.99	5.9	Rutting	15.62	37
845	10	2.3793	2.2885	2.3313	2.4843	2849	12	4.23	7.15	4.6	Stripping	15.14	70
6113	2	2.4107	2.3045	2.3608	2.4269	3103	9	0.67	8.14	5.9	Control	15.2	100
6213	19	2.3717	2.2580	2.2134	2.4529	3006	12	3.31	9.54	5	Rutting	15.77	25
7114	4	2.3760	2.2516	2.3903	2.4827	3342	8	4.30	9.6	4.5	Control	15.18	99

Table 9.4 Continued

CORE #	GTM BULK SG 30 REV. (pcf)	GTM BULK SG 60 REV. (pcf)	ANGLE (INITIAL)	ANGLE (MAX.)	GTM ROLLER PRESSURE 30 REV. (PSI)	GTM ROLLER PRESSURE 60 REV. (PSI)	C.I.*	GSF* 30 REV.	GSF* 60 REV.	S.I.*	MAX. SHEAR STRAIN
4213	154.2	157	10.3	10.8	52	51.3	0.982	20.05	20.33	1.05	2.36
124	144.9	147.7	11	11.6	44.3	43.3	0.981	22.56	23.08	1.05	2.54
7213	143.8	146.2	9.7	9.6	49.3	47.3	0.984	20.07	20.92	0.99	2.10
816	137.4	139.8	9.5	9.4	47.3	49.3	0.983	20.43	19.60	0.99	2.06
316	144	146	9.1	9	35	34.3	0.986	31.83	32.48	0.99	1.97
327	144.2	146.7	9.6	9.9	55.7	54	0.983	18.09	18.66	1.03	2.17
835	144.9	147.9	9.6	9.9	53.7	52.7	0.980	18.59	18.95	1.03	2.17
525	140.2	142.7	9.5	9.4	57.3	58.3	0.982	16.37	16.09	0.99	2.06
7413	143.4	146.2	9.3	10.1	55.3	52.3	0.981	17.82	18.84	1.09	2.21
535	143.8	146	10	10.2	56.3	52.7	0.985	17.71	18.92	1.02	2.23
235	143.1	145.7	9.4	9.5	49.7	46	0.982	19.51	21.08	1.01	2.08
515	144.6	146.8	9.9	9.8	49.7	50.3	0.985	20.16	19.92	0.99	2.14
546	146.2	149	9.1	9.2	54.7	54.7	0.981	18.38	18.38	1.01	2.01
345	142.7	145.2	9.3	9.4	45	43	0.983	21.58	22.58	1.01	2.06
7312	–	141.1	9.4	9.2	25.7	26.7	0.000	20.00	20.00	0.98	2.01
214	143.2	146.1	9.5	9.3	59	55	0.980	16.71	17.92	0.98	2.03
335	142.9	145.2	9.6	9.8	51	50.3	0.984	20.16	20.44	1.02	2.14
825	141	144.1	9.7	9.7	51	52	0.978	18.95	18.59	1.00	2.12
845	142.8	145.4	10.5	10.3	53.3	51	0.982	17.71	18.51	0.98	2.25
6113	143.8	146.3	9.8	9.9	58.7	59	0.983	16.95	16.87	1.01	2.17
6213	140.9	144.4	9.9	10.5	58.7	56.7	0.976	16.30	16.87	1.06	2.30
7114	140.5	143.3	10.2	10.8	59	59.3	0.980	16.46	16.38	1.06	2.36

*NOTES: C.I. – COMPACTIBILITY INDEX S.I. – STABILITY INDEX

GSF – GYRATORY SHEAR FACTOR

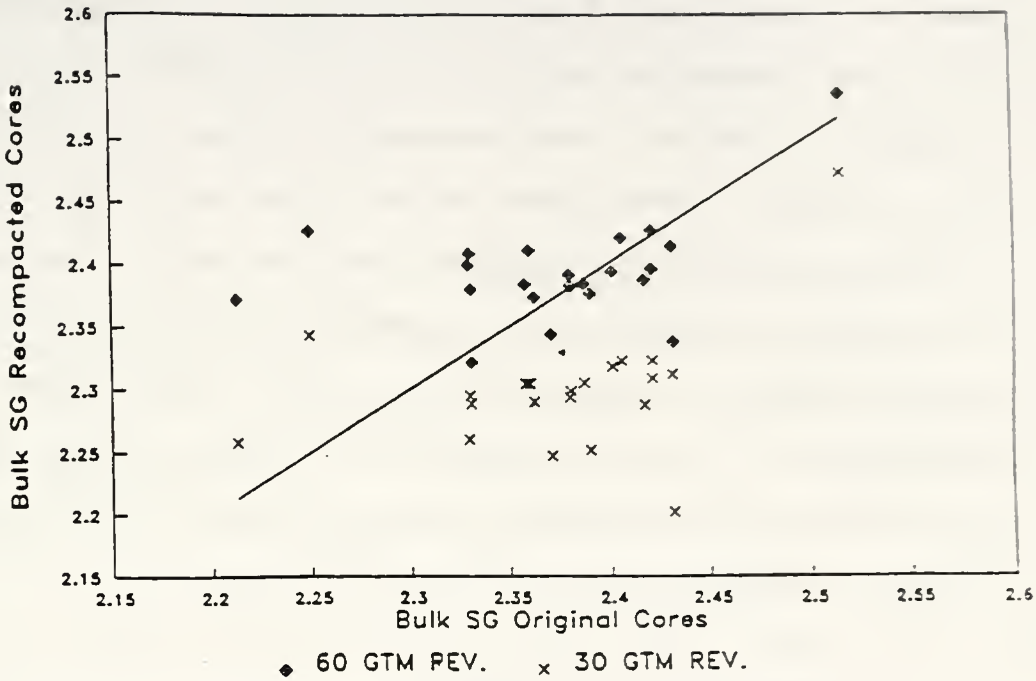

Figure 9.1. Comparison of Recompacted and Field Bulk Specific Gravity

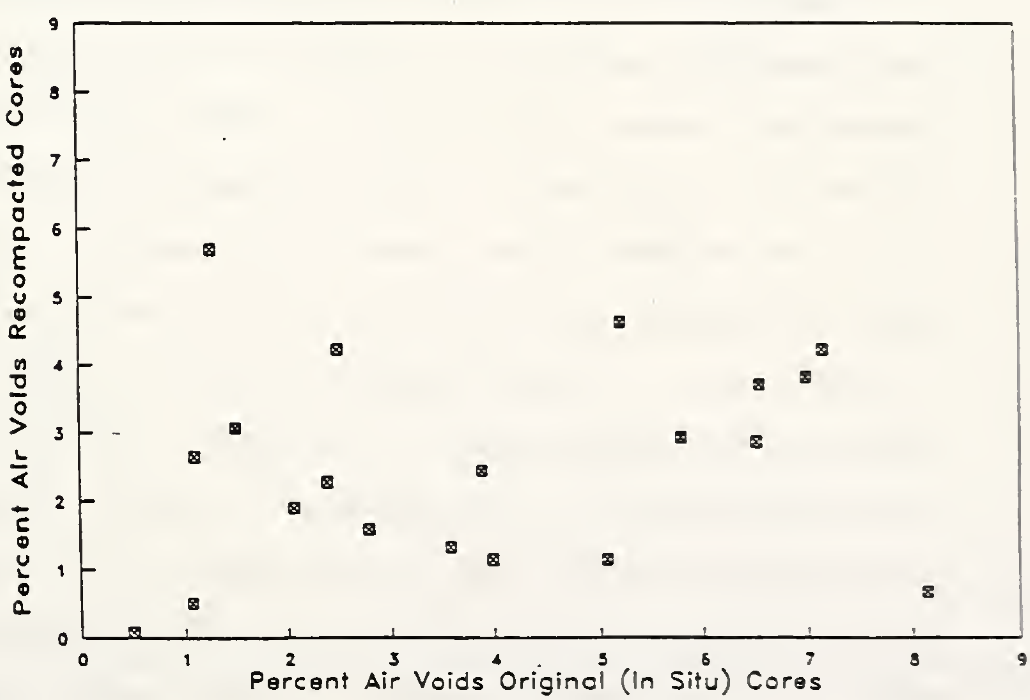

Figure 9.2. Comparison of Recompacted and Field Percent Air Voids

60 revolutions is similar. The difference is approximately 0.1 or 6 pcf. As a result, subsequent analyses and plots of physical properties are shown only for the 60 revolution GTM compaction effort. One conclusion is that any differences in the mixture compositions do not have an effect on the bulk specific gravity achievable with the GTM. The recompacted bulk specific gravities (60 revolutions) plotted in Figure 9.1 have minimal correlation with the field core specific gravities ($r^2 = 0.27$). Figure 9.2 is a plot of the recompacted air voids (60 revolutions) and air voids of the field cores. Again, the correlation is low ($r^2 = 0.35$).

9.5.2 Frequency Distributions

Figures 9.3 and 9.4 are frequency distributions plots for bulk specific gravity of both the in situ cores and recompacted cores, respectively. These plots show several interesting relationships. The distributions have differences as well as similarities. Both distributions indicate the highest frequency of occurrence of bulk specific gravity is the same, 2.4. This indicates that the GTM, with the compaction conditions used in this study, recompacts material to the same density as is achieved in situ. However, this bulk specific gravity is lower than that achieved with original asphalt and aggregate in the mix design as shown in Table 3.3. In this table, the GTM bulk specific gravity at optimum asphalt content is 2.53. The mixture on which the data in Table 3.3 is based is a #9 binder, which is similar to the binder mixes from the in situ pavements.

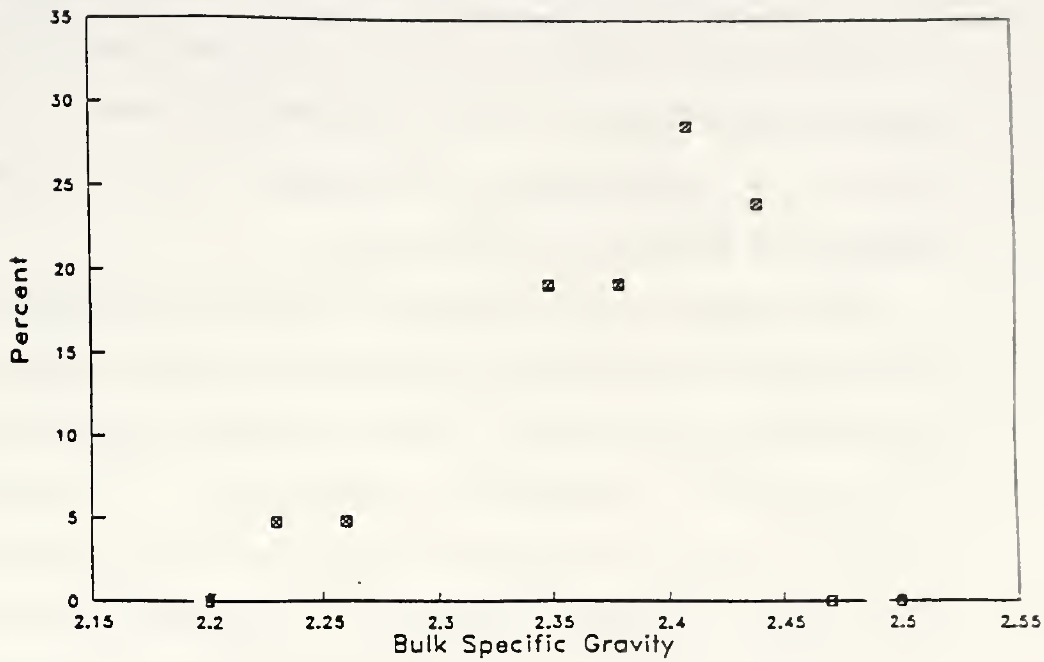

Figure 9.3. Bulk Specific Gravity Frequency Distribution (In Situ Cores)

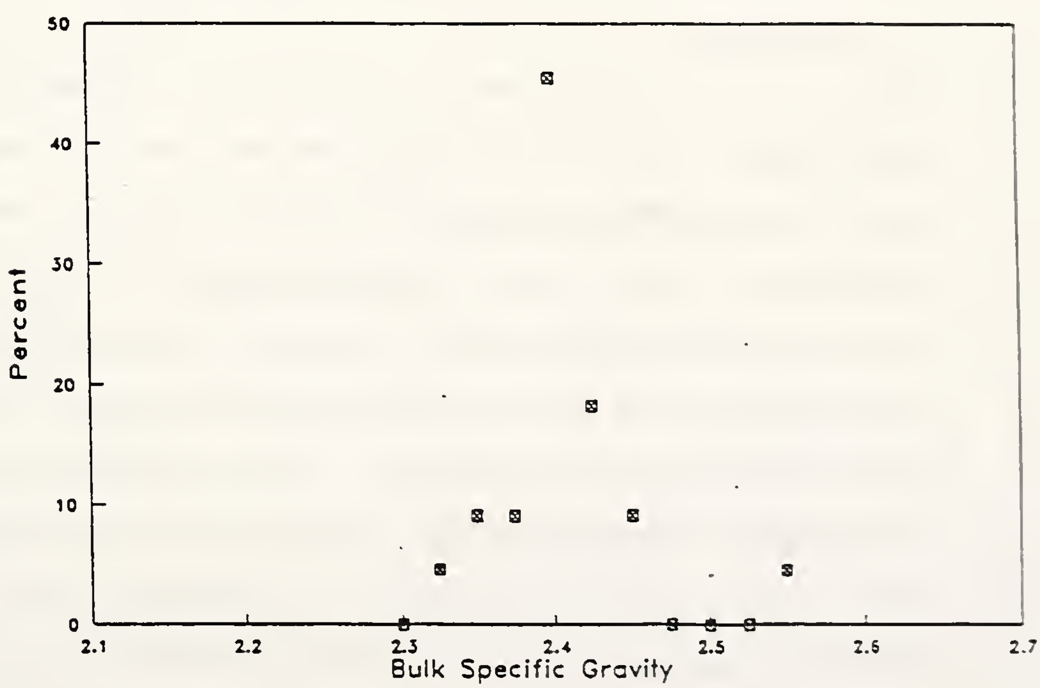

Figure 9.4. Bulk Specific Gravity Frequency Distribution (Recompacted Cores)

However, a temperature of 275°F was used during compaction. The in situ bulk specific gravity is lower than the optimum mix design bulk specific gravity, discounting the compaction temperature difference, by an amount equivalent to 6 to 8 pcf. This is a significant difference and suggests higher constructed density is achievable.

The forms of the frequency distributions are different. GTM compaction produces a reasonably normal distribution of bulk specific gravities. This would be expected because of the controlled compaction conditions. In contrast, the frequency distribution of bulk specific gravities from the in situ cores is skewed. There is a significant tail of lower bulk specific gravities. This indicates that lack of uniform field compaction produces greater variation.

Frequency distributions of air voids are plotted in Figure 9.5 and 9.6 for in situ and recompacted cores, respectively. Because of the dependency of air voids on bulk specific gravity these distributions exhibit characteristics that mirror those of bulk specific gravity in Figures 9.3 and 9.4. As with the bulk specific gravity distributions, the air void distribution for in situ cores is skewed. The tail is toward higher air void content. Both distributions indicate the highest frequency of air voids within approximately the same range, 2.3 to 2.5 percent. As expected, this indicates the GTM is effective in compacting mixtures to an air void level that agrees with in situ air voids. Also, GTM compaction for original mix design produces a lower range of air voids. The value of the lowest air void content is lower than that in the field.

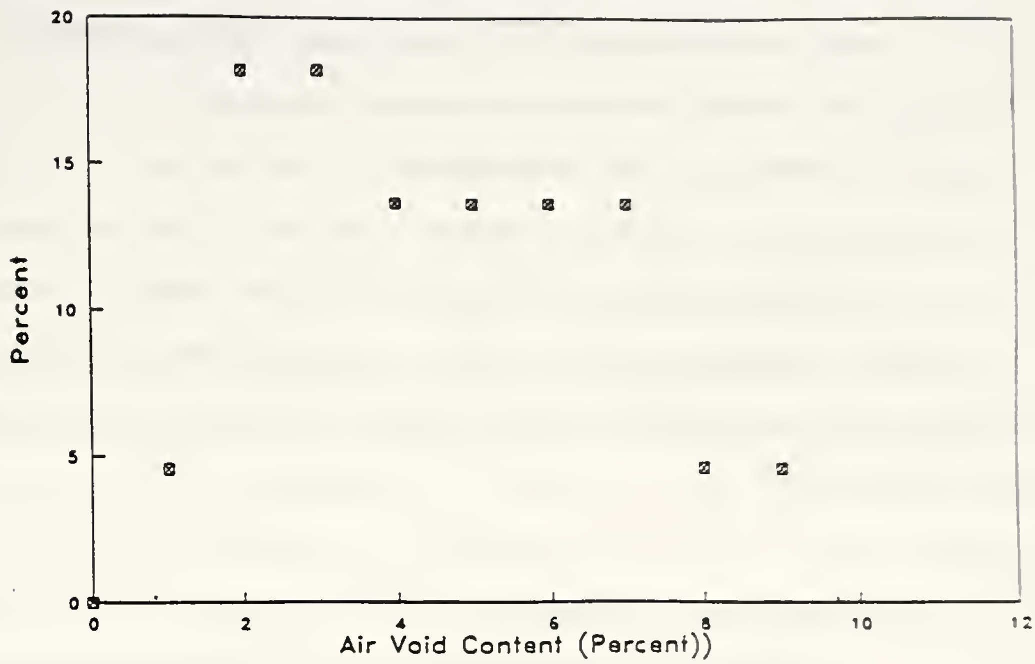

Figure 9.5. Air Void Frequency Distribution (In Situ Cores)

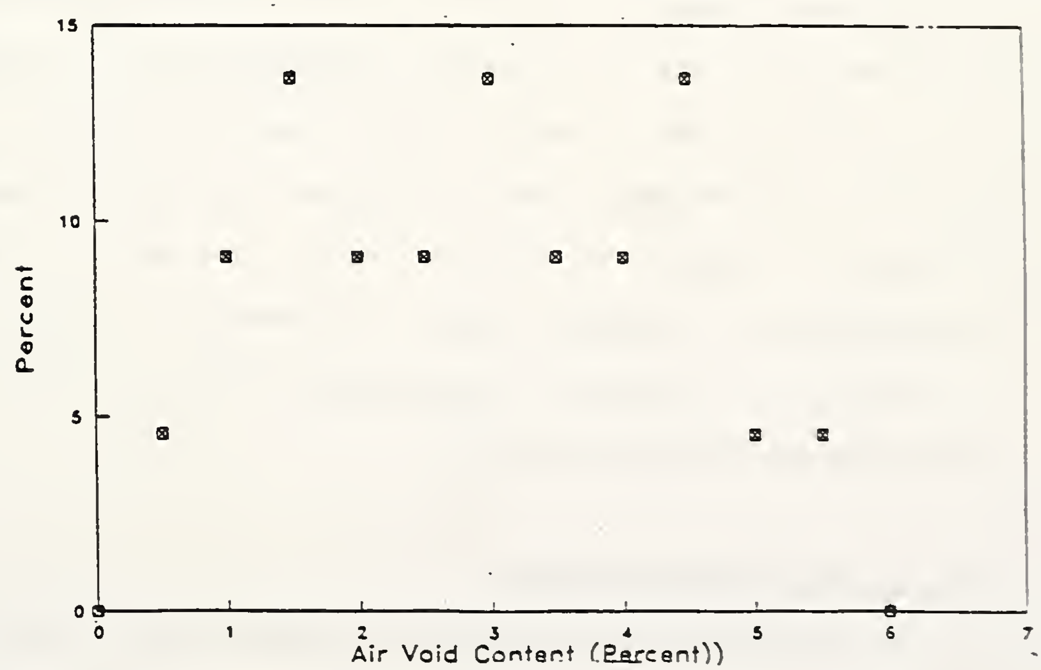

Figure 9.6. Air Void Frequency Distribution (Recompacted Cores)

This suggests that the GTM is capable of discriminating mixtures with more or less resistance to compaction.

The data from Table 3.3 for the GTM mix design of the #9 binder mix indicates an air void content of 1.4 percent. This air void content is too low. Review of the mix design indicates the asphalt content is too high by approximately 0.75 percent asphalt content. A lower asphalt content would result in improvement of the mix design by producing a higher air void content, higher voids in the mineral aggregate and lower flow.

9.5.3 Asphalt Content

The asphalt content of in situ pavements shown in Table 9.4 ranges from 4.5 to 5.9 percent. In general, pavements with lower asphalt content are performing satisfactory. Such an evaluation has to take into consideration the pavement age.

As pointed out above, GTM compaction tends to identify, at the mix design stage, mixtures with high asphalt content through evaluation of air voids, voids in the mineral aggregate or Marshall flow. As shown in Table 9.4 this is also true, in general, when material from in situ pavement is recompacted using the GTM.

9.6 Core Recompactions

Evaluation of recompacted cores and in situ pavement physical properties relative to pavement performance involved consideration of several factors. In general, as shown in Table 9.4, mixture with adequate air voids after GTM compaction exhibited acceptable performance. The in situ air voids of these mixtures are in agreement with air voids resulting from GTM recompaction. Exceptions are cores 816 and 316. Cores from these pavements indicate very low in situ air voids. However, the pavements are only 5 years old and have relatively low asphalt contents of 4.6 and 4.7 percent, respectively. Both pavements are classified as control pavements (no distress). However, the pavement for core 316 is in poorer condition (PCI = 60) and has lower recompacted air voids (3.07 percent). Overall, air voids and asphalt content are related to pavement condition. There does not seem to be a significant relationship between the voids in the mineral aggregate and measures of performance.

CHAPTER 10. CONCLUSION AND RECOMMENDATION

As a result of this research, a number of significant observations are made that explain the performance of asphalt pavements in Indiana. The observations are based on analyses of physical and mechanical properties of asphalt mixture samples obtained from in service pavements as well as those prepared in the laboratory. These properties were related to the in service pavement condition. The conclusions that can be drawn from this study are:

1. From the study of compactive effort and mix design the mix design criteria recommended by the Asphalt Institute results in an asphalt content that is too high. This is justification for use of a modified mix design criteria that produces a lower asphalt content.
2. Comparison of bulk densities produced during mix design and those from recompacting material from in service pavements indicates that higher constructed density is achievable. A higher compactive effort during construction would produce both higher and more uniform density.
3. A gyratory compactive effort of one degree angle of gyration, 120 psi pressure and 60 revolutions at a temperature of 250°F produces a mean bulk density and air voids that compares with those of in service pavements.
4. GTM recompaction of mixture from in service pavements indicates that the original asphalt content was too high.

5. Mixtures from badly rutted pavement sections with high truck traffic tended to be gap graded. Also, in many cases these gradations were out of the specification limits in the larger sizes.
6. Dynamic testing of field cores produced bituminous concrete modulus values comparable to theoretical dynamic modulus values. Thus, considering the inherent variabilities present in bituminous concrete and given the uncertain nature of asphalts, the theoretical dynamic modulus of bituminous concrete was shown to be a useful substitute in indicating and predicting mixture behavior. The theoretical dynamic modulus is much easier to obtain and can be used as a check when testing bituminous concrete in the laboratory.
7. The dynamic modulus values for bituminous concrete cores from pavement sections with thermal cracking were consistently high at all test temperatures and loading frequencies. Moduli for rutted pavements were low.
8. The lowest modulus values were obtained at high temperature and at slow dynamic loading, similar to a hot day with slow moving, heavy trucks.
9. A factorial analysis with three factors; truck traffic, base type and wheel path; all at two levels; showed that trucks and base pavement type had a measured effect on distress.
10. A criterion for identifying mixtures with distress potential using discriminant analysis has been developed.

This criterion identifies mixtures that will perform well or rut, thermally crack or strip. Mix designs produced in the laboratory could be evaluated using this criterion prior to use in the field.

11. Field samples taken from within a continuous five mile stretch were homogenous, with no significant difference between mixture properties.

It is recognized that INDOT has adopted mix design criteria that is similar to the criteria recommended in this report. Also, quality control procedures now being used should help minimize the variations in gradations and achieve higher and more uniform densities. The tests and analyses utilized in this current study will be helpful in evaluating the benefit of such changes.

10.1 Recommendations for Future Research

Asphalt mix design is an evolving process brought about by changes in materials, loading, base conditions, agency criteria and cost. Because of such changes, there is a continuing need to address a number of issues:

1. Establish a program to obtain limiting criteria for accepting or rejecting a mix design using bituminous concrete dynamic modulus. This research should obtain sufficient samples from pavements with various types of distress, each at low, medium and high levels. The samples should be tested at a range of pavement service temperatures to simulate

in service conditions. The results are intended to associate dynamic modulus with distress type and level, and could be used to develop criteria for predicting performance at the mix design stage.

2. Laboratory dynamic testing should be conducted on bituminous concrete at higher frequencies and test temperatures with better data acquisition equipment.

3. Stripping is a phenomenon that has gained the attention of pavement engineers such that effective measures are being sought to combat it. There is a need to carry out a two-prong study regarding stripping:

    i. Develop a procedure for the identification of stripping by visual or non-destructive methods, and quantify the distress for incorporation into pavement condition surveys. Presently, stripping is not included in any pavement condition survey procedure.

    ii. Stripping is a load related distress. Thus a unique test procedure needs to be developed that simulates the effect of a moving load on a pavement with a high moisture content. A fast moving load can cause high velocity jets of water to pulse through the voids in the bituminous mixture, causing the asphalt film to strip from the aggregate surface. A test that simulates this effect could in the laboratory determine the stripping resistance of a mixture at the laboratory mix design stage.

4. A procedure using discriminant analysis has been developed in this study that identifies mixtures that are prone to rut, thermally crack, or perform well. This procedure should be expanded in two areas:

    i. Expand the data base used to develop the vectors with which an individual asphalt mixture is compared with in predicting its distress category.
    ii. Use the procedure to identify other distresses in bituminous pavements.
    iii. Implement the procedure in Indiana for determining acceptability of a given mix design before it is approved for field use.

LIST OF REFERENCES

Acott, M., "The Design of Hot Mix Asphalt for Heavy Duty Pavements", National Asphalt Paving Association, Quality Improvement Series 111/86, Maryland 1986.

ASTM D 3381-92, American Society for Testing and Materials, Philadelphia, PA, Volume 04.03, 1993.

Badaruddin, S.R., McDaniel, R.S., "Cold In-Place Recycling For Rehabilitation And Widening of Low Volume Flexible Pavements", Transportation Research Record, Transportation Research Board, 71st. Annual Meeting, Washington D.C., (1992).

Badaruddin, S.R., "Performance Evaluation of Bituminous Mixtures Placed Under Quality Assurance", Interim Report, Indiana Department of Transportation, November 1993.

Baladi, G., "Fatigue Life and Permanent Deformation Characteristics of Asphalt Concrete Mixes", Transportation Research Record 1227, Transportation Research Board, Washington, D.C.,1989.

Barksdale, R.D., "Laboratory Evaluation of Rutting in Base Course Materials, Proceedings, Third International Conference on the Structural Design of Asphalt Pavements, Volume 1, London, 1972.

Bibbens, R.F., C.A. Bell, and G.R. Hicks, "Effect of Season of Year on Pavement Response", Transportation Research Record 993, Transportation Research Board, Washington, D. C., 1984.

Bolk, H.J.N.A., "The Creep Test", SCW Record 5, Study Center for Road Construction, Netherlands, 1981.

Bonnaure, F., Gest, G. and Uge, P., "A New Method of Predicting The Stiffness of Asphalt Paving Mixtures", Proceedings, Association of Asphalt Paving Technologists, Volume 46, 1977.

Brown, E.R.., and S.A. Cross, " A study of In-Place Rutting of Asphalt Pavements", Proceedings, Association of Asphalt Paving Technologists, Volume 58, 1989.

Brown, E.R. and Cross, S.A.,"Comparison of Laboratory and Field Density of Asphalt Mixtures", Transportation Research Record 1300, Transportation Research Board, Washington D.C., 1991.

Brown, S.F., and C.A. Bell, "The Validity of Design Procedures for the Permanent Deformation of Asphalt Pavements", Proceedings, Fourth International Conference on the Structural Design of Asphalt Pavements, Volume 1, University Of Michigan, Ann Arbor, 1977.

Brown, S.F., J.N. Preston and K.E. Cooper, "Application of New Concepts in Asphalt Mix Design", Proceedings, Association of Asphalt Paving Technologists, Volume 60, 1991.

Claessen, A.I.M., J.M. Edwards, P. Sommer, and P. Uge, " Asphalt Pavement Design - The Shell Method", Proceedings, Fourth International Conference on the Structural Design of Asphalt Pavements, Volume 1, University of Michigan, Ann Arbor, 1977.

Coffman, B.S., Proceedings, Second International Conference on the Structural Design of Asphalt Pavements, August 1967, p.819.

Consuegra, A., Little, D.,N., Von Quintas, H. and Burati, J., "Comparative Evaluation of Laboratory Compaction Devices Based on Their Ability to Produce Mixtures with Engineering Properties Similar to Those Produced in the Field", Transportation Research Record No. 1228, Transportation Research Board, Washington D.C. (1989).

Department of the Army, "Pavement Maintenance Management", Technical Manual TM 5-623, Washington, D.C., November, 1982.

Dukatz, E.L. Jr., and C.R. Marek," Quality Control Aspects of Production and Handling Aggregates for Use in Asphalt Concrete Mixtures", Proceedings, Association of Asphalt Paving Technologists, Volume 55, 1986.

Elliot, J.F., and F. Moavenzadeh, " Analysis of Stress and Displacements in Three Layer Viscoelastic Systems", Highway Research record 345, Highway Research Board, Washington, D.C., 1971.

Fehsenfeld, F.M., Sr. and Kriech, A.J., "A Comparison Of Mix Design procedure For Mix Design", Heritage Research Group, Indianapolis, USA, 1987.

Finn F.L., Monismith, C.L. and Markevich N.J., "Pavement Performance and Asphalt Concrete Mix Design", Proceedings, Association of Asphalt Paving Technologists, Volume 52, 1983.

Goetz, W.H., " The Evolution of Asphalt Concrete Mix Design" Asphalt Concrete Mix Design : Development of a More Rational Approaches, ASTM STP 1041, W. L. Gartner, Ed., American Society for Testing and Materials, Philadelphia, 1985.

Heukelom, W., "An Improved Method of Characterizing Asphaltic Bitumen with the Aid of Their Mechanical Properties", Proceedings, Association of Asphalt Paving Technologists, Volume 42, 1973.

Hughes, C.S., NCHRP Report No. 152, Compaction of Asphalt Pavement, Transportation Research Board, National Research Council, Washington, D.C., USA, 1989.

Huhtala, M., J. Pihlajamaki, and M. Pienimaki, "Effects of Tires and Tire Pressures on Road Pavement", Transportation Research Record 1227, Transportation Research Board, Washington D.C., 1989.

INDOT, "Quality Assurance Program", 1986, (Not Published).

INDOT, Indiana State Specifications For Construction of Roads And Highways, 1988.

INDOT, "Quality Assurance Questionnaire Results", Division Of Research, (Not Published), 1991.

Jimenez, R.A., "A look at the Art of Asphaltic Concrete Mixture Design", Proceedings, Association of Asphalt Paving Technologists, Volume 55, 1986.

Kandhal, S.P. and W.S. Koehler,"Marshall Mix Design Method: Current Practices", Proceedings, Association of Asphalt Paving Technologists, Volume 54, 1985.

Kandhal, P.S., and W.S. Koehler, "Effect of Rheological Properties of Asphalts on Pavement Cracking", Asphalt Rheology : Relationship to Mixture, ASTM STP 941, Philadelphia, 1985.

Kenis, W. J., "Predictive Design Procedures - A Design Method for Flexible Pavements Using the VESYS structural Sub-System", Proceedings, International Conference on the Structural Design of Asphalt Pavements, Volume 1, University of Michigan, Ann Arbor, 1977

Labtech Notebook Version 4, Manual, Data Acquisition Software, Laboratory Technology Corporation, Maryland, 1986.

Lindly, J.K. "Development of an Overlay Design Procedure for Flexible Pavements in Indiana", Ph.D Thesis, Purdue University, 1987.

Littel, R. C., Freund, R. J., and Spector, P. L., SAS System for Linear Models, Third Ed., SAS Institute Inc., 1991.

Lottman, R.P., "Predicting Moisture-Induced Damage to Asphaltic Concrete", NCHRP Report 192, Transportation Research Board, Washington, D.C., 1978.

Lottman, R.P., "Predicting Moisture-Induced Damage to Asphaltic Concrete", NCHRP Report 246, Transportation Research Board, Washington, D.C., 1982.

Mahboub, K. and D.N. Little Jr., "An Improved Asphalt Concrete Mix Design Procedure", Proceedings, Association of Asphalt Paving Technologists, Volume 59, 1990.

Mahoney, J.P., "The Relationship Between Axle Configuration, Wheel Loads and Pavement Structures", Vehicle/Pavement Interaction, SP 765, Society of Automotive Engineers, Pennsylvania, 1988.

McLeod , N.W., "Asphalt Cements : Pen-Vis Number and its Application to Moduli of Stiffness", ASTM Journal of Testing and Evaluation, Volume 4, No.4, 1976.

McLeod, N.W., "Relationship of Paving Asphalt Temperature Susceptibility as Measured by PVN to Paving Asphalt Specifications, Asphalt Paving Mixture Design and Asphalt Pavement Performance," Proceedings, Association of Asphalt Paving Technologists, Volume 58, 1989.

Monismith, C.L., F.N. Finn, and B.A. Vallerga, "A Comprehensive Asphalt Concrete Mix Design System", Asphalt Concrete Mix Design : Development of a More Rational Approaches, ASTM STP 1041, W. L. Gartner, Ed., American Society for Testing and Materials, Philadelphia, 1985.

Morrison, D.F., Multivariate Statistical Methods, 2nd Ed., McGraw-Hill, New York, 1976.

Moulthrop, J.S., R.J. Cominsky, "Strategic Highway Research Project for Asphalt Research - An Overview", Proceedings, Association of Asphalt Paving Technologists, Volume 60, 1991.

Perl, M., J. Uzan, and A. Sides, "Visco-Elasto-Plastic Constitutive Law for a Bituminous Mixture Under repeated Loading", Transportation Research Record 911, Transportation Research Board, Washington, D.C., 1984.

Pfeiffer, V. Ph., and P.M. Van Doormaal, "The Rheological Properties of Asphaltic and Bitumen", Journal of the Institute of Petroleum Technology, Volume 22, 1936.

Pumphrey, N.D., "Development of an Asphaltic Concrete Overlay Design Procedure for Rigid Pavements in Indiana", Ph.D Thesis, Purdue University, 1989.

Roberts, F.L., Kandhal, P.S., Brown, E.R., D.Y. Lee and Kennedy, T.W., Hot Mix Asphalt Materials, Mixture Design and Construction, NAPA Education Foundation, Lanham, Maryland, USA, 1991.

Romain, J.E., "Rut Depth Prediction in Asphalt Pavements", Proceedings, Third International Conference on the Structural Design of Asphalt Pavements, Volume 1, London, 1972.

Root, R.E., "The Effects of Testing and Production Procedures on Mix Design Results", Proceedings, Association of Asphalt Paving Technologists, Volume 58, 1989.

Roque, R., M. Tia, and, B.E. Ruth, " Asphalt Rheology to Define the Properties of Asphalt Concrete Mixtures and Performance of Pavements", Asphalt Rheology : Relationship to Mixture, ASTM STP 941, Philadelphia, 1985.

Santucci, L.E., "Design as a Factor in Pavement Performance", Proceedings, Association of Asphalt Paving Technologists, Volume 54, 1985.

Scherocman, J.A., and L.E. Wood, "Pavement Performance Framework for Success", Proceedings, Association of Asphalt Paving Technologists, Volume 58, 1989.

Sebaaly, P., and N. Tabatabee, "Effect of Tire Pressure and Type on Response of Flexible Pavements", Transportation Research Record 1227, Transportation Research Board, Washington, D.C., 1989.

Shahin, M.Y. and S.D. Kohn, "Pavement Maintenance Management For Roads And Parking Lots," Construction Engineering Research Laboratory, U.S. Army Corps of Engineers, Report No. CERL-TR-M-294, October 1981.

Shell Pavement Design Manual, Shell Petroleum Company, London, 1978.

Sousa, J.B. and Monismith, C.L., "Dynamic Response of Paving Materials", Transportation Research Record 1136, Transportation Research Board, Washington D.C., 1987.

Sousa, J.B., J. Craus, C.L. Monismith, "Summary Report on Permanent Deformation in Asphalt Concrete", Strategic Highway Research Program : SHRP-A/IR-91-04, National Research Council, Washington, D.C., 1991.

Strategic Highway Research Plans", Final Report, NCHRP Project 20-20, FHWA, May 1986.

Stuart, K.D., "Moisture Damage in Asphalt Mixtures - A State-of-the-Art Report", Final report, FHWA Report No: FHWA-RD-90-019, Virginia, 1990.

Sullivan, M., "Trends in Truck Transportation - Issues Pertaining to Truck/Pavement Interaction", Vehicle/Pavement Interaction SP 765, Society of Automotive Engineers, Pennsylvania, 1988.

Taylor, M.A. and N.P. Khosla, "Stripping of Asphalt Pavement: State-of-the-Art", Transportation Research Record 911, Transportation Research Board, Washington, D. C.,1974

Terrel, R.L., and J.W. Shute, "Summary Report on Water Sensitivity", Strategic Highway Research Program : SR-OSU-A-003A-89-3, National Research Council, Washington D.C., 1989.

The Asphalt Institute, "Causes and Prevention of Stripping in Asphalt Pavements (ES-10)," College Park, Maryland, 1981.

The Asphalt Institute, "Mix Design Methods for Asphalt Concrete (MS-2)," College Park, Maryland, USA, 1979.

Thomas, T. W., "Detection of Sand Particles Using Automatic Image Analysis", MSCE Thesis, Purdue University, 1993.

Valkering, C.P., D.J.L. Lancon, E. deHilster, and D.A. Stoker, "Rutting Resistance of Asphalt Mixes Containing Non-Conventional and Polymer-Modified Binders", Proceedings, Association of Asphalt Paving Technologists, Volume 59, 1990.

Vallerga, B.A. and W.R. Lovering, " Evolution of the Hveem Stabilometer Method of Designing Asphalt Mixtures", Proceedings, Association Asphalt Paving Technologists, Volume 54, 1985.

Van de loo, P.J., "The Creep Test - A Key Tool in Asphalt Mix Design and the Prediction of Pavement Rutting", Proceedings, Association of Asphalt Paving Technologists, Volume 47, 1978.

Van Til, C.J., B.F. McCullough and R.G. Hicks," Evaluation of AASHTO Interim Guides for Design of Pavement Structures", NCHRP Report 128, Highway Research Board, 1972.

Von Quintas, H.L., Scherocman, J.A., Hughes, C.S. and Kennedy, T.W., NCHRP Report 338, "Asphalt-Aggregate Mixture Analysis System **(AAMAS)**, Transportation research Board, National Research Council, Washington, D.C., 1991.

White, T.D., "Marshall Procedures for Design and Quality Control of Asphalt Mixtures", Proceedings, Association of Asphalt Paving Technologists", Volume 54, 1985.

Yandell, W.O. and R.B. Smith, "Towards Maximum Performance Mix Design for Each Situation", Asphalt Concrete Mix Design : Development of a More Rational Approaches, ASTM STP 1041, W. L. Gartner, Ed., American Society for Testing and Materials, Philadelphia, 1985.

Yeager, L.L. and Wood, L.E., "A Recommended Procedure for the Determination of the Dynamic Modulus of Asphalt Mixtures", JHRP-74-18, 1974.

Yoder, E.J., and M.W. Witczak, Principles of Pavement Design, Second Ed., John Wiley and Sons Inc., Pub., 1975.

Yoder, E.J., and B. Colluci-Rios, "Truck Size and Weight Issues", Proceedings, of the 66th Purdue Road School, Purdue University, March 1980.

Zaghloul, S. M. and White, T. D., "Use of a Three Dimensional-Dynamic Finite Element Program for Analysis of Flexible Pavements", Transportation Research Record 1388, Transportation Research Board, National Academy of Sciences, 1993, pp. 60-69.

APPENDIX A - MATERIAL SPECIFICATION

Figure A.1. Gradation - Showing the Actual and Specification

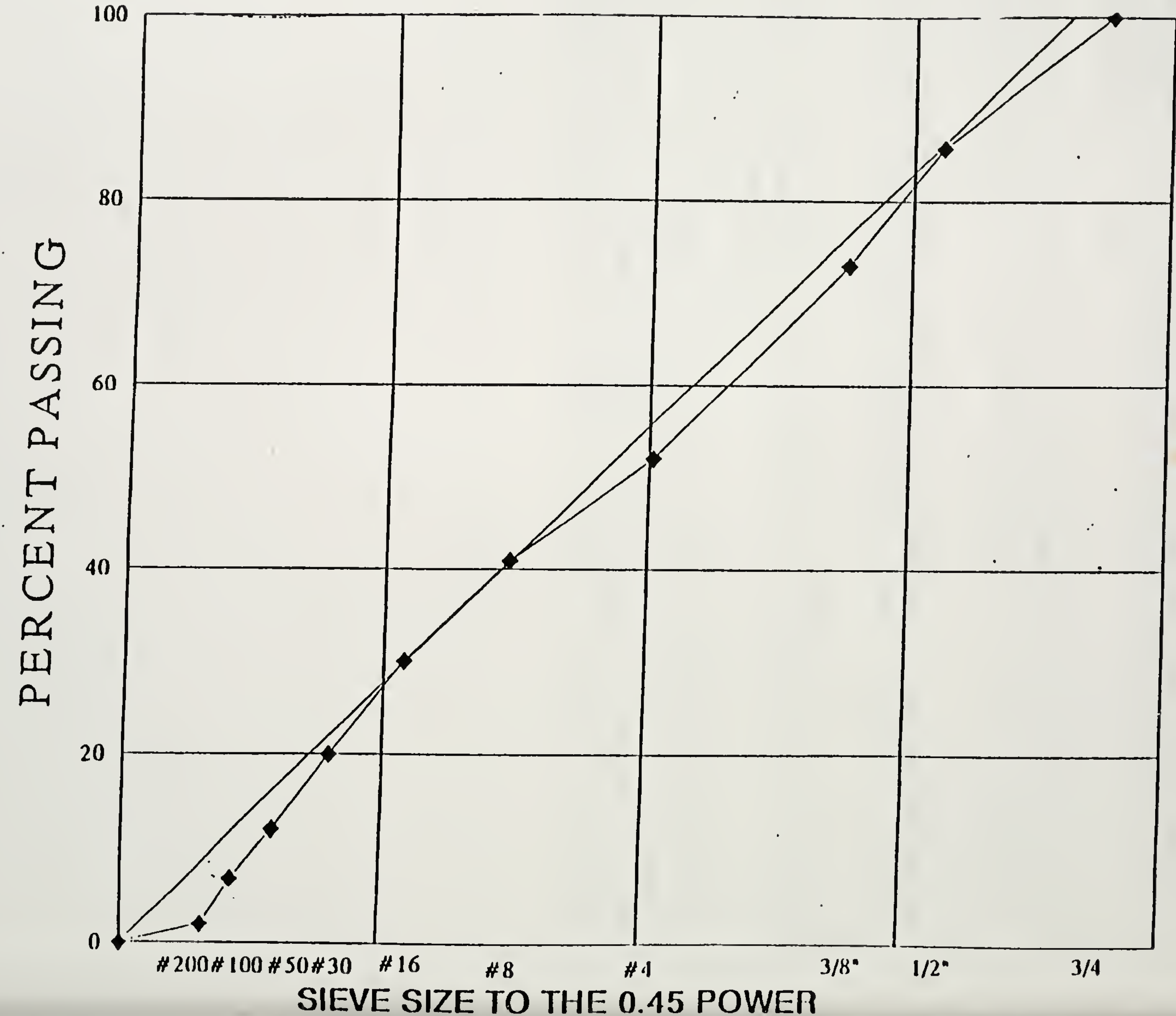

APPENDIX B - SAMPLING AND FIELD CONDITION SURVEY

APPENDIX B

ANOVA for Bulk Specific Gravity

SOURCE	df	SS x 10^{-3}	MSE x 10^{-3}	F	F_{crit}
LOCATION L	3	0.8440	2.8133	<1	18.9
W/PATH W	1	0.7156	7.1560	1.2	5.318
L x W	3	3.0568	10.1893	1.72	4.066
ERROR	8	4.7415	5.9268		
TOTAL	15				

The F-test is not significant at 10%. Thus bulk specific gravity values for the entire 5.4 mile pavement section can be assumed to be from the same population.

Table B.1. Number of Observations per Sample Using t For Difference of Means

Single-Sided Test	Alpha 0.01					Alpha 0.01					Alpha 0.03					Alpha 0.05					
Double-Sided Test	Alpha 0.01					Alpha 0.02					Alpha 0.05					Alpha 0.1					
Beta =	0.01	0.05	0.1	0.2	0.5	0.01	0.05	0.1	0.2	0.5	0.01	0.05	0.1	0.2	0.5	0.01	0.05	0.1	0.2	0.5	
0.3										123					87					61	0.3
0.4					85					70				100	50			108	78	35	0.4
0.5				96	55			106	82	45		106	86	64	32		88	70	51	23	0.5
0.6		101	85	67	39		90	74	58	32	104	74	60	45	23	89	61	49	36	16	0.6
0.7	100	75	63	50	29	90	66	55	43	24	76	55	44	34	17	66	45	36	26	12	0.7
0.75	88	66	55	44	26	79	58	48	38	21	67	48	39	29	15	57	40	32	23	11	0.75
0.8	77	58	49	39	23	70	51	43	33	19	59	42	34	26	14	50	35	28	21	10	0.8
0.85	69	51	43	35	21	62	46	38	30	17	52	37	31	23	12	45	31	25	18	9	0.85
0.9	62	46	39	31	19	55	41	34	27	15	47	34	27	21	11	40	28	22	16	8	0.9
0.95	55	42	35	28	17	50	37	31	24	14	42	30	25	19	10	36	25	20	15	7	0.95
1	50	38	32	26	15	45	33	28	222	13	38	27	23	17	9	33	23	18	14	7	1
1.1	42	32	27	22	13	38	28	23	19	11	32	23	19	14	8	27	19	15	12	6	1.1
1.2	36	27	23	18	11	32	24	20	16	9	27	20	16	12	7	23	16	13	10	5	1.2
1.3	31	23	20	16	10	28	21	17	14	8	23	17	14	11	6	20	14	11	9	5	1.3
1.4	27	20	17	14	9	24	18	15	12	8	20	15	12	10	6	17	12	10	8	4	1.4
1.5	24	18	15	13	8	21	16	14	11	7	18	13	11	9	5	15	11	9	7	4	1.5
1.6	21	16	14	11	7	19	14	12	10	6	16	12	10	8	5	14	10	8	6	4	1.6
1.7	19	15	13	10	7	17	13	11	9	6	14	11	9	7	4	12	9	7	6	3	1.7
1.8	17	13	11	10	6	15	12	10	8	5	13	10	8	6	4	11	8	7	5		1.8
1.9	16	12	11	9	6	14	11	9	8	5	12	9	7	6	4	10	7	6	5		1.9
2	14	11	10	8	6	13	10	9	7	5	11	8	7	6	4	9	7	6	4		2
2.5	10	8	7	6	4	9	7	6	5	4	8	6	5	4		6	5	4	3		2.5
3	8	6	6	5	4	7	6	5	4	3	6	5	4	4		5	4	3			3
3.5	6	5	5	4	3	6	5	4	4		5	4	4	3		4	3				3.5
4	6	5	4	4		5	4	4	3		4	4	3			4					4

Selecting Sample Size to Core From Pavement

		LOCATION				
		L1	L2	L3	L4	Y_j
WHEEL PATH	INSIDE	2.3841 2.3192	2.4161 2.3799	2.3839 2.3442	2.3900 2.3890	2.3761
	BETWEEN	2.3960 2.4221	2.3689 2.3990	2.3788 2.3802	2.3700 2.3980	2.3890
	Y_i	2.3810	2.3910	2.3721	2.3870	2.3820

$d_1 = U_{out} - U_{in} =$ Mean Bulk Specific (outside - between) wheelpath

$= 2.3890 - 2.3761$

$= 0.013$

Sample Standard Deviation (SSD) = 0.0201

$D_1 = d_1$ / SSD = 0.013/0.0201

$= 0.65$

From table in Appendix B, for alpha and beta equal to 10%, the minimum number of core samples required is 40. Thus for the entire section there were 4 subsections, so a minimum of about ten cores are required for each; five from the wheelpath and five from between the wheelpath.

APPENDIX C - LABORATORY DATA

APPENDIX C

KEY TO THE DATA

CODE	Identification for each core, location and distress
L	Layer type, A is surface, B is binder, C is base
N30	The percent of silicious material on the #30 sieve
N50	The percent of silicious material on the #50 sieve
N100	The percent of silicious material on the #100 sieve
CONT#	Contract number of pavement section studied
TRUCKS	Average annual daily truck traffic
KINV	Kinematic viscosity
ABSV	Absolute viscosity
PVN	Penetration-viscosity number
BULK SG	Bulk specific gravity
MAXSG	Maximum specific gravity
MARSH	Marshall stability
FLOW	Flow, 0.01 inch
Q	Ratio of Marshall stability with flow
PEN	Penetration
ASP %	Percent asphalt content by mixture weight
PCI	Pavement condition index
WHEEL	Wheelpath (cores from wheelpath or between wheelpath)
HT	Core height
WEIGHT	Core weight
CO	County number
CLI	Climate
AIR %	Percent air voids in compacted bituminous mixture
AGE	Age of pavement at the time cores were taken

CI	Compactibility index
SI	Stability index
GSF	Gyratory shear factor
E1HZ20	Dynamic modulus of bituminous concrete tested at 1 cycle per second (Hz) and at 20 degrees centigrade

Table C.1. Pavement Sections to Core in the Laporte District

HIGHWAY	CODE	DISTRESS	LOCATION
1) SR114	25	RAVELING	ELEVEN MILES BEFORE JCT US421 GOING EAST ON E/BOUND LANE.
2) SR14	23	THERMAL CRACKING	ABOUT 6.2 MILES BEFORE JCT US35 GOING WEST ON W/BOUND LANE.
3) I-65	35	RAVELING	BETWEEN MILEPOST 207-208 GOING NORTH RIGHT LANE.
4) US31S	13	THERMAL CRACKING	JUST BEFORE CO. ROAD 1500N IN FULTON COUNTY GOING SOUTH , TAKE CORES FROM PASSING LANE.
5) SR14E	41	ZERO	ABOUT 1.5 MILES BEFORE JCT SR39 IN PULASKI COUNTY GOING EAST TAKE CORES FROME/BOUND LANE.
6) SR14W	42	RUT	JUST AFTER JCT SR39 GOING WEST IN PULASKI COUNTY TAKE CORES FROM WEST BOUND LANE.
7) SR8E	42	RUT	ABOUT 3.3 MILES EAST OF JCT US35 IN STARKE COUNTY TAKE CORES FROM E/BOUND LANE.
8) SR8E	43	THERMAL CRACKING	ABOUT 3.3 MILES EAST OF JCT US35 IN STARKE COUNTY TAKE CORES FROM E/BOUND LANE.

Table C.2. Pavement Sections to Core in the Seymour District

CORES ALREADY TAKEN

HIGHWAY	CODE	DISTRESS	LOCATION
1) I-65	73	THERMAL CRACKING	BETWEEN MILEPOSTS 35-34 GOING SOUTH(ie. JUST BEFORE JCT SR256) . TAKE CORES FROM LANES ie. 14 + 14 CORES*.

CORES TO TAKE

HIGHWAY	CODE	DISTRESS	LOCATION
1) SR446N	61	ZERO	ABOUT 0.1 MILE NORTH OF JCT US50 TAKE CORES FROM THE NORTH BOUND LANE
2) US421N	81	ZERO	ABOUT 2.2 MILES NORTH OF JCT SR350 GOING NORTH TAKE CORES FROM THE LEFT WHEEL PATH. (Also just after Co. Rd. 600n in Ripley County)
3) I-65N	74	STRIPPING	BETWEEN MILEPOST 30 - 31 TAKE CORES FROM RIGHT LANE.
4) SR56W	85 82	RAVELING	ABOUT 0.7 MILES AFTER JCT SR39 GOING WEST TAKE CORES FROM WEST BOUND LANE.
5) I-65S	71	ZERO	SOUTHBOUND JUST BEFORE JCT SR44 ON RIGHT LANE.

NOTE: PLEASE TAKE 7 CORES FROM THE WHEEL PATH AND 7 MORE FROM OUTSIDE THE WHEEL PATH FOR EACH LANE. EACH SECTION HAS BEEN MARKED WITH INITIALS "TW" IN YELLOW EITHER ON THE SHOULDER OR ON THE PAVEMENT EDGE.

Table C.3. Pavement Sections to Core in the Greenfield District

HIGHWAY	CODE	DISTRESS	LOCATION
2) SR37N	82	RUTTING	0.5 MILE NORTH OF JCT I-69 NORTH BOUND LEFT LANE.
3) SR1	83	THERMAL CRACKING	ABOUT 2.8 MILES NORTH OF JCT SR38 N/BOUND LANE.
4) SR37	84	STRIPPING	ABOUT 0.5 MILES BEFORE JCT SR38 GOING SOUTH ON RIGHT LANE.

NOTE

PLEASE TAKE 7 CORES FROM THE WHEEL PATH AND 7 MORE FROM OUTSIDE THE WHEELPATH.
ALL SECTIONS ARE MARKED WITH THE INITIALS "TW".

Table C.4. Pavement Sections to Core in the Crawfordsville District

HIGHWAY	CODE	DISTRESS	LOCATION
1) I-74	72	RUTTING	BETWEEN MPS 17 AND 18 GOING EAST TAKE CORES FROM THE RIGHT LANE

THE PAVEMENT SECTION HAS BEEN MARKED WITH THE INITIAL 'TW' AT TWO LOCATIONS BETWEEN WHICH POINTS THE CORES ARE TO BE TAKEN.

Table C.5. Pavement Sections to Core in the Fort Wayne District

HIGHWAY	CODE	DISTRESS	LOCATION
1) US 24	11	ZERO	IN HUNTINGTON CITY JUST AFTER JCT US224 GOING NORTH, NORTH BOUND RIGHT LANE.
2) US31	12	RUTTING	ONE MILE BEFORE JCT SR16 GOING SOUTH, S/BOUND RIGHT LANE.
3) SR8	21	ZERO	JUST BEFORE INDIANA/OHIO STATE LINE WEST BOUND LANE.
4) SR8 W	21	ZERO	ABOUT 2 MILES BEFORE JCT SR1N GOING WEST TAKE CORES FROM W/BOUND LANE.
6) I-69	31	ZERO	BETWEEN MILEPOSTS 130-131 GOING NORTH, N/BOUND LANE.
7) US31	32	RUTTING	NORTH OF JCT US24 BEFORE COUNTY ROAD 275N ON N/BOUND RIGHT LANE.
8) I-69	33	THERMAL CRACKING	BETWEEN MILEPOSTS 64-63 GOING SOUTH ON S/BOUND LEFT LANE.
9) I-69	34	STRIPPING	BETWEEN MILEPOSTS 114-115 NORTH BOUND ON N/BOUND RIGHT LANES.

NOTE: PLEASE TAKE 7 CORES FROM THE WHEELPATH AND 7 FROM OUTSIDE THE WHEELPATH.
THE SECTIONS ARE MARKED WITH INITIALS "TW"

Table C.6. Pavement Sections to Core in the Vincennes District

	HIGHWAY	CODE	DISTRESS	LOCATION
1)	I-64	5 1	ZERO	ABOUT 2 MILES AFTER JCT SR37N GOING WEST, OR BETWEEN MILEPOST 86-84. TAKE CORES FROM BOTH LANES (ie. 14 + 14)*.
2)	I-64	5 2	RUTTING	ABOUT 2 MILES BEFORE JCT SR145 GOING WEST, OR BETWEEN MILEPOST 75-74. TAKE CORES FROM THE RIGHT LANE ALONG THE LEFT WHEEL PATH.
3)	I-64	5 3	THERMAL CRACKING	JUST BEFORE JCT SR161 GOING WEST, OR BETWEEN MILEPOST 55-54 FROM THE LEFT LANE.
4)	I-64	5 4	STRIPPING	ABOUT 1.2 MILES BEFORE JCT SR162 GOING WEST OR BETWEEN MILEPOST 65-64. TAKE CORES FROM THE RIGHT LANE ALONG THE LEFT WHEEL PATH.
5)	I-64	5 5	RAVELING	JUST BEFORE JCT SR161 GOING WEST, OR BETWEEN MILEPOST 55-54 TAKE CORES FROM THE RIGHT LANE.
6)	US41N	EXTRA 75	T.CRACK & RAVELING	ABOUT 3.8 MILES BEFORE JCT SR550 GOING NORTH FROM THE LEFT LANE IN KNOX COUNTY.
7)	US41N	EXTRA	RUTTING	ABOUT 3.8 MILES BEFORE JCT SR550 GOING NORTH TAKE CORES FROM THE RIGHT LANE ALONG THE LEFT WHEEL PATH IN KNOX COUNTY.
8)	SR245E	6 2	RUTTING	ABOUT 4 MILES AFTER JCT SR62 EAST BOUND RIGHT LANE TAKE CORES FROM LEFT WHEEL PATH.

* NOTE: PLEASE TAKE 7 CORES FROM THE WHEEL PATH AND 7 MORE FROM OUTSIDE THE WHEEL PATH FOR EACH LANE. EACH SECTION ABOVE HAS BEEN MARKED WITH THE INITIALS "TW" ON THE PAVEMENT SHOULDER.

Table C.7. Individual Core Location and Characteristics

CODE	CONTRACT NUMBER	ROUTE TYPE	ROUTE NO.	CO.	WHEEL	N30 %	N50 %	N100 %	TRUCKS DAILY	KIN. VISC. (CSt.)	ABS. VISC. (POISE)	PVN	BULK SG	MAX. SG	MARSHALL STABILITY (LBS.)	FLOW (0.01")
111	R14093	US	24	35	WP	8.8	33	23.4	1480	1305	48120	−0.4	2.2588	2.4927	<1"	14
112	R14093	US	24	35	WP	8.8	33	23.4	1480	1259	48215	−0.4	2.2553	2.5296	<1"	18
113	R14093	US	24	35	WP	8.8	33	23.4	1480				2.2671		<1"	20
114	R14093	US	24	35	WP	8.8	33	23.4	1480				2.2646		<1"	19
115	R14093	US	24	35	WP	8.8	33	23.4	1480				2.2356			
116	R14093	US	24	35	WP	8.8	33	23.4	1480				2.2117			
117	R14093	US	24	35	WP	8.8	33	23.4	1480				2.1719			
118	R14093	US	24	35	OWP	8.9	32	25	0				2.2204	2.4948	<1"	14
119	R14093	US	24	35	OWP	8.9	32	25	0				2.2365	2.4952	<1"	15
1110	R14093	US	24	35	OWP	8.9	32	25	0				2.2426		1125	15
1111	R14093	US	24	35	OWP	8.9	32	25	0				2.2163		<1"	13
1112	R14093	US	24	35	OWP	8.9	32	25	0							
1113	R14093	US	24	35	OWP	8.9	32	25	0							
1114	R14093	US	24	35	OWP	8.9	32	25	0							
121	R9210	US	31	52	WP	19	53	63.3	1621	603	8475	−0.8	2.4131	2.42	2407	10
122	R9210	US	31	52	WP	19	53	63.3	1621	615	8977	−0.8	2.4198	2.449	2454	12
123	R9210	US	31	52	WP	19	53	63.3	1621				2.4191		1647	13
124	R9210	US	31	52	WP	19	53	63.3	1621				2.4441		1561	15
125	R9210	US	31	52	WP	19	53	63.3	1621				2.4093			
126	R9210	US	31	52	WP	19	53	63.3	1621				2.4022			
127	R9210	US	31	52	WP	19	53	63.3	1621				2.3931			
128	R9210	US	31	52	OWP	17	56	63.2	0	564	8856	−1.1	2.3727	2.4562	0	14
129	R9210	US	31	52	OWP	17	56	63.2	0	555	8931	−1.1	2.3756	2.4659	0	12
1210	R9210	US	31	52	OWP	17	56	63.2	0	556			2.3675		0	14
1211	R9210	US	31	52	OWP	17	56	63.2	0	539			2.3697		1484	
1212	R9210	US	31	52	OWP	17	56	63.2	0				2.3737			

Table C.7. (cont.)

CODE	CONTRACT NUMBER	ROUTE TYPE	ROUTE NO.	CO.	WHEEL	#30 %	#50 %	#100 %	TRUCKS	KIN. VISC.	ABS. VISC.	PVN	BULK S.G.	MAX. S.G.	MARSHALL STABILITY	FLOW
1213	R9210	US	31	52	OWP	17	56	63.2	0				2.3926			
1214	R9210	US	31	52	OWP	17	56	63.2	0				2.3775			
211	R14925	SR	8	17	OWP	21	45	44.4	78	938	20541	−0.4	2.3728	2.4959	2350	14
212	R14925	SR	8	17	OWP	21	45	44.4	78	867	20436	−0.5	2.3652	2.4948	1244	17
213	R14925	SR	8	17	OWP	21	45	44.4	78				2.3255		1441	18
214	R14925	SR	8	17	OWP	21	45	44.4	78				2.3502		1750	
215	R14925	SR	8	17	OWP	21	45	44.4	78				2.3312			
216	R14925	SR	8	17	OWP	21	45	44.4	78				2.4192			
217	R14925	SR	8	17	OWP	21	45	44.4	78				2.3906			
218	R14925	SR	8	17	WP	20	43	46	0	938	20541	−0.4	2.3629	2.5302	1432	17
219	R14925	SR	8	17	WP	20	43	46	0	867	20436	−0.5	2.3373	2.5013	3779	14
2110	R14925	SR	8	17	WP	20	43	46	0				2.3278			
2111	R14925	SR	8	17	WP	20	43	46	0				2.3251			
2112	R14925	SR	8	17	WP	20	43	46	0				2.3144			
2113	R14925	SR	8	17	WP	20	43	46	0				2.4134			
2114	R14925	SR	8	17	WP	20	43	46	0				2.4073			
231	R13183	SR	14	66	WP				95	657.3	12593	−0.7	2.4018	2.4757		
232	R13183	SR	14	66	WP				95	656.8	12561	−0.7	2.3766	2.4672		
233	R13183	SR	14	66	WP				95	632.9			2.3489			
234	R13183	SR	14	66	WP				95	637.7			2.2328			
235	R13183	SR	14	66	WP				95				2.2823			
236	R13183	SR	14	66	WP				95							
237	R13183	SR	14	66	WP				95							
238	R13183	SR	14	66	OWP				0	633	12471	−0.8	2.4056	2.4823		
239	R13183	SR	14	66	OWP				0	620	12398	−0.8	2.3812	2.4743		
2310	R13183	SR	14	66	OWP				0							
2311	R13183	SR	14	66	OWP				0							

Table C.7. (cont.)

CODE	CONTRACT NUMBER	ROUTE TYPE	ROUTE NO.	CO.	WHEEL	#30 %	#50 %	#100 %	TRUCKS	KIN. VISC.	ABS. VISC.	PVN	BULK S.G.	MAX. S.G.	MARSHALL STABILITY	FLOW
2312	R13183	SR	14	66	OWP				0							
2313	R13183	SR	14	66	OWP				0							
2314	R13183	SR	14	66	OWP				0							
311	R14625	I	69	2	WP	17	47	57.4	4033	694.5	22572	−0.9	2.4367	2.4707	1658	14
312	R14625	I	69	2	WP	17	47	57.4	4033	672	22581	−0.9	2.4291	2.4514	1352	12
313	R14625	I	69	2	WP	17	47	57.4	4033				2.4181		1270	11
314	R14625	I	69	2	WP	17	47	57.4	4033				2.4212		1350	14
315	R14625	I	69	2	WP	17	47	57.4	4033				2.4111			
316	R14625	I	69	2	WP	17	47	57.4	4033				2.4483			
317	R14625	I	69	2	WP	17	47	57.4	4033				2.4361			
318	R14625	I	69	2	OWP	16	48	56.4	0	662.3	25747	−0.9	2.3805	2.4648	1103	15
319	R14625	I	69	2	OWP	16	48	56.4	0	675.7	25840	−0.9	2.3832	2.4712	1792	17
3110	R14625	I	69	2	OWP	16	48	56.4	0	661.8			2.3949		1349	18
3111	R14625	I	69	2	OWP	16	48	56.4	0	654			2.3835		1509	15
3112	R14625	I	69	2	OWP	16	48	56.4	0				2.3049			
3113	R14625	I	69	2	OWP	16	48	56.4	0				2.3729			
3114	R14625	I	69	2	OWP	16	48	56.4	0				2.3864			
321	R10114	US	31	52	OWP	20	48	47.7	1563	888	22112	−0.8	2.4045	2.4223	2447	16
322	R10114	US	31	52	OWP	20	48	47.7	1563	905.1	22500	−0.8	2.4113	2.4512	1654	16
323	R10114	US	31	52	OWP	20	48	47.7	1563				2.3507		2699	
324	R10114	US	31	52	OWP	20	48	47.7	1563				2.4045			
325	R10114	US	31	52	OWP	20	48	47.7	1563				2.4454			
326	R10114	US	31	52	OWP	20	48	47.7	1563				2.3988			
327	R10114	US	31	52	OWP	20	48	47.7	1563				2.4223			
328	R10114	US	31	52	WP	18	48	53.1	0	708.2	14165	−1	2.4107	2.4648	2602	13
329	R10114	US	31	52	WP	18	48	53.1	0	725.3	14137	−1	2.4345	2.4712	1619	16
3210	R10114	US	31	52	WP	18	48	53.1	0				2.4413		2068	16

Table C.7. (cont.)

CODE	CONTRACT NUMBER	ROUTE TYPE	ROUTE NO.	CO.	WHEEL	#30 %	#50 %	#100 %	TRUCKS	KIN. VISC.	ABS. VISC.	PVN	BULK S.G.	MAX. S.G.	MARSHALL STABILITY	FLOW
3211	R10114	US	31	52	WP	18	48	53.1	0				2.4411		1981	20
3212	R10114	US	31	52	WP	18	48	53.1	0				2.4448			
3213	R10114	US	31	52	WP	18	48	53.1	0				2.4301			
3214	R10114	US	31	52	WP	18	48	53.1	0				2.4138			
331	R12322	US	31	27	WP				2243	1292	39456	−0.6	2.3601	2.469	1498	15
332	R12322	US	31	27	WP				2243	1242	39489	−0.6	2.3659	2.4863	2121	17
333	R12322	US	31	27	WP				2243				2.3737		1790	21
334	R12322	US	31	27	WP				2243				2.3391		3157	20
335	R12322	US	31	27	WP				2243				2.3655			
336	R12322	US	31	27	WP				2243				2.2839			
337	R12322	US	31	27	WP				2243				2.3719			
338	R12322	US	31	27	OWP				0	1588	41523	−0.3	2.3659	2.4858	2234	14
339	R12322	US	31	27	OWP				0	1575	41636	−0.3	2.3569	2.4755	2427	16
3310	R12322	US	31	27	OWP				0				2.3469		2145	18
3311	R12322	US	31	27	OWP				0				2.4052		3586	20
3312	R12322	US	31	27	OWP				0				2.3464			
3313	R12322	US	31	27	OWP				0				2.3408			
3314	R12322	US	31	27	OWP				0				2.3776			
341	R12060	I	69	17	WP				2356	666	16454	−0.8	2.4121	2.5078	2114	18
342	R12060	I	69	17	WP				2356	623	16441	−0.9	2.3913	2.4838	1411	11
343	R12060	I	69	17	WP				2356				2.4255		2396	14
344	R12060	I	69	17	WP				2356				2.4161		1885	
345	R12060	I	69	17	WP				2356				2.4077			
346	R12060	I	69	17	WP				2356				2.3198			
347	R12060	I	69	17	WP				2356							
348	R12060	I	69	17	OWP				0	796	17387	−0.7	2.3644	2.5126	1715	18
349	R12060	I	69	17	OWP				0	755	17342	−0.8	2.3606	2.4915	2253	17

Table C.7. (cont.)

CODE	CONTRACT NUMBER	ROUTE TYPE	ROUTE NO.	CO.	WHEEL	#30 %	#50 %	#100 %	TRUCKS	KIN. VISC.	ABS. VISC.	PVN	BULK S.G.	MAX. S.G.	MARSHALL STABILITY	FLOW
3410	R12060	I	69	17	OWP				0				2.3173		1457	22
3411	R12060	I	69	17	OWP				0				2.3818		1907	19
3412	R12060	I	69	17	OWP				0				2.3662			
3413	R12060	I	69	17	OWP				0				2.3046			
3414	R12060	I	69	17	OWP				0				2.3907			
411	RS16390	SR	14	66	WP	23	57	74.6	67				2.4333	2.5388	2844	11
412	RS16390	SR	14	66	WP	23	57	74.6	67				2.4121	2.5343	1877	14
413	RS16390	SR	14	66	WP	23	57	74.6	67				2.4847		2717	14
414	RS16390	SR	14	66	WP	23	57	74.6	67				2.4024		<1"	13
415	RS16390	SR	14	66	WP	23	57	74.6	67				2.4447			
416	RS16390	SR	14	66	WP	23	57	74.6	67				2.4629			
417	RS16390	SR	14	66	WP	23	57	74.6	67				2.4454			
418	RS16390	SR	14	66	OWP	23	57	73	0				2.4051	2.5167	2096	11
419	RS16390	SR	14	66	OWP	23	57	73	0				2.4246	2.5463	1613	11
4110	RS16390	SR	14	66	OWP	23	57	73	0				2.4121		1882	15
4111	RS16390	SR	14	66	OWP	23	57	73	0				2.3665		1342	16
4112	RS16390	SR	14	66	OWP	23	57	73	0				2.4038			
4113	RS16390	SR	14	66	OWP	23	57	73	0				2.4667			
4114	RS16390	SR	14	66	OWP	23	57	73	0				2.3798			
421	RS16390	SR	8	75	OWP	16	55	68.5	67	486	4712	−0.8	2.5078	2.5134	2140	7
422	RS16390	SR	8	75	OWP	16	55	68.5	67	506	4792	−0.8	2.4774	2.4774	2168	9
423	RS16390	SR	8	75	OWP	16	55	68.5	67				2.5078		2182	9
424	RS16390	SR	8	75	OWP	16	55	68.5	67				2.5186		<1"	8
425	RS16390	SR	8	75	OWP	16	55	68.5	67				2.5159			
426	RS16390	SR	8	75	OWP	16	55	68.5	67				2.5052			
427	RS16390	SR	8	75	OWP	16	55	68.5	67				2.5052			

Table C.7. (cont.)

CODE	CONTRACT NUMBER	ROUTE TYPE	ROUTE NO.	CO.	WHEEL	#30 %	#50 %	#100 %	TRUCKS	KIN. VISC.	ABS. VISC.	PVN	BULK S.G.	MAX. S.G.	MARSHALL STABILITY	FLOW
429	RS16390	SR	8	75	WP	15	52	68.4	0	603	8416	−0.7	2.4975	2.5155	1901	11
4210	RS16390	SR	8	75	WP	15	52	68.4	0				2.5258		2156	11
4211	RS16390	SR	8	75	WP	15	52	68.4	0				2.4921		1729	
4212	RS16390	SR	8	75	WP	15	52	68.4	0				2.5125			
4213	RS16390	SR	8	75	WP	15	52	68.4	0				2.5011			
4214	RS16390	SR	8	75	WP	15	52	68.4	0				2.4404			
431	RS11377	SR	8	75	WP				164	837	22267	−0.8	2.4478	2.5166		
432	RS11377	SR	8	75	WP				164	806	22318	−0.8	2.4176	2.4849		
433	RS11377	SR	8	75	WP				164				2.2991			
434	RS11377	SR	8	75	WP				164				2.2684			
435	RS11377	SR	8	75	WP				164				2.2329			
436	RS11377	SR	8	75	WP				164							
437	RS11377	SR	8	75	WP				164							
438	RS11377	SR	8	75	OWP				0	1396	65733	−0.4	2.2551	2.5027		
439	RS11377	SR	8	75	OWP				0	1352	66038	−0.5	2.2357	2.4231		
4310	RS11377	SR	8	75	OWP				0				2.2549			
4311	RS11377	SR	8	75	OWP				0				2.1638			
4312	RS11377	SR	8	75	OWP				0				2.1929			
4313	RS11377	SR	8	75	OWP				0				2.2361			
4314	RS11377	SR	8	75	OWP				0							
511	R14151	I	64	13	OWP	30	58	61.9	2880	632.9		−0.7	2.3781	2.4706	<1"	11
512	R14151	I	64	13	OWP	30	58	61.9	2880	627.7		−0.7	2.3534	2.4575	1906	10
513	R14151	I	64	13	OWP	30	58	61.9	2880				2.3406		1601	
514	R14151	I	64	13	OWP	30	58	61.9	2880				2.4065			
515	R14151	I	64	13	OWP	30	58	61.9	2880				2.3984			
516	R14151	I	64	13	OWP	30	58	61.9	2880				2.3957			
517	R14151	I	64	13	OWP	30	58	61.9	2880				2.3506			

Table C.7. (cont.)

CODE	CONTRACT NUMBER	ROUTE TYPE	ROUTE NO.	CO.	WHEEL	#30 %	#50 %	#100 %	TRUCKS	KIN. VISC.	ABS. VISC.	PVN	BULK S.G.	MAX. S.G.	MARSHALL STABILITY	FLOW
518	R14151	1	64	13	WP	30	59	62.8	0	812		−0.4	2.3993	2.4302	<1"	8
519	R14151	1	64	13	WP	30	59	62.8	0	819		−0.4	2.3921	2.429	2527	9
5110	R14151	1	64	13	WP	30	59	62.8	0				2.3956		2105	10
5111	R14151	1	64	13	WP	30	59	62.8	0				2.3862			9
5112	R14151	1	64	13	WP	30	59	62.8	0				2.3881			
5113	R14151	1	64	13	WP	30	59	62.8	0				2.4207			
5114	R14151	1	64	13	WP	30	59	62.8	0				2.4019			
521	R14150	1	64	62	WP	43	73	60.1	2850	892	18324	−0.4	2.3803	2.4533	2523	8
522	R14150	1	64	62	WP	43	73	60.1	2850	885	18357	−0.5	2.3763	2.4364	2500	9
523	R14150	1	64	62	WP	43	73	60.1	2850				2.3745		2119	9
524	R14150	1	64	62	WP	43	73	60.1	2850				2.3569		2025	9
525	R14150	1	64	62	WP	43	73	60.1	2850				2.3481			
526	R14150	1	64	62	WP	43	73	60.1	2850				2.3872			
527	R14150	1	64	62	WP	43	73	60.1	2850				2.3787			
528	R14150	1	64	62	OWP	42	76	64.5	0	833	18241	−0.4	2.2972	2.4493	1191	9
529	R14150	1	64	62	OWP	42	76	64.5	0	795	18198	−0.5	2.2974	2.4411	1251	7
5210	R14150	1	64	62	OWP	42	76	64.5	0				2.3214			9
5211	R14150	1	64	62	OWP	42	76	64.5	0				2.3276			9
5212	R14150	1	64	62	OWP	42	76	64.5	0				2.2582			
5213	R14150	1	64	62	OWP	42	76	64.5	0				2.3218			
5214	R14150	1	64	62	OWP	42	76	64.5	0				2.2482			
531	R9581	1	64	87	WP				2890	789.8	16275	−0.9	2.3643	2.443	1550	15
532	R9581	1	64	87	WP				2890	780.7	16253	−0.9	2.3619	2.4318	1432	13
533	R9581	1	64	87	WP				2890	748			2.3707		1936	15
534	R9581	1	64	87	WP				2890	742			2.3594		1310	16
535	R9581	1	64	87	WP				2890				2.3363			
536	R9581	1	64	87	WP				2890				2.3812			

Table C.7. (cont.)

CODE	CONTRACT NUMBER	ROUTE TYPE	ROUTE NO.	CO.	WHEEL	#30 %	#50 %	#100 %	TRUCKS	KIN. VISC.	ABS. VISC.	PVN	BULK S.G.	MAX. S.G.	MARSHALL STABILITY	FLOW
537	R9581	I	64	87	WP				2890				2.3553			
538	R9581	I	64	87	OWP				0	701	15652	−1	2.3357	2.4293	1596	15
539	R9581	I	64	87	OWP				0	713	15651	−1.1	2.3358	2.4597	1207	16
5310	R9581	I	64	87	OWP				0				2.2644		1628	15
5311	R9581	I	64	87	OWP				0				2.2987		1937	20
5312	R9581	I	64	87	OWP				0				2.3835			
5313	R9581	I	64	87	OWP				0				2.3846			
5314	R9581	I	64	87	OWP				0				2.3772			
541	R14149	I	64	19	WP				3001	766.8	12360	−0.6	2.3643	2.4962	1649	10
542	R14149	I	64	19	WP				3001	771.9	12374	−0.5	2.3797	2.468	1640	13
543	R14149	I	64	19	WP				3001				2.3481		2278	14
544	R14149	I	64	19	WP				3001				2.3632		864	12
545	R14149	I	64	19	WP				3001				2.3887			
546	R14149	I	64	19	WP				3001				2.4286			
547	R14149	I	64	19	WP				3001				2.3939			
548	R14149	I	64	19	OWP				0	673	12008	−0.5	2.3349	2.4893	1572	16
549	R14149	I	64	19	OWP				0	709	12052	−0.5	2.3389	2.4632	1418	16
5410	R14149	I	64	19	OWP				0				2.3125		1128	15
5411	R14149	I	64	19	OWP				0				2.2961		1068	17
5412	R14149	I	64	19	OWP				0				2.2828			
5413	R14149	I	64	19	OWP				0				2.3591			
5414	R14149	I	64	19	OWP				0				2.3517			
611	RS17953	SR	446	47	WP	25	48	48.1	66	668.2		−0.8	2.3631	2.4482	1084	14
612	RS17953	SR	446	47	WP	25	48	48.1	66	646.5		−0.9	2.3532	2.4083	1115	11
613	RS17953	SR	446	47	WP	25	48	48.1	66				2.3627		1048	17
614	RS17953	SR	446	47	WP	25	48	48.1	66				2.3303		2274	15
615	RS17953	SR	446	47	WP	25	48	48.1	66				2.3459			

Table C.7. (cont.)

CODE	CONTRACT NUMBER	ROUTE TYPE	ROUTE NO.	CO.	WHEEL	#30 %	#50 %	#100 %	TRUCKS	KIN. VISC.	ABS. VISC.	PVN	BULK S.G.	MAX. S.G.	MARSHALL STABILITY	FLOW
616	RS17953	SR	446	47	WP	25	48	48.1	66				2.3613			
617	RS17953	SR	446	47	WP	25	48	48.1	66				2.3768			
618	RS17953	SR	446	47	OWP	25	46	50	0	675		−0.8	2.2711	2.4565	412	13
619	RS17953	SR	446	47	OWP	25	46	50	0	670		−0.8	2.2427	2.4573	407	15
6110	RS17953	SR	446	47	OWP	25	46	50	0				2.2681		454	14
6111	RS17953	SR	446	47	OWP	25	46	50	0				2.2455		272	13
6112	RS17953	SR	446	47	OWP	25	46	50	0				2.2429			
6113	RS17953	SR	446	47	OWP	25	46	50	0				2.2522			
6114	RS17953	SR	446	47	OWP	25	46	50	0				2.2283			
621	RS11071	SR	245	74	WP	32	60	57.7	57	1265	39871	0.01	2.3461	2.4411	1276	12
622	RS11071	SR	245	74	WP	32	60	57.7	57	1311	39813	0.07	2.3448	2.4567	2232	12
623	RS11071	SR	245	74	WP	32	60	57.7	57				2.3561		1496	12
624	RS11071	SR	245	74	WP	32	60	57.7	57				2.3319		1524	16
625	RS11071	SR	245	74	WP	32	60	57.7	57				2.3451			
626	RS11071	SR	245	74	WP	32	60	57.7	57				2.3611			
627	RS11071	SR	245	74	WP	32	60	57.7	57				2.3635			
628	RS11071	SR	245	74	OWP	29	60	56.4	0	919	29668	−0.7	2.2071	2.4779	<1"	11
629	RS11071	SR	245	74	OWP	29	60	56.4	0	920	29618	−0.7	2.2581	2.4589	1305	16
621	RS11071	SR	245	74	OWP	29	60	56.4	0				2.2459		1750	16
6211	RS11071	SR	245	74	OWP	29	60	56.4	0						1775	
6212	RS11071	SR	245	74	OWP	29	60	56.4	0				2.2543			
6213	RS11071	SR	245	74	OWP	29	60	56.4	0				2.2584			
6214	RS11071	SR	245	74	OWP	29	60	56.4	0				2.2667			
711	R17914	I	65	41	WP	13	40	39.3	3765	850.4		−0.6	2.2134	2.4859	1413	18
712	R17914	I	65	41	WP	13	40	39.3	3765	885.3		−0.6	2.2217	2.4782	1194	15
713	R17914	I	65	41	WP	13	40	39.3	3765				2.2091		1926	15
714	R17914	I	65	41	WP	13	40	39.3	3765				2.2133		884	23

Table C.7. (cont.)

CODE	CONTRACT NUMBER	ROUTE TYPE	ROUTE NO.	CO.	WHEEL	#30 %	#50 %	#100 %	TRUCKS	KIN. VISC.	ABS. VISC.	PVN	BULK S.G.	MAX. S.G.	MARSHALL STABILITY	FLOW
715	R17914	1	65	41	WP	13	40	39.3	3765				2.2049			
716	R17914	1	65	41	WP	13	40	39.3	3765				2.2476			
717	R17914	1	65	41	WP	13	40	39.3	3765				2.2152			
718	R17914	1	65	41	OWP	14	41	41.7	0	1031		−0.4	2.2224	2.4552	1213	15
719	R17914	1	65	41	OWP	14	41	41.7	0	1022		−0.4	2.2113	2.4493	1154	16
7110	R17914	1	65	41	OWP	14	41	41.7	0				2.2104		1958	16
7111	R17914	1	65	41	OWP	14	41	41.7	0				2.2181		1428	
7112	R17914	1	65	41	OWP	14	41	41.7	0				2.2008			
7113	R17914	1	65	41	OWP	14	41	41.7	0				2.2183			
7114	R17914	1	65	41	OWP	14	41	41.7	0				2.2144			
721	R15317	1	74	23	WP	20	50	65	3383	563	7837	−0.9	2.4316	2.4572	709	14
722	R15317	1	74	23	WP	20	50	65	3383	571	7841	−0.8	2.4323	2.4584	1980	13
723	R15317	1	74	23	WP	20	50	65	3383				2.4303			15
724	R15317	1	74	23	WP	20	50	65	3383				2.4119			14
725	R15317	1	74	23	WP	20	50	65	3383				2.4371			
726	R15317	1	74	23	WP	20	50	65	3383				2.4332			
727	R15317	1	74	23	WP	20	50	65	3383				2.4572			
728	R15317	1	74	23	OWP	19	53	68.7	0	555	6852	−1.2	2.4054	2.4582	1558	14
729	R15317	1	74	23	OWP	19	53	68.7	0	560	6887	−1	2.3992	2.4894	1854	12
7210	R15317	1	74	23	OWP	19	53	68.7	0				2.3684		1321	14
7211	R15317	1	74	23	OWP	19	53	68.7	0				2.3428		1227	15
7212	R15317	1	74	23	OWP	19	53	68.7	0				2.4141			
7213	R15317	1	74	23	OWP	19	53	68.7	0				2.3976			
7214	R15317	1	74	23	OWP	19	53	68.7	0				2.3744			
731	R10930	0	65	72	WP				5676	981.1	36728	−0.6	2.3648	2.515		
732	R10930	1	65	72	WP				5676	1007	36827	−0.6	2.3574	2.47		0
733	R10930	1	65	72	WP				5676				2.3805			0

Table C.7. (cont.)

CODE	CONTRACT NUMBER	ROUTE TYPE	ROUTE NO.	CO.	WHEEL	#30 %	#50 %	#100 %	TRUCKS	KIN. VISC.	ABS. VISC.	PVN	BULK S.G.	MAX. S.G.	MARSHALL STABILITY	FLOW
734	R10930	I	65	72	WP				5676				2.3291			0
735	R10930	I	65	72	WP				5676				2.3456			
736	R10930	I	65	72	WP				5676				2.3423			
737	R10930	I	65	72	WP				5676				2.3392			
738	R10930	I	65	72	OWP				0	1135	41213	−0.4	2.3497	2.4982		0
739	R10930	I	65	72	OWP				0	1112	41176	−0.5	2.3112	2.4836		0
7310	R10930	I	65	72	OWP				0				2.3312			0
7311	R10930	I	65	72	OWP				0				2.3436			0
7312	R10930	I	65	72	OWP				0				2.2634			
7313	R10930	I	65	72	OWP				0				2.3226			
7314	R10930	I	65	72	OWP				0				2.2501			
741	R11240	I	65	72	WP				5786	405	3843	−1.2	2.3988	2.462	4792	8
742	R11240	I	65	72	WP				5786	411.4	3850	−1.2	2.3945	2.4589	3336	10
743	R11240	I	65	72	WP				5786	414.9			2.3944		3975	7
744	R11240	I	65	72	WP				5786	389.5			2.3612		3166	9
745	R11240	I	65	72	WP				5786				2.3824			
746	R11240	I	65	72	WP				5786				2.3976			
747	R11240	I	65	72	WP				5786				2.4031			
748	R11240	I	65	72	OWP				0	467.2	4121	−1.2	2.3852	2.456	1880	12
749	R11240	I	65	72	OWP				0	475.4	4129	−1.1	2.3795	2.46	2184	11
7410	R11240	I	65	72	OWP				0	455.1			2.3921		2164	14
7411	R11240	I	65	72	OWP				0	454			2.3936		1786	12
7412	R11240	I	65	72	OWP				0				2.3811			
7413	R11240	I	65	72	OWP				0				2.3695			
7414	R11240	I	65	72	OWP				0				2.3783			
811	RS15171	US	421	69	WP	28	48	52.7	217	835		−1	2.4244	2.4667	1692	16
812	RS15171	US	421	69	WP	28	48	52.7	217	824		−1	2.4427	2.4637	1874	15

Table C.7. (cont.)

CODE	CONTRACT NUMBER	ROUTE TYPE	ROUTE NO.	CO.	WHEEL	#30 %	#50 %	#100 %	TRUCKS	KIN. VISC.	ABS. VISC.	PVN	BULK S.G.	MAX. S.G.	MARSHALL STABILITY	FLOW
813	RS15171	US	421	69	WP	28	48	52.7	217				2.4219		1893	16
814	RS15171	US	421	69	WP	28	48	52.7	217				2.4235		1734	15
815	RS15171	US	421	69	WP	28	48	52.7	217				2.4211			
816	RS15171	US	421	69	WP	28	48	52.7	217				2.4121			
817	RS15171	US	421	69	WP	28	48	52.7	217				2.4074			
818	RS15171	US	421	69	OWP	27	50	50.4	0	845		−1	2.4309	2.4914	2215	16
819	RS15171	US	421	69	OWP	27	50	50.4	0	840		−1	2.4291	2.4822	2241	18
8110	RS15171	US	421	69	OWP	27	50	50.4	0				2.4244		1925	19
8111	RS15171	US	421	69	OWP	27	50	50.4	0				2.4084		2095	20
8112	RS15171	US	421	69	OWP	27	50	50.4	0				2.4327			
8113	RS15171	US	421	69	OWP	27	50	50.4	0				2.4097			
8114	RS15171	US	421	69	OWP	27	50	50.4	0				2.4172			
821	R15415	SR	37	29	WP	15	33	42	303	1151		−0.5	2.3392	2.5022	2514	13
822	R15415	SR	37	29	WP	15	33	42	303	1111		−0.6	2.3224	2.4685	1175	17
823	R15415	SR	37	29	WP	15	33	42	303				2.3529		2099	13
824	R15415	SR	37	29	WP	15	33	42	303				2.3136		2016	17
825	R15415	SR	37	29	WP	15	33	42	303				2.2998			
826	R15415	SR	37	29	WP	15	33	42	303				2.3096			
827	R15415	SR	37	29	WP	15	33	42	303				2.3312			
828	R15415	SR	37	29	OWP	15	36	38.5	0	1314	63930	−0.5	2.3174	2.494	2109	16
829	R15415	SR	37	29	OWP	15	36	38.5	0	1292	63999	−0.5	2.3135	2.4997	2696	15
8210	R15415	SR	37	29	OWP	15	36	38.5	0				2.2907		1553	19
8211	R15415	SR	37	29	OWP	15	36	38.5	0				2.3099		1916	15
8212	R15415	SR	37	29	OWP	15	36	38.5	0				2.2787			
8213	R15415	SR	37	29	OWP	15	36	38.5	0				2.3438			
8214	R15415	SR	37	29	OWP	15	36	38.5	0				2.2941			
831	R10396	SR	1	89	OWP				179	541.8	6464	−0.8	2.4309	2.4354	2117	16

Table C.7. (cont.)

CODE	CONTRACT NUMBER	ROUTE TYPE	ROUTE NO.	CO.	WHEEL	#30 %	#50 %	#100 %	TRUCKS	KIN. VISC.	ABS. VISC.	PVN	BULK S.G.	MAX. S.G.	MARSHALL STABILITY	FLOW
832	R10396	SR	1	89	OWP				179	542.3	6438	−0.8	2.4339	2.4658	3085	16
833	R10396	SR	1	89	OWP				179				2.4365		2444	17
834	R10396	SR	1	89	OWP				179				2.4302		2352	19
835	R10396	SR	1	89	OWP				179				2.4352			
836	R10396	SR	1	89	OWP				179				2.4436			
837	R10396	SR	1	89	OWP				179				2.4347			
838	R10396	SR	1	89	WP				0	545		−0.8	2.4066	2.4701	1110	13
839	R10396	SR	1	89	WP				0	551		−0.8	2.4056	2.4597	1215	11
8310	R10396	SR	1	89	WP				0				2.3909		1394	18
8311	R10396	SR	1	89	WP				0				2.4162		1303	18
8312	R10396	SR	1	89	WP				0				2.4061			
8313	R10396	SR	1	89	WP				0				2.4144			
8314	R10396	SR	1	89	WP				0				2.4255			
841	R12196	SR	37	29	WP				1056	1067	33865	−0.9	2.3353	2.5039	1511	16
842	R12196	SR	37	29	WP				1056	1029	33935	−1	2.3453	2.5138	1863	15
843	R12196	SR	37	29	WP				1056				2.3261		1477	19
844	R12196	SR	37	29	WP				1056				2.3008		1457	16
845	R12196	SR	37	29	WP				1056				2.3238			
846	R12196	SR	37	29	WP				1056				2.3222			
847	R12196	SR	37	29	WP				1056				2.3583			
848	R12196	SR	37	29	OWP				0	1406		−0.3	2.3369	2.4928	1840	9
849	R12196	SR	37	29	OWP				0	1434		−0.3	2.3437	2.4963	2085	14
8410	R12196	SR	37	29	OWP				0				2.3637		1733	17
8411	R12196	SR	37	29	OWP				0				2.3629		2151	16
8412	R12196	SR	37	29	OWP				0				2.3759			
8413	R12196	SR	37	29	OWP				0				2.3755			
8414	R12196	SR	37	29	OWP				0				2.3764			

APPENDIX D - DISCRIMINANT ANALYSIS AND EXAMPLE

The S and X Matrices develcped in the Analysis

	PVN	BSG	MARSH	FLOW	PEN	ASP	AIR
PVN	0.08804	−0.00816	35.28151	−0.17159	−0.25181	−0.00661	0.394064
BSG	−0.0082	0.006999	21.12563	−0.0143	0.186875	0.002926	−0.22969
MARSH	35.2815	21.12563	322339.7	216.8768	−1148.75	−55.9983	−528.171
FLOW	−0.1716	−0.0143	216.8768	7.324185	−12.1487	−0.13263	1.989165
PEN	−0.2518	0.186875	−1148.75	−12.1487	55.90739	1.088235	−9.53925
ASP	−0.0066	0.002926	−55.9983	−0.13263	1.088235	0.16605	−0.08185
AIR	0.39406	−0.22969	−528.171	1.989165	−9.53925	−0.08185	9.045371
E1HZ20	−36253	21071.93	105500000	156234.6	−686653	−48472.3	−780075
E1HZ30	−18268	10584.03	65040193	159254	−698213	−38344.5	−377860
E4HZ30	−23196	13431.04	81569076	198452.2	−861735	−45732.8	−479429
E8Z20	−52277	30091.43	146910000	212530.3	−909506	−60621.8	−1113977
E8HZ30	−26391	15146.72	91108790	220885.7	−952804	−50138.7	−541679

	E1HZ20	E1HZ30	E4HZ30	E8HZ20	E8HZ30
PVN	−36252.8	−18268.2	−23196.3	−52276.7	−26391
BSG	21071.93	10584.03	13431.04	30091.43	15146.72
MARSH	105500000	65040193	81569076	146910000	91108790
FLOW	156234.6	159254	198452.2	212530.3	220885.7
PEN	−686653	−698213	−861735	−909506	−952804
ASP	−48472.3	−38344.5	−45732.8	−60621.8	−50138.7
AIR	−780075	−377860	−479429	−1113977	−541679
E1HZ20	1.23E+11	7.32E+10	9.16E+10	1.718E+11	1.03E+11
E1HZ30	7.32E+10	4.55E+10	5.68E+10	1.018E+11	6.36E+10
E4HZ30	9.16E+10	5.68E+10	7.10E+10	1.276E+11	7.94E+10
E8Z20	1.72E+11	1.02E+11	1.28E+11	2.407E+11	1.43E+11
E8HZ30	1.03E+11	6.36E+10	7.94E+10	1.430E+11	8.88E+10

POOLED WITHIN−CLASS COVARIANCE MATRIX (S MATRIX)

	PVN	BSG	MARS	FLOW	PEN	ASP	AIR
ZERO	−0.6386	2.3199918	1632.6071	14.702381	23.9285714	5.0714286	5.8991141
RUT	−0.8076	2.3508245	1695.7143	13.321429	24.8571429	5.1142857	4.3956421
TC	−0.7327	2.3707143	1815.1667	15.777778	23.1666667	5.4	3.8791185
STRIP	−0.682	2.3563	1771.3125	15.229167	27.125	5.2	5.3321268

	E1HZ20	E1HZ30	E4HZ30	E8HZ20	E8HZ30
ZERO	1140587.9	625219.75	789306.95	1618163.92	888576.28
RUT	1227441.5	662296.14	839010.53	1751397.59	944358.76
TC	1258513	684633.5	871943.54	1810092.1	984032.75
STRIP	1027234.4	547130.7	692681	1464826.67	779416.64

SAMPLE VECTOR MATRIX (Mean Laboratory Measured Data or X−Matrix)

APPENDIX D

WORK EXAMPLE FOR CLASSIFYING UNKNOWN BITUMINOUS MIXTURE INTO DISTRESS CATEGORY

	PVN	BSG	MARSH	FLOW	PEN	ASP	AIR
X DATA	-0.69	2.3499	1750	15	25	5.1	4.5
X-ZERO	-0.051	0.0299082	117.39286	0.297619	1.0714286	0.0285714	-1.3991
X-RUT	0.1176	-0.000924	54.285714	1.6785714	0.1428571	-0.014286	0.10436
X-TC	0.0427	-0.020814	-65.16667	-0.777778	1.8333333	-0.3	0.62088
X-STRIP	-0.008	-0.0064	-21.3125	-0.229167	-2.125	-0.1	-0.8321

	E1HZ20	E1HZ30	E4HZ30	E8HZ20	E8HZ30
X DATA	1122335	590000	750000	1600000	900000
X-ZERO	-18253	-35219.75	-39306.95	-18163.92	13123.718
X-RUT	-105107	-72296.14	-89010.53	-151397.6	-44358.76
X-TC	-136178	-99633.5	-121943.5	-210092.1	-84032.75
X-STRIP	95100.6	42869.296	57319.003	135173.33	120583.36

Data from a set of samples for a bituminous pavement with unknown distress is evaluated. The necessary data for the analysis is tabulated above. The $(X - X_i)$ matrix was computed using data in Table 8.3. Finally, the D_i^2 was evaluated using Equation 8.2 and the results are shown below:

$D_{zero}^2 = 8.5E20$ $\qquad D_{rut}^2 = 2.6E22$

$D_{tc}^2 = 5.2E22$ $\qquad D_{strip}^2 = 2.5E22$

The minimum D_i^2 is 8.5E20 thus the unknown pavement belongs to the ZERO distress category.